Plasma Proteome Analysis

Using Peptide Group-Specific Immunoprecipitation

"Triple X Proteomics"

Dissertation

der Mathematisch-Naturwissenschaftlichen Fakultät

der Eberhard Karls Universität Tübingen

zur Erlangung des Grades eines

Doktors der Naturwissenschaften

(Dr. rer. nat.)

vorgelegt von

Sonja Schneider

aus Temeschburg

Tübingen

2012

Tag der mündlichen Qualifikation:	02.05.2012
Dekan:	Prof. Dr. Wolfgang Rosenstiel
1. Berichterstatter:	Prof. Dr. Stefan Stevanovic
2. Berichterstatter:	Prof. Dr. Thilo Stehle

Acknowledgments

This thesis was performed at the Natural and Medical Sciences Institute at the University of Tübingen in the department of biochemistry. Parts of the experimental work were also carried out at the University of Victoria Genome British Columbia Proteomics Centre, Victoria, BC, Canada under the supervision of Dr. Christoph Borchers and at Agilent Technologies, Waldbronn, Germany under the supervision of Dr. Stefan Buckenmaier.

First of all, I would like to thank my supervisor Prof. Dr. Stefan Stevanovic for excellent supervision of this thesis. I would also like to acknowledge Prof. Dr. Thilo Stehle for agreeing to act as 2nd examiner. I am very grateful to Dr. Thomas Joos for giving me the opportunity to write my PhD thesis at the NMI and for all his support during the last 3 years.

I especially wish to express my sincere gratitude to my advisor Oliver Poetz. I appreciate all the time he invested, the detailed and constructive comments and especially his crucial support throughout this thesis. I am very thankful for being given the chance to work abroad and for all his encouragement and ideas during the time in Canada.

In addition, I would like to thank Dr. Christoph Borchers for giving me the opportunity to learn MRM quantification techniques in his lab and to spend a great time in Victoria in the summer 2010. I would like to take this opportunity to acknowledge Boehringer Ingelheim Fonds for the financial support of my research stay in Victoria.

Many thanks to Dr. Caroline May from the Medical Proteome Centre in Bochum for the amino acid analysis of my peptides.

Furthermore, I would like to thank Dr. Stefan Buckenmaier for the great assistance during my experiments, carried out at Agilent Technologies in Waldbronn.

Also, I wish to thank all my colleagues at the NMI for the great working atmosphere. In particular, I would like to thank the TXP/MS group: David, Thomas, Chris, Dieter and Conny for all the inspiring discussions and support. Also I would like to thank the other graduate students Katrin, Nadja, Michael, Steffi and Yvonne for a great time during my stay at the NMI.

I am very grateful to my parents for their love and support throughout my education.

Finally, I owe my loving thanks to my husband Nico for all his understanding during busy times and my stay abroad. I am very fortunate to be your wife.

Contents

List of Figures

List of Tables

Abbreviations

AA	Amino acid
AB	Antibody
ABC	Ammonium bicarbonate
ABCN	Ammonium bicarbonate + 0.3 % NOG
ACN	Acetonitrile
AQUA	Absolute quantification
A.U.	Arbitrary units
BSA	Bovine serum albumin
CE	Collison energy
CHCA	α-Cyano-4-hydroxycinnamic acid
Cy5	Cyanine dye 5
Da	Dalton
2-DE	2D electrophoresis
DMSO	Dimethyl sulfoxide
DNA	Deoxyribonucleic acid
DOA	8-Amino-3,6-dioxa-octanoic acid
EDC	1-Ethyl-3-[3-dimethylaminopropyl]carbodiimide hydrochloride
ELISA	Enzyme-linked immunosorbent assay
ESI	Electrospray ionization
FA	Formic acid
FPLC	Fast protein liquid chromatography
HA	Hemagglutinin
HUPO	Human Proteome Organization
IAA	Iodoacetamide
ICAT	Isotope-coded affinity tags
Ig	Immunoglobulin

IP	Immunoprecipitation
iTRAQ	Isobaric tags for relative and absolute quantification
KDa	Kilo Dalton
KLH	Keyhole limpet hemocyanin
LC	Liquid chromatography
LOD	Limit of detection
LOQ	Limit of quantification
MALDI	Matrix-assisted laser desorption/ionization
MES	2-(N-morpholino)ethanesulfonic acid
MFI	Median fluorescence intensity
MRM	Multiple reaction monitoring
MudPIT	Multidimensional protein identification technology
MS	Mass spectrometry
MW	Molecular weight
m/z	Mass-to-charge ratio
NHS	N-hydroxysuccinimide
NOG	N-octyl-β-d-glucopyranoside
n.a.	Not applicable
n.d.	Non/not determined
n.k.	Not known
n.i.	Not identified
PAC	Prespotted anchor chip
PBS	Phosphate buffered saline
PBSN	Phosphate buffered saline + 0.3 %NOG
PCR	Polymerase chain reaction
PE	Phycoerythrin

PMF	Peptide mass fingerprint
PMSF	Phenylmethanesulfonylfluoride
QQQ	Triple quadrupole
rbt	Rabbit
RIA	Radioimmunoassay
RNA	Ribonucleic acid
RPM	Revolutions per minute
RT	Room temperature
S.D.	Standard deviation
SDS-PAGE	Sodium dodecyl sulfate polyacrylamide gel electrophoresis
SILAC	Stable isotope labeling with amino acids in cell culture
SIS	Stable isotope standard
SISCAPA	Stable isotope standards and capture by anti-peptide antibodies
SMCC	Succinimidyl-4-[N-maleimidomethyl]cyclohexane-1-carboxylat
SMPB	Succinimidyl 4-[p-maleimidophenyl]butyrate
S/N	Signal to noise ratio
TCEP	Tris(2-carboxyethyl)phosphine
TFA	Trifluoroacetic acid
TOF	Time of flight
TXP	Triple X proteomics
UC	Ultracentrifugation

Chapter 1.

Introduction

1.1. The plasma proteome

"Blut ist ein ganz besondrer Saft." Johann Wolfgang von Goethe, Faust I, Verse 1740 / Mephistopheles

Blood immerses most tissues in the human body and therefore contains useful diagnostic information. As such, the composition of blood plasma proteins can reflect the diseased or healthy state of a patient (Jacobs *et al.*, 2005). Plasma is composed of the classical plasma proteins, many of which are involved in coagulation, immune defense, small molecule transport and protease inhibition. Additionally, plasma also contains proteins originating from cell or tissue leakage or active secretion (Anderson and Anderson, 2002). Proteins are responsible for catalytic, structural and signaling activities within an organism. Thus the detection and quantification of individual proteins can enable disease characterization at the molecular level. For example, tissue proteins in plasma can be used as leakage markers, as tumors or other disease processes often lead to the release of proteins into the blood system. Proteins, which are differentially regulated as a result of a pharmacological response or a therapeutic intervention, can furthermore act as predictive or monitoring biomarkers (Anderson, 2010).

The identification of reliable biomarkers, which accurately report health and disease status, has gained considerable interest in recent years (Veenstra *et al.*, 2005). The plasma proteome is the most complex human-derived proteome containing proteins present at concentrations which differ in more than 10 orders of magnitude (Jacobs *et al.*, 2005; Anderson, 2005; Hortin *et al.*, 2008; Whiteaker *et al.*, 2007b). Serum albumin, the protein with the highest abundance in plasma, is present at a concentration ranging from 35 to 50 mg/ml (Masaki *et al.*, 2006), whereas in contrast proteins like e.g. interleukin-6 are present in the low pg/ml range (Ridker *et al.*, 2000).

As blood plasma is readily available and easily accessible without highly invasive techniques, it has huge potential as a sample source for routine clinical diagnosis assays.

1.2. Plasma proteome analysis

The first report of a disease diagnosis, based on the analysis of blood, was that made by Hippocrates (Secretion *et al.*, 1998). He proposed that diseases result from the imbalance of the four humors: blood, phlegm, yellow bile and black bile. His ideas remained basic to medical practice for over a thousand years. Although medical practice and principles have changed a great deal over the centuries, blood has remained one of the most clinically significant samples (Anderson and Anderson, 2002).

However, the analysis of plasma is complicated by its complexity and the dynamic range of its constituents (Anderson, 2005). In contrast to the polymerase chain reaction for the amplification of DNA or RNA, there is no protein amplification technique available. Hence, without fractionation and enrichment techniques prior to detection, the signals of low abundant proteins are often suppressed by those derived from high abundant proteins (Sun *et al.*, 2005).

There are two basic approaches of plasma proteome analysis: non-targeted and targeted proteome analysis. The goal of non-targeted plasma proteome analysis is the discovery and identification of new biomarkers in blood plasma. Other applications of non-targeted analysis, in addition to new biomarker discovery, include sample classification, quality control and peptide fingerprinting. Obviously, non-targeted discovery experiments are not directly leading to biomarkers, that can be instantly used in clinical diagnostics. Non-targeted experiments provide "candidates", which have to be validated using "targeted plasma proteome analysis" to be useful in clinical diagnostics (Carr and Anderson, 2008). Hence, targeted plasma proteome analysis is the precise identification and quantification of multiple and already known plasma proteins.

1.2.1. Tools for non-targeted plasma proteome analysis

A great variety of techniques exist for the analysis of plasma proteins e.g. one-dimensional (SDS-PAGE) or two-dimensional electrophoresis. The application of 2-D electrophoresis to plasma analysis (Anderson and Anderson, 1977) enabled the resolution of over 300 species (2-DE map of human plasma), the identification of which was carried out by immunodetection. The detection of many lower abundant proteins is nevertheless limited without additional separation steps like classical chromatographic separation techniques - such including size exclusion, ion exchange, lectin binding, and hydrophobic interaction using aliphatic carbon chain coated surfaces.

1.2.2. Tools for targeted plasma proteome analysis

The gold standard for the diagnosis and monitoring of diseases in blood plasma are immunoassays like the radioimmunoassay (RIA, Yalow and Berson (1960)) and the

enzyme-linked immunosorbent assay (ELISA, Lequin (2005)), mostly carried out as *sandwich* ELISA.

Over the past years, protein microarrays have become more and more important, enabling high-throughput analysis in a miniaturized format (Nielsen and Geierstanger, 2004). In protein microarrays, purified proteins or sera/lysate samples are immobilized either on a planar surface or on small microspheres creating protein arrays in suspension. Schwenk *et al.* (2008) developed multiplexed antibody microarrays using color-coded microspheres to screen for target proteins in complex serum samples.

Immunoassays enable the high throughput accurate quantification of low abundant plasma proteins (down to the low pg/ml range) in highly complex samples (Ridker *et al.*, 2000). However, up to now only 1% of the human gene products can be quantitatively measured by laboratory-developed tests available for clinical use in the US. The rate of developing new assays is only one per year (Anderson, 2010).

1.3. Plasma proteome analysis by mass spectrometry

Mass spectrometry (MS) is an established tool for the detection and identification of protein biomarkers in clinical samples like human plasma. In line with classical plasma analyzing methods (see above), MS-based proteome analysis can be carried out in a non-targeted and a targeted manner.

1.3.1. Non-targeted MS analysis

Non-targeted MS analysis, also known as "shotgun" proteomics, is achieved by coupling multidimensional separation with mass spectrometry (Wolters *et al.*, 2001). Washburn *et al.* (2001) described an unbiased (non-targeted) method incorporating multidimensional liquid chromatography and tandem mass spectrometry, termed multidimensional protein identification technology (MudPIT) for the analysis of the yeast (*Saccharomyces cerevisiae*) proteome. Adkins *et al.* (2002) then went on to apply "shotgun" proteomics to the analysis of the plasma proteome.

As MS based proteome analysis evolved, different quantification strategies were established, including ^{18}O proteolytic labeling (Yao *et al.*, 2001; Miyagi and Rao, 2007), isotope-coded affinity tags (ICAT, Gygi *et al.* (1999, 2002)), isobaric tags for relative and absolute quantification (iTRAQ^{TM}, Aggarwal *et al.* (2006); Melanson *et al.* (2006)) and stable isotope labeling with amino acids in cell culture (SILAC, Ong *et al.* (2002); Everley *et al.* (2004)).

1.3.2. Targeted MS analysis

Targeted MS analysis is typically carried out using multiple reaction monitoring (MRM) techniques using triple quadrupole mass spectrometers. MRM enables the identification of e.g. peptides via analysis of specific transitions from parent ion (whole peptide) to fragment ions (peptide fragments). Protein quantification using stable isotope dilution coupled to MRM was described by Gerber *et al.* (2003). This strategy for absolute quantification (termed AQUA) uses synthetic, stable isotope-labeled peptides as internal standards to enable quantification by comparing the signals from the exogenous labeled and endogenous unlabeled type.

Mass spectrometry based assays are particularly affected by ionization suppression. Signals corresponding to the low abundant proteins are masked by those derived from the high abundant proteins (Liu *et al.*, 2006). To obtain limits of detection (LOD) and quantification (LOQ) in the clinically relevant range, either an enrichment of the low abundant proteins and/or a depletion of the high abundant proteins must be performed. Keshishian *et al.* and Fortin *et al.* e.g. investigated the combination of immunodepletion of the most abundant proteins in plasma with MRM based MS assays and were successfully able to reach LODs in the low ng/ml concentration range (Keshishian *et al.*, 2009; Fortin *et al.*, 2009a). Around the same time Fortin *et al.* (2009b) published a method, where they obtained LODs in the low ng/ml range without immunodepletion (using 100 μl plasma in both publications). Instead, they used a combination of solid-phase extraction and multiple reaction monitoring to the power of three (MRM^3, adding another fragmentation step after the one already implemented in the method).

By incorporating stable isotope peptide standards into a workflow with immunoaffinity purification prior to MRM analysis, Anderson *et al.* introduced SISCAPA (stable isotope standards and capture by anti-peptide antibodies) for plasma protein quantification (Anderson *et al.*, 2004). Two years later, they developed multiplex assays based on MRM mass spectrometry for plasma proteins of high to medium abundance down to those present in only hundreds of ng/ml (Anderson and Hunter, 2006).

With the use of peptide-specific antibodies for the immunoenrichment of target peptides with subsequent MRM read-out using 10 μl plasma (Whiteaker *et al.*, 2010), similar sensitivities were obtained compared to Keshishian *et al.* and Fortin *et al.*. With 1 ml plasma volume, the detection limit was even extended to the low pg/ml range (Whiteaker *et al.*, 2010).

1.4. Sandwich immunoassays vs. mass spectrometry

Clinical validation of biomarkers is traditionally carried out by ELISAs due to their specificity and sensitivity and the capacity for high sample throughput (Rifai *et al.*,

2006). However, immunodetection by specific antibodies used by methods like RIA or ELISA carry the risk of generating false-positives, resulting from non-specific binding of other proteins in a complex sample (Spencer, 2004). The limitation of such immmunodetection methods is, that they do not enable the identification of the generated signal, so that positive signals could be produced from non-specific molecules, that bind to the applied antibodies in the immunoassay (Minutti *et al.*, 2004). Moreover, the assay development is highly time-consuming, cost intensive and rarely successful in terms of finding adequate specific antibodies for the application in RIAs, ELISAs and other immunodetection methods (Ackermann and Berna, 2007).

Immunodetection assays are therefore dependent upon the generation of high quality protein antibodies. Unfortunately, the list of available antibodies for human plasma biomarker candidates is short. These limitations create a bottleneck in the biomarker pipeline (Paulovich *et al.*, 2008) and make it impractical to develop immunoassays for all putative biomarkers. To enhance the validation frequency of new candidate biomarkers more affordable "intermediate" methodologies with shorter development time and comparable multiplexing options are required.

A combination of immunoaffinity enrichment and mass spectrometry has proven to be a useful tool for the detection and quantification of clinically relevant plasma proteins (Ackermann and Berna, 2007; Whiteaker *et al.*, 2011) and exhibits several advantages compared to immunoassays. Similar to a sandwich immunoassay, a capture antibody first binds to its analyte, but instead of using a second analyte specific antibody, a mass spectrometer is used for the detection. The resulting immunoaffinity mass spectrometry method, when combined with stable isotopes (SISCAPA), has been shown to be suitable for plasma protein quantification (Anderson *et al.*, 2004). As the sample is digested to peptides, potential signal interferences from endogenous antibodies and other non-specific bound molecules, which can affect accurate quantification of the analyte, can be excluded. Furthermore, the optional fragmentation of the analyte peptide to smaller peptide components enables the determination of the amino acid sequence and along with that, the identification of the associated protein by database search engines. This procedure eliminates the generation of false-positives.

Although immunoaffinity MS does not match the speed and sample throughput of ELISAs it has 100 percent specificity, because the detection of the protein by the specific immunoaffinity capture and the MS read-out represent two statistically independent events. This technique is, however, limited by the availability of appropriate specific peptide antibodies. The production of thousands of antibodies would be necessary to cover the complete human proteome (Anderson *et al.*, 2009a), which is a very cost-intensive and time-consuming endeavor.

With the limit of detection and quantification in the ng/ml range (SISCAPA, using 10 μl plasma), the sensitivity of the mass spectrometric analysis is still a limiting factor (Whiteaker *et al.*, 2010), compared to the sensitivity of ELISA assays (down to the

low pg/ml range). However, the potential for multiplexing is inherent to MRM MS. Additionally, sample throughput can be greatly increased with the use of a matrix-assisted laser desorption/ionization (MALDI) mass spectrometer compared to LCMS systems.

1.4.1. Immunoaffinity MS using antibodies directed against short amino acid sequences - TXP Proteomics

A possible alternative to reduce the number of antibodies is achieved by enriching subproteomes like the glycoproteome (Zhang *et al.*, 2003) in a semi-targeted approach. Plasma contains a huge number of glycosylated proteins, where albumin is the only one, which is known not to be glycosylated (Montreuil *et al.*, 1997). But compared to immunoaffinity pre-fractionation methods, the complexity of such subproteomes can still be extremely high due to the huge number of glycosylated proteins in plasma and the heterogeneity in the glycosylation.

The Triple X Proteomics approach tackles this problem through the application of group specific antibodies. These antibodies are directed against short terminal epitopes (4 to 5 amino acids) at the N- or C-terminus of tryptic digested peptides (Poetz *et al.*, 2009). 3 to 4 amino acids of the epitope are variable, whereas the terminal amino acid is determined by the cleaving site of the chosen enzyme. Therefore, the concept was named triple X - referring to the 3 variable amino acids of the terminal epitope. The antibodies are capable of enriching groups of signature peptides with the same N- or C-terminal motif. The introduction of these antibodies leads to a very efficient enrichment of the targeted analytes and a reduction in sample complexity (Hoeppe *et al.*, 2010). Figure 1.1 displays the binding mechanism of TXP antibodies. Group specific enrichment is achieved by antibodies binding to peptides with the C-terminal ending EGYR, but not to peptides which do not carry this sequence nor those carrying the N-terminal EGYR sequence. Compared to the classical immunoaffinity enrichment MS techniques, which employ the One Antibody-One Analyte approach, TXP antibodies are capable of enriching several peptides with one single TXP antibody. To cover the human proteome a total of 21,500 antibodies would be necessary using the One Antibody-One Analyte approach, and with double coverage (2 peptides per protein) as many as 43,000 antibodies would be required (Anderson *et al.*, 2009a). In contrast, with the application of TXP antibodies, less than 2,000 (single coverage) would be theoretically necessary to cover the complete proteome (Poetz *et al.*, 2009; Planatscher *et al.*, 2010).

Figure 1.1.: Principle of Triple X antibody enrichment. The anti-EGYR TXP antibody, directed against the C-terminal sequence EGYR binds all peptides with the C-terminal ending EGYR, but not peptides with other sequences nor the N-terminal sequence EGYR. With TXP antibodies it is therefore possible to enrich peptides group-specifically due to their target sequence.

1.5. Goal of the thesis

The main goal of this thesis is to develop a high-throughput immunoaffinity assay using TXP antibodies with subsequent MS read-out to target a group of candidate biomarkers in human plasma. The triple X concept starts with an *in silico* digestion of the chosen proteome to select possible TXP epitopes for the generation of TXP antibodies.

About 300 potential biomarkers, taken from literature (Anderson, 2005; Polanski and Anderson, 2007), are examined using bioinformatics tools for appropriate TXP antibody epitopes. The potential candidate biomarkers cover different indications in the field of cancer and cardiovascular research. All peptides are filtered for compatibility with MS analysis. The terminal sequences of the final peptide list is searched and optimized for a minimal number of common epitopes with the aim of covering the whole biomarker list.

Polyclonal TXP antibodies are generated against the chosen TXP-epitopes by rabbit immunization. The resulting antisera are characterized regarding specificity and selectivity using microsphere-based peptide microarrays. Antisera, tested positively for high specificity and selectivity, are used for antibody purification using affinity chromatography.

The purified TXP antibodies are further characterized for specificity and cross-reactivity in immunoaffinity MS assays using synthetic peptides. Successfully tested antibodies are applied to immunoaffinity MS assays using enzymatically digested plasma as sample. The captured peptides are eluted and analyzed by MSMS. Figure 1.2 illustrates the Triple X Proteomics concept, modified after Hoeppe *et al.* 2010.

For the MS read-out, two different types of mass spectrometry platforms were used: a MALDI-TOF/TOF instrument (gaining higher throughput screening) and a nanoflow

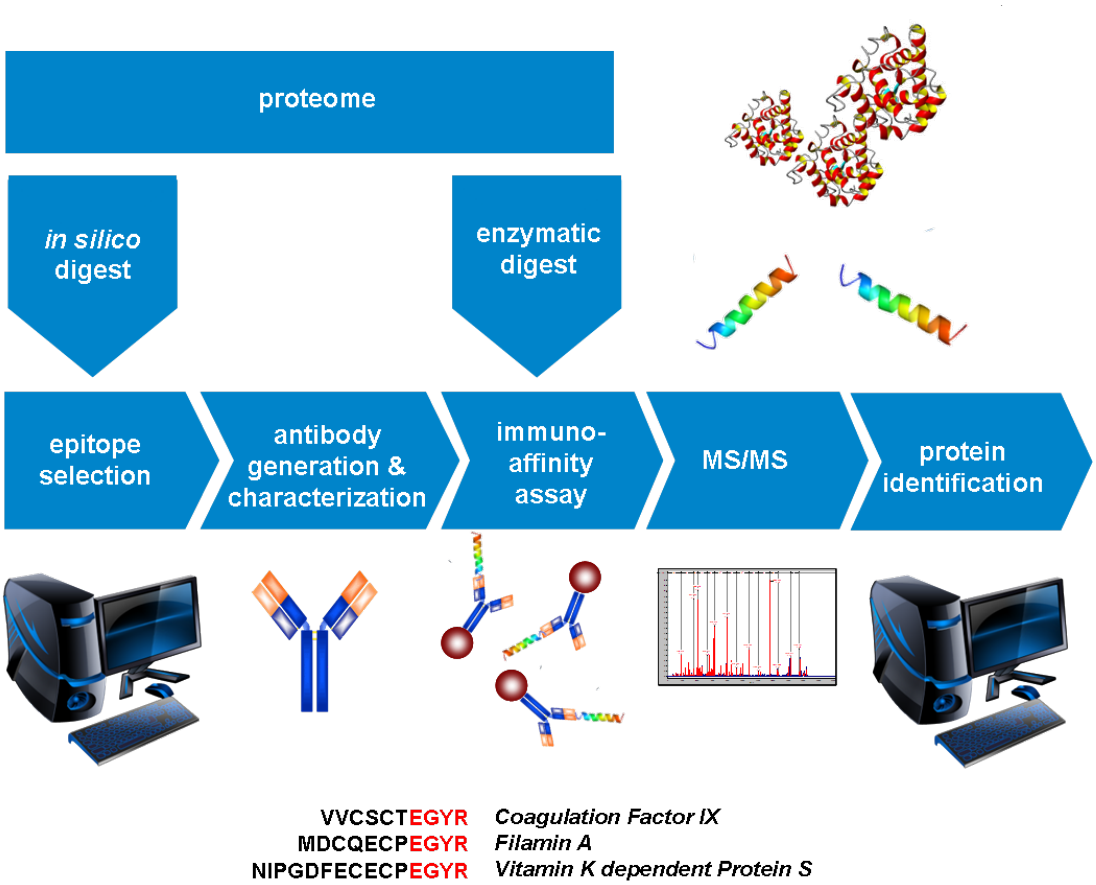

Figure 1.2.: Triple X Proteomics concept, modified after Hoeppe *et al.* 2010

HPLC coupled to an ESI (electrospray ionization) triple quadrupole for MRM for the quantitative aspect of the thesis.

For **discovery** and **identification** of captured peptides a MALDI TOF/TOF read-out was preferred. With TOF/TOF systems, peptides can be fragmented which enables database searches in order to identify the peptides, derived from a tryptic plasma digest. In contrast to LCMS measurements MALDI has a considerably higher throughput, which provides fast and reproducible measurements.

In addition to the establishment of an immunoaffinity MS assay, the quantification of the analytes was also carried out in a **targeted, quantitative approach**. Due to limited quantification capabilities of MALDI MS, MRM assays were developed to address the quantitative aspect of this work using a triple quadrupole mass spectrometer.

Following issues are examined and discussed in this thesis:

- Specificity and cross-reactivity of the TXP antibodies
- Suitability of the TXP immunoaffinity assay for MS read-out
- Suitability of the TXP immunoaffinity assay for plasma analysis

- Quantification of the captured peptides using MS read-out

In summary, the feasibility of applying the described group specific peptide enrichment affinity assays to the analysis of the highly complex blood plasma was examined for the detection and quantification of biomarkers in human blood plasma.

Chapter 2.

Experimental procedures

2.1. Material, hardware and software

Material

Blood collection tubes	4 x 7.5 ml Plasma Lithium-Heparin S-Monovette tubes, Sarstedt, Nümbrecht, Germany
C18 purification	ZipTip Pipette Tips Millipore, Billerica, MA, USA
Disposables	Greiner Bio-One GmbH, Frickenhausen, Germany Eppendorf, Hamburg, Germany Beckman Coulter, Brea, CA, USA
1 ml HiTrap Column (NHS-activated HP)	GE Healthcare Bio-Sciences AB, Uppsala, Sweden
5 ml HiTrap™ Desalting Column	GE Healthcare Bio-Sciences AB, Uppsala, Sweden
Filter	Ultrafree-MC (Durapore, 0.65 µm) Millipore, Billerica, MA, USA
Microspheres	Carboxylated Microspheres Luminex, Austin, TX, USA
MALDI targets	Prespotted Anchor Chips Bruker Daltonik GmbH, Bremen, Germany
Magnetic microspheres	Dynabeads Protein G Invitrogen, Carlsbad, CA, USA

Microtiter filterplates	1.2 µm Durapore PVDF Millipore, Billerica, MA, USA
PCR-plates	KingFisher 96 KF plate (200 µł) ThermoFisher Scientific,Waltham, MA, USA
PCR tip comb	KingFisher 96 tip comb for PCR magnets ThermoFisher Scientific,Waltham, MA, USA
Single use cuvettes	UVette Eppendorf, Hamburg, Germany
Syringe filter	Rotilabo, sterile (0.22 µm PES) Carl Roth, Karlsruhe, Germany
Syringe needles	19-gauge 100 Sterican B. Braun Melsungen AG, Melsungen, Germany 21-gauge Safety Multifly 0.8 mm/19 mm needle Sarstedt, Nümbrecht, Germany

Hardware

Balances	Explorer E12140 OHAUS, Pine Brook, NJ, USA MC1 Research RC210 Sartorius AG, Göttingen, Germany
Microsphere array analyzer	Luminex 100/200 Luminex, Austin, TX USA
Centrifuges	Hettich Rotanta/RPC RP5094 rotor Hettich Lab technology, Tuttlingen, Germany 5415D and 5810R Eppendorf, Hamburg, Germany
Chromatographic Systems	ÄKTAxpress GE Healthcare Bio-Sciences AB, Uppsala, Sweden Agilent 1260 Infinity LC including HPLC-Chip Cube Agilent Technologies, Santa Clara, CA, USA
Gel-documentation	Kodak Image Station 440 CF Kodak Eastman, Rochester, NY, USA

MALDI mass spectrometer	MALDI-TOF/TOF Ultraflex III Bruker Daltonik, Bremen, Germany
Triple quadrupole mass spectrometer	6410 Triple Quadrupole LC-MS Agilent 6400 Series Triple Quad LC/MS system Agilent Technologies, Santa Clara, CA, USA
HPLC Chip	Large Capacity Chip (II) G420-62010 Agilent Technologies, Santa Clara, CA, USA
Magnets	Invitrogen DynaMag™, Carlsbad, CA, USA
Magnetic microsphere handler	Thermo Scientific KingFisher Flex and KingFisher 96 ThermoFisher Scientific,Waltham, MA, USA
Orbital shaker	KL-2 Edmund Bühler GmbH, Hechingen, Germany
pH meter	pH meter 766 Knick, Berlin, Germany
Photometer	BioPhotometer plus Eppendorf, Hamburg, Germany
Pipettes	Eppendorf, Hamburg, Germany
SDS PAGE System	XCell Sure Lock Mini Cell, Power Ease 500 Invitrogen, Carlsbad, CA, USA
Shaker	Vortex Genie 2 Scientific Industries, Bohemia, NY, USA
Syringe pump	Model 22 Harvard Apparatus, Holliston, MA, USA
Thermomixer	Thermomixer comfort Eppendorf, Hamburg, Germany
Swivel roller mixer	RM5 Assistent, Sondheim, Germany
Ultra pure water system	Arium 61316/611VF Sartorius, Göttingen, Germany
Ultracentrifuge	TL-100 Beckman Coulter, Brea, CA, USA

Ultrasonic bath	RK 31 Bandelin, Berlin, Germany

Software

Data collection microsphere based arrays	Exponent 3.1 Luminex, Austin, TX, USA
Data collection MALDI	FlexControl 3.0
	Bruker Daltonik, Bremen, Germany
Data evaluation MALDI	FlexAnalysis 3.0, Biotools 3.1
	Bruker Daltonik, Bremen, Germany
Data collection MRM	Mass Hunter Workstation Acquisition Software B.03.01
	Agilent, Santa Clara, CA, USA
Data evaluation MRM	Skyline/MacCoss Lab Seattle, WA, USA
Statistics	SigmaPlot 10, Systat software, Inc. Chicago, IL, USA
	StatistiXL 1.8, Excel Add-on

2.2. Reagents and chemicals

Antigen generation

DMSO	Fluka (Sigma-Aldrich) St. Louis, MO, USA
KLH	Pierce (Thermo Fisher Scientific) Waltham, MA, USA
Sodium azide	Merck KGaA Darmstadt, Germany
PBS	PAA Laboratories GMbH Pasching, Austria
Sulfo-MBS	Pierce (Thermo Fisher Scientific) Waltham, MA, USA
Peptides	Intavis AG Reutlingen, Germany
TCEP	Fluka (Sigma-Aldrich) St. Louis, MO, USA

Microsphere based microarrays

BSA (Albumin Fraction V Protease-free)	Carl Roth Karlsruhe, Germany
Blocking reagent for ELISA	Roche Mannheim, Germany
Di-sodiumhydrogenphosphate	Fluka (Sigma-Aldrich) St. Louis, MO, USA
EDC	Pierce (Thermo Fisher Scientific) Waltham, MA, USA
Donkey anti rabbit phycoerythrin	Jackson Immunoresearch West Grove PA, USA
Donkey anti sheep phycoerythrin	Jackson Immunoresearch West Grove, PA, USA
Goat anti mouse phycoerythrin	Jackson Immunoresearch West Grove, PA, USA

Mouse anti c-myc	Clone 9E10, Institute for molecular immunology Helmholtzzentrum, Munich, Germany
MES	Sigma-Aldrich St. Louis, MO, USA
Sulfo-NHS	Pierce (Thermo Fisher Scientific) Waltham, MA, USA
Sulfo-SMPB	Pierce (Thermo Fisher Scientific) Waltham, MA, USA
Tween20®	Merck KGaA Darmstadt, Germany
Activation buffer	100 mM sodium hydrogen phosphate, pH 6.2
Blocking buffer	Blocking reagent for ELISA (Roche) solved in H_2O_{dd} + 0.05 % (v/v) Tween20®
Coupling buffer	50 mM MES, pH 5.0
Washing buffer	0.05 % (v/v) Tween20®in PBS

Antibody purification

Ammonium acetate	Merck KGaA Darmstadt, Germany
Citrate	Sigma-Aldrich St. Louis, MO, USA
Ethanolamine	Carl Roth Karlsruhe, Germany
Maleimide activated BSA (SMCC)	Pierce (Thermo Fisher Scientific) Waltham, MA, USA
Sodium chloride	Carl Roth Karlsruhe, Germany
Hydrochloride acid	Carl Roth Karlsruhe, Germany
Activation buffer	1 mM hydrochloride acid
Binding buffer	PBS

Deactivation buffer I	0.5 M ethanolamine, 0.5 M sodium chloride, pH 8.3
Deactivation buffer II	0.1 M acetate, 0.5 M sodium chloride, pH 4.0
Elution buffer antibody purification	0.1 M citrate, pH 2.5

Immunoaffinity enrichment

Ammonium bicarbonate	Fluka (Sigma-Aldrich) St. Louis, MO, USA
Ammonium phosphate	Sigma-Aldrich St. Louis, MO, USA
PBS	PAA Laboratories GmbH Pasching, Austria
Formic acid	Biosolve Valkenswaard, Netherlands
n-Octyl-ß-D-glucopyranoside	Applichem Darmstadt, Germany
Triethanolamine	Carl Roth Karlsruhe, Germany
Trifluoroacetic acid	Biosolve Valkenswaard, Netherlands
Stopping solution	150 mM Ethanolamine, pH 9.0
Elution buffer TXP MALDI	1 % Formic acid
Elution buffer TXP MRM	1 % Formic acid + 0.1 % n-octyl-ß-D-glucopyranosid
Washing buffer PBSN (1, 2)	PBS + 0.3 % n-octyl-ß-D-glucopyranosid
Washing buffer ABCN (3, 4, 5)	50 mM ammonium bicarbonate pH 7.4 + 0.3 % n-octyl-ß-D-glucopyranosid

C18 Chromatography using ZipTip pipette tips

Acetonitrile	Merck KGaA Darmstadt, Germany

Wetting solution	100 % acetonitrile
Equilibration solution	0.1 % TFA
Methanol	Merck KGaA Darmstadt, Germany
Washing buffer ZipTip	0.1 % TFA + 5 % Methanol
Elution buffer ZipTip	80 % Acetonitrile + 0.1 % TFA

Plasma sample preparation

Acetic acid	Biosolve Valkenswaard, Netherlands
Ammonium phosphate	Sigma-Aldrich St. Louis, MO, USA
Iodoacetamide	Sigma-Aldrich St. Louis, MO, USA
Phenylmethylsulfonylfluoride	Roche Diagnostics Mannheim, Germany
ProteoExtract Albumin/IgG Removal Kit	Calbiochem (Merck KGaA) Darmstadt, Germany
Tris(2-carboxyethyl)phosphine	Sigma-Aldrich St. Louis, MO, USA
Trypsin	Sigma-Aldrich St. Louis, MO, USA
Trypsin Gold	Promega Madison, WI, USA

Ultracentrifugation

Goat anti human IgG Cy3	Jackson Immunoresearch West Grove, PA, USA
Goat anti human IgG Cy5	Jackson Immunoresearch West Grove, PA, USA
Goat anti rabbit IgG(F_c)	Jackson Immunoresearch West Grove, PA, USA

HA-peptide	Intavis AG Reutlingen, Germany
Rat anti HA	Clone 3F10, Institute for molecular immunology Helmholtzzentrum, Munich, Germany
Streptavidin	Pierce (Thermo Fisher Scientific) Waltham, MA, USA
Streptavidin-phycoerythrin conjugate	Jackson Immunoresearch West Grove, PA, USA
Sucrose	Sigma-Aldrich St. Louis, MO, USA

MALDI MS

Ammonium phosphate	Sigma-Aldrich St. Louis, MO, USA
Washing Buffer MS	10 mM ammonium phosphate + 0.1 % TFA

SDS PAGE

Antioxidants	NUPage Antioxidant Invitrogen, Carlsbad, CA, USA
Ethanol	Merck KGaA Darmstadt, Germany
Running buffer	NuPage SDS MES or MOPS Running buffer Invitrogen, Carlsbad, CA, USA
Sample buffer	NuPage LDS Sample buffer Invitrogen, Carlsbad, CA, USA
Protein Standard	SeeBlue Plus2 Pre-Stained Standard Invitrogen, Carlsbad, CA, USA
Reducing Agent	NuPage Sample Reducing Agent Invitrogen, Carlsbad, CA, USA
Coomassie Solution	0.2 % (w/v) Coomassie Brilliant Blue, 50 % methanol, 10 % acetic acid

Destaining Solution I	50 % ethanol, 10 % acetic acid
Destaining Solution II	10 % ethanol, 5 % acetic acid

2.3. Generation of polyclonal antibodies

2.3.1. Bioinformatical antigen selection

The sequences of 300 potential biomarker taken from literature, see Anderson (2005) and Polanski and Anderson (2007), were examined using bioinformatic tools for appropriate TXP antibody epitopes. The potential biomarkers cover different indications in the field of cancer and cardiovascular research. Short peptide sequences, that cover all plasma proteins of interest, were identified. The bioinformatic selection process after Planatscher *et al.* (2010) was separated into four distinct modules, see Fig. 2.1. The first module (preprocessing) digested the human proteome of the Uniprot database, the second step (filter) removed all peptides with unfavorable properties, the third step (optimization) was the selection of optimal antibodies and the last step generated a comprehensive report of the results. All plasma proteins were digested *in silico* with trypsin. The cleavage site was specified to cut after R (arginine) or K (lysine) if no P (proline) followed. A complete *in silico* digest was assumed, so every position matching the cleavage site definition was actually cut. This digest resulted in a list of peptide sequences each with the identifier of the protein they were derived from.

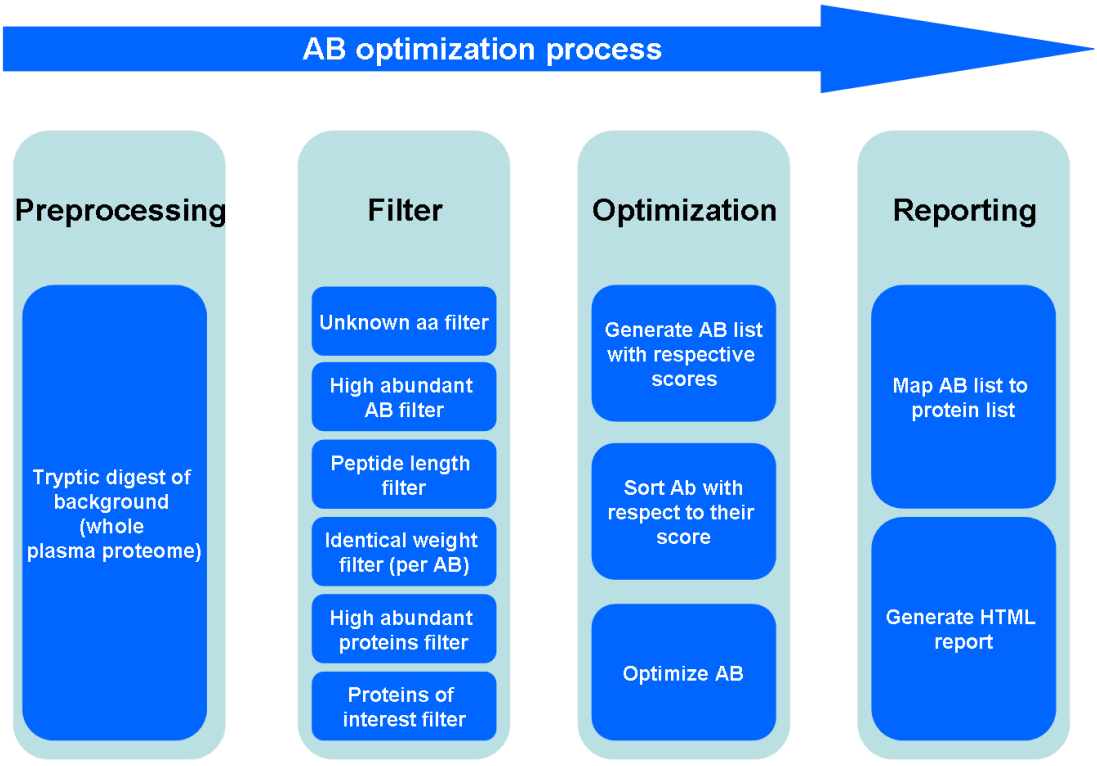

Figure 2.1.: Bioinformatical processing, after Planatscher

Given the peptide list, the filter steps aimed to remove all peptides which have some unfavorable properties for the MS measurement. Following filters were applied: (1) Unknown aa filter removes peptides with uncertain amino acids. (2) High abundant AB filter excludes termini that are present in more than 700 other peptides. (3) Peptide

length filter excludes peptides too small or too long for the MS (smaller than 500 or bigger than 5,000 Da). (4) Identical weight filter (per AB): isobaric peptide filter excludes peptides of similar mass. (5) High abundant proteins filter excludes termini that are present in high abundant proteins. (6) Proteins of interest filter.

All peptides that remained in the list after filtering could be utilized for the selection of TXP epitopes. The software generated a report with the selected TXP sequences. The procedure is described in detail in Planatscher *et al.* (2010).

TXP sequences were chosen to cover a broad range of the plasma proteins → from the most high abundant plasma protein albumin (41 mg/ml, (Polanski and Anderson, 2007)) down to very low abundant proteins with a concentration in a low pg/ml range. The selected sequences were used to generate peptide-tag specific antibodies to capture the relevant target fragments, see table 3.1.

2.3.2. Peptide conjugation onto carrier proteins

The peptides for the immunization were conjugated to the carrier protein *keyhole limpet hemocyanin* (KLH). KLH was reconstituted in sterile H_2O_{dd} to a concentration of 10 mg/ml. Sulfo-SMCC was freshly dissolved in DMSO to a concentration of 40 mg/ml, mixed with the KLH solution in a ratio of 1:10 and incubated at room temperature for 1 h on a swivel roller mixer. Excess coupling reagent, which had not reacted, was removed by size exclusion chromatography using a HiTrap desalting column on an ÄKTAxpress chromatography system. The peptides for immunization, that contained cysteine, were dissolved in PBS at a concentration of 4 mg/ml, and reduced with one equivalent TCEP to ensure the reduced thiol groups. The pre-activated KLH and the peptides were mixed 1:1 (w/w) and gently agitated on a swivel roller mixer for 3 h at RT. For storage reasons, 0.01 % sodium azide was added. The immunization of the rabbits was carried out at Pineda Antibody Service, Berlin, Germany after a standard protocol. Two rabbits were immunized using the same antigen. Prior to immunization pre-immune serum was drawn from the rabbits. To test the immune reaction of the rabbits against the used antigen, blood samples were taken after the 41th and the 60st day after immunization and analyzed by an antibody binding assay, see section 3.1.1. The rabbits were sacrificed after day 81 to obtain polyclonal serum. 0.05 % sodium azide was added to the sera and aliquoted upon receipt. The sera were stored at -20 °C to the day of antibody purification.

2.4. Microsphere-based peptide microarrays

Peptide microarrays were performed using different, distinguishable populations of color-coded carboxylated polystyrene-microspheres as solid phase. The read-out of the microsphere-

based peptide microarrays was carried out on a Luminex L100 System, which is similar to a fluorescence activated cell sorter (Luminex, Austin, TX, USA).

2.4.1. Characterization of polyclonal antisera

The characterization of the polyclonal antibodies was performed using microsphere-based peptide microarrays. To increase the capacity, the microspheres are linked with bovine serum albumin (BSA) before the peptides are coupled on the microspheres using a heterobifunctional crosslinker. The peptide loaded microspheres were incubated with antiserum and the bound antibodies were detected by a fluorescence marked detection antibody. To prevent false positive signals, spacer and peptide linker were changed. Free peptides (with TXP sequence at the C- or N-terminus) and blocked peptides (amidated C-terminus and acetylated N-terminus) were used.

2.4.1.1. Peptide conjugation onto microspheres

A two-step procedure using standard EDC/NHS chemistry was used for the covalent coupling of peptides to carboxylated fluorescent microspheres (Luminex) for the generation of microsphere-based peptide micorarrays. The first step of the coupling procedure was the linkage of BSA prior to peptide coupling to increase the capacity. The microsphere stock solution was centrifuged 2 min at 10,000 g, sonicated and vortexed for 10 s before usage. 300 μl (3.75 x 10^6) per coupling reaction of every microsphere type was transferred to a filter unit, centrifuged (at a quick spin up to 3,000 g) and washed twice with 300 μl activation buffer each. 300 μl freshly prepared activation solution (containing 50 mg/ml sulfo-NHS and 50 mg/ml EDC, dissolved in activation buffer) was added to each filter unit and incubated at RT for 20 min in the dark on a swivel roller mixer. After the incubation the microspheres were centrifuged and washed twice with coupling buffer. 500 μl BSA solution (100 μg/ml in coupling buffer) was added to the filter units and incubated at RT for 2 h in the dark on a swivel roller mixer. To remove unbound BSA, the microspheres were washed three times with 500 μl washing buffer and subsequently resuspended in washing buffer.

A microsphere count using the Luminex 100 was carried out to determine the microsphere recovery. The microsphere solution was centrifuged at 10,000 g for 1 min, sonicated for 10 s and then vortexed thoroughly. 2 μl of the microsphere solution was resuspended in 1,000 μl washing buffer and then 100 μl was transferred to each well of a 96-well plate. The microsphere count was carried out in duplicates.

The second step of the procedure was the coupling of the peptides to the BSA-microspheres. 10^6 BSA-microspheres were transferred into a filter unit. For the activation of the BSA-microspheres sulfo-SMPB was dissolved in DMSO at 15 mg/ml, and

diluted with PBS in a ratio of 1:10. After centrifugation of the filter units 100 µl activation solution was added to the microspheres and incubated for 60 min at RT in a thermomixer at 650 rpm. Unbound sulfo-SMPB was removed from the microspheres by two washing steps with PBS.

Peptides were reduced with an equivalent amount of TCEP in order to disrupt disulfide bridges and to prevent re-oxidation. 50 µl 1mM peptides and 50 µl 1 mM TCEP were mixed and incubated in a thermomixer for 20 min at RT and 250 rpm. 150 µl PBS was added to the reduced peptides. 250 µl of the reduced peptides were transferred to the activated microspheres and incubated for 60 min at RT and 650 rpm in a thermomixer. The filter units were briefly centrifuged and the microspheres were washed with 400 µl washing buffer three times. 100 µl blocking reagent (Roche) and 0.05 % sodium azide was added to the filter units. The microspheres were resuspended with 100 µl blocking reagent and 0.05 % sodium azide and transferred into a fresh microcentrifuge tube. A second microsphere counting was carried out. The microspheres were stored at 4 °C in the dark.

2.4.1.2. Antibody binding assay

Equal amounts of peptide-coupled microspheres were pooled for the multiplex serum characterization of the purified antibodies. GSG-tag as well as blocked GSG-tag peptides were used for characterization. The 96-well filter plates were pre-blocked with 100 µl blocking buffer for 15 min. The blocking buffer and all the following solutions were removed by vacuum filtration. 30 µl of the microsphere mix was transferred into 96-well filter plates (500 microspheres of each microsphere type per well), mixed with 30 µl diluted rabbit serum (1:10,000 and 1:20,000) and incubated for 1 h at RT in a thermomixer at 650 rpm. PBS was used as negative control. The microspheres were subsequently washed twice with 100 µl washing buffer. 30 µl of phycoerythrin labeled anti-species specific detection antibody (2.5 µg/mL) was added and incubated for 45 min at RT and 650 rpm. To remove residual detection antibody the microspheres were washed twice with washing buffer. The microspheres were resuspended in 100 µl blocking buffer and the microsphere type-specific fluorescence was determined with a Luminex 100 IS system. Median fluorescence intensity (MFI) was calculated by at least 100 microspheres per population.

2.5. Microsphere-based immunoassays

To quantify the amount of peptide, antibody and peptide-antibody-complex in controls or fractions obtained from ultracentrifugation (see section 2.8.1), a model system with biotinylated hemagglutinin (HA) peptide (Biotin-Doa-Doa-YPYDVPDYA-NH_2)

and the corresponding monoclonal rat anti-HA antibody (Clone 3F10) was established using microsphere-based immunoassays (Luminex).

2.5.1. Protein conjugation onto microspheres

A standard EDC/NHS chemistry procedure was used for the covalent coupling of donkey anti-rat antibodies or streptavidin to carboxylated fluorescent microspheres (Luminex). The microsphere stock solution was centrifuged 2 min at 10,000 g, sonicated and vortexed for 10 s before usage. 300 μl (1.25 x 10^7) per coupling reaction of every microsphere type is transferred to a filter unit, centrifuged (at a quick spin up to 3,000 g) and washed twice with 300 μl activation buffer each. 150 μl freshly prepared activation solution (containing 50 mg/ml sulfo-NHS and 50 mg/ml EDC, dissolved in activation buffer) was added to each filter unit and incubated at RT for 20 min in the dark on a swivel roller mixer. After the incubation the microspheres were centrifuged and washed twice with coupling buffer. 250 μl protein solution (20 μg protein) was added to the filter units and incubated at RT for 2 h in the dark on a swivel roller mixer. To remove protein excess, the microspheres were washed three times with 400 μl washing buffer and subsequently resuspended 100 μl of blocking reagent and 0.05 % sodium azide. The microsphere suspension was transferred to a fresh microcentrifuge tube and stored for further use at 4 °C. The recovery of the protein-coated microspheres was determined as described in section 2.4.1.1.

2.5.2. Sandwich immunoassay for the determination of rat IgG

The HA-peptide and HA-antibody were incubated in trypsin-digested human blood plasma matrix for 1 h at room temperature on a swivel roller mixer. After the incubation the sample was pipetted onto the pre-prepared sucrose gradient, and the ultracentrifugation was started. Following ultracentrifugation, the samples were fractionated into 50 μl fractions. For the microsphere-based immunoassays the samples were transferred into 96-well filter plates (Millipore). For each well of an assay, 30 μl containing 1,000 microspheres and 30 μl sample (both diluted in blocking reagent, supplemented with 0.05 % Tween 20), were mixed in a 96-well filter plate. The detection of free antibodies and peptide-antibody complexes was performed by the incubation of the samples with donkey anti-rat antibody-coupled microspheres for 1 h at 650 rpm at RT. After washing the microspheres were incubated with 30 μ of PE-labelled anti-rat detection antibody (2.5 μg/ml) for 45 min.

Following the last incubation and washing steps, 100 μl Roche blocking reagent/0.05 % Tween 20 was added and the microsphere type specific fluorescence was determined with a Luminex 100 IS system.

2.5.3. Immunoassay for the determination of the biotinylated HA-peptide and peptide-antibody complex

The HA-peptide and HA-antibody were incubated in trypsin-digested human blood plasma matrix for 1 h at room temperature on a swivel roller mixer. After the incubation the sample was pipetted onto the pre-prepared sucrose gradient, and the ultracentrifugation was started. Following ultracentrifugation the samples were fractionated into 50 μl fractions. For the microsphere-based immunoassays the samples were transferred into 96-well filter plates (Millipore).

For each well of an assay, 30 μl containing 1,000 microspheres and 30 μl sample (both diluted in blocking reagent supplemented with 0.05 % Tween 20), were mixed in a 96-well filter plate. The detection of free peptides was performed by incubation of the samples with streptavidin-coated microspheres for 1 h at 650 rpm at RT. After washing, the microspheres were incubated for another 1 h with 30 μl rat anti-HA antibody (1 μg/ml). After washing, the microspheres were incubated with 30 μl PE-labelled anti-rat detection antibody (2.5 μg/ml) for 45 min. Following the last incubation and washing steps, 100 μl Roche blocking reagent/0.05 % Tween 20 was added and the microsphere type specific fluorescence was determined with a Luminex 100 IS system.

The detection of peptide-antibody complexes was performed by incubation of the samples with donkey anti-rat antibody-coupled microspheres for 1 h at 650 rpm at RT. After washing with 100 μl PBS/0.05 % Tween 20, the microspheres were incubated with 30 μl sample streptavidin-PE conjugate (2.5 μg/ml) for 45 min. Following the last incubation and washing steps, 100 μl Roche blocking reagent/0.05 % Tween 20 was added and the microsphere type specific fluorescence was determined with a Luminex 100 IS system.

2.6. Antibody purification

The generated polyclonal antibodies were purified using peptide affinity based chromatography. Pre-activated sepharose columns were used as solid phase matrix, on which BSA and peptides were covalently immobilized. By the use of the prepared peptide columns the specific antibodies were extracted from rabbit serum, acidic eluted and fractionated.

2.6.1. Preparation of peptide columns

Commercially available pre-activated sepharose columns, packed with N-hydroxysuccinimide activated sepharose were used as starting material and purged with activation buffer. BSA was dissolved in PBS as a 20 % solution and coupled over the

amino-reactive group onto the matrix material. The remaining amine-reactive groups were blocked by purging the columns alternately with deactivation buffer I and II. Sulfosuccinimidyl 4-(p-maleimidophenyl)butyrate (sulfo-SMPB) was used for the activation of BSA. 1 mg of each peptide was dissolved in PBS. The peptides were reduced with freshly prepared TCEP-solution in a half-equimolar concentration. The reduced peptides, containing a cysteine for immobilization, a GSG-tag as a spacer and the targeted epitope sequence were added and incubated over night at 4 °C. The columns were washed to remove unbound peptides and the free maleimide groups were blocked with 1 mM cysteine solution. The columns were washed again, to remove excess cysteine. The columns were filled with 1 ml PBS + 0.01 % sodium azide and stored at 4 °C. To prevent false positive signals, spacer and peptide linker were changed.

2.6.2. Affinity and gel filtration chromatography

Polyclonal antibodies were immunopurified using an FPLC chromatography system (ÄKTAxpress, GE Healthcare). About 15 ml rabbit serum was thawed and filtered with a syringe filter (pore size 0.22 μm) before purification. The corresponding peptide column and a gel filtration column (5 ml desalting column, GE Healthcare) were inserted in the FPLC system. The columns were purged (5 column volumes) and equilibrated before the rabbit serum was applied on the affinity column with a flow rate of 0.5 ml/min. Unbound serum components were removed by column purging after the serum application (5 column volumes). The bound TXP antibodies were eluted using Elution buffer for Antibody Purification (0.1 M citrate, pH 2.5). Acidic buffer was replaced by PBS by subsequent gel filtration (three gel filtration columns (5 ml each) were used in series). The protein content was determined photometrically. The fractions with the highest concentration were combined and 0.05 % sodium azide was added. The antibodies were stored at 4 °C.

2.7. Plasma sample preparation methods

2.7.1. Blood collection

Blood from healthy male and female donors (voluntary colleagues) was collected by venous puncture using a 21-gauge Safety Multifly 0.8 mm / 19 mm needle (Sarstedt). A total of 30 ml blood per donor was collected into 4 x 7.5 ml Plasma Lithium-Heparin S-Monovette® tubes (Sarstedt). After inverting the tubes to mix blood and heparin, samples were centrifuged at room temperature for 10 min at 4,000 rpm using a Rotanta/RP5094 rotor to pellet the cells. Plasma supernatant was collected immediately after centrifugation, transferred into 1.5 ml Eppendorf tubes in 60 μl tube aliquots and stored at -80 °C.

2.7.2. Depletion of high abundant proteins

Albumin and IgGs from plasma were removed by using the ProteoExtract Albumin/IgG Removal Kit from Calbiochem. 35 μl plasma was used per depletion column as recommended by the manufacturer. The plasma was diluted 10-fold with the ProteoExtract Albumin/IgG Binding buffer. The blue cap from a ProteoExtract column was removed and the column was inverted on a paper towel to remove the column storage buffer. The lower tip of the column was removed and an Eppendorf tube was placed under the column. 850 μl ProteoExtract Binding Buffer was added to the column and passing allowed by gravity-flow. The collection tube was discarded and replaced by a fresh sample collection tube before the diluted sample was added. The sample was allowed to pass through the resin bed by gravity-flow. The flow-through was collected in the sample collection tube. The column was washed by adding 600 μl of ProteoExtract Binding buffer. The washing step was repeated and the wash fractions were collected in the sample collection tube. The diluted plasma sample was subsequently digested.

2.7.3. Digest

Tryptic plasma digests were prepared by diluting 60 μl of whole plasma with 540 μl of 50 mM triethanolamine pH 8.5. Thereafter, 30 μl of 10 % NOG solution and 3 μl of the reducing agent TCEP (5 mM) were added. The samples were denatured for 5 min at 100 °C. After cooling down to room temperature, the samples were alkylated for 30 min at room temperature in the dark with 10 mM iodoacetamide final concentration. 100 μg of modified Trypsin Gold, Mass spectrometry grade (Promega, Madison, WI, USA) was resuspended in 100 μl 50 mM acetic acid. 98 μl of the resuspended trypsin was added to the alkylated plasma samples (40:1 substrate:enzyme ratio). Digestion was carried out for 16 h at 37 °C and 650 rpm in a Thermomixer (Eppendorf, Hamburg, Germany). Trypsin activity was stopped by heating the sample to 100 °C for 5 min and by adding 6.6 μl of 200 mM PMSF. The digested samples were spun at 13,000 x g for 10 min. The supernatant was partially directly used in volumes of 50 μl (about 5 μl original plasma amount) or 200 μl aliquots of the supernatant were lyophilized and reconstituted in 50 μl deionized water when needed.

2.7.4. Desalting and concentration

For the desalting and concentrating of peptides, C18 ZipTips (Millipore) were used. The sample was acidified with TFA to a total concentration of 0.1 %. ZipTip pipette tips were equilibrated using the maximum volume setting of 10 μl of a 10 μl pipette by aspirating and dispensing wetting solution (100 % ACN) followed by equilibrating solution (0.1 % TFA) through the tip. The peptides were bound to the ZipTip pipette tip by aspirating and dispensing the sample 10 cycles for maximum binding. After

washing the bound peptides using the washing solution (0.1 % TFA, 5 % methanol) four times the peptides were eluted with 5 µl 80 % ACN containing 0.1 % TFA. 0.25 µl of the eluates were spotted onto a prespotted anchor chip (Bruker).

2.8. Immunoaffinity enrichment using TXP antibodies

The generated polyclonal TXP antibodies were used to enrich peptides out of a complex mixture (synthetic peptide mix or plasma digest). Protein G-coated magnetic microspheres captured the peptide-antibody complex and the peptides were eluted in an acidic buffer. To enable automatic handling, magnetic microspheres from Invitrogen were used. These microspheres are coated with Protein G, an immunoglobulin-binding protein expressed in *Streptococcus*. Protein G binds to the FC region of the antibodies and is therefore applicable to antibody purification.

An automated immunoaffinity assay was established to allow automatic handling (KingFisher, ThermoFisher Scientific) using magnetic microspheres coated with Protein G. PCR plates for the TXP immunoprecipitation were prepared before the assay was started in the KingFisher System. 8 PCR plates were used for the whole procedure:

1. sample plate (containing sample plus TXP antibodies $\mapsto$ 100 µl)
2. microsphere plate (containing magnetic microspheres in PBSN $\mapsto$ 100 µl)
3. washing plate 1 (containing PBSN $\mapsto$ 100 µl)
4. washing plate 2 (containing PBSN $\mapsto$ 100 µl)
5. washing plate 3 (containing ABCN $\mapsto$ 100 µl)
6. washing plate 4 (containing ABCN $\mapsto$ 100 µl)
7. washing plate 5 (containing ABCN $\mapsto$ 100 µl)
8. elution plate (containing elution buffer $\mapsto$ 20 µl)

The sample was incubated with the TXP-antibody for 1 h at RT in the sample plate. The sample was mixed every 10 min for 2 min. 5 µl magnetic Protein G microspheres per µg antibody were added (transferred from microsphere plate) and incubated again for 1 h at RT (with the same mixing intervals as described above). After the capture of the peptide-antibody complex with the magnetic microspheres, the microspheres were transferred to washing plate 1 where they were washed for 2 min. The washing with PBSN was supposed to remove non-captured analytes from the microsphere complex. The microspheres were transferred to washing plate 2, where the washing step with PBSN was repeated. After the washing steps in PBSN, the washing buffer was changed to ABCN in washing plate 3 to 5 to desalt the samples for the MS read-out. The washing

procedure was carried out as described before. After the 5th and last washing step in ABCN, the microspheres were transferred to the elution plate, containing 20 µl 1% formic acid as elution buffer for the MALDI read-out. For the MRM read-out, 0.1 % NOG was added to the elution buffer to avoid that the peptides are adsorbed on any vial surfaces during transfer. The peptides were eluted from the antibodies and the microspheres in 2 min constant shaking. After elution procedure the microspheres were finally back-transferred to the microsphere plate.

2.8.1. In solution peptide/IgG complex separation by ultracentrifugation

50 µl plasma digest samples were incubated for 1 h at room temperature with 5 or 10 µg of the respective antibodies. The incubated samples were either directly processed by Protein G magnetic microsphere enrichment (see below) or processed as follows. A three-step sucrose density gradient was prepared manually by carefully pipetting the density layers into a 1.5 ml centrifugation tube (Beckman Coulter). The sucrose density gradient was prepared as follows: bottom: 350 µl 30 % sucrose/PBS, middle: 350 µl 20 % sucrose/PBS, top: 450 µl 10 % sucrose/PBS. The sample was carefully loaded on top of the sucrose gradient and the sample tubes were placed in a TL-100 ultracentrifuge (Beckman Coulter) with the fixed angle rotor TLA-55. As a visual separation control a Cy3 antibody was mixed with the digested plasma sample. The centrifugation was carried out at 4 °C and 55,000 rpm (135,000 x g average rcf) for 15 h. After centrifugation, the tubes were punctured at the bottom with a 20-gauge needle and fractions with defined volumes were taken using a pipette. Depending on the experiment, the samples were either fractionated into 50 µl fractions or were fractionated (bottom → top) into 500 µl, 400 µl and 300 µl fractions. The fractions were further processed by TXP immunoprecipitation (see below).

Per sample 20 µl plasma was digested, lyophilized and subsequently reconstituted in 50 µl deionized water. 5 µg TXP antibody was added and either a normal TXP immunoprecipitation was performed or a TXP immunoprecipitation with inserted ultracentrifugation. The experiments were carried out in triplicates, so that for one TXP antibody six samples were measured (three for normal TXP immunoprecipitation, three for the TXP immunoprecipitation combined with UC step).

2.9. Mass spectrometry read-out

2.9.1. MALDI MS

To prevent the microspheres from being spotted on the PAC target, the elution plate (see section 2.8) was placed on a plate magnet (DynaMag™, Invitrogen). 1 µl of the

elution of the TXP immunoprecipitation was spotted at least in triplicates on a pre-spotted anchor chip. After the spots were completely dry the entire PAC target was immersed in MS washing buffer for a few seconds to reduce sodium adduct formation.

MS and MSMS spectra were obtained using the Ultraflex III MALDI TOF/TOF mass spectrometer (Bruker Daltonik) with the FlexControl 3.0 software package. The experiments were carried out in positive ion reflectron mode with a deflector cut-off up to 550 Da. All spectra were analyzed using the flexAnalysis 3.0 software (Bruker Daltonik). The spectrometer was calibrated using prespotted calibrants on the PAC targets. The spectra were recorded with 1,000 shots and the masses were automatically annotated with the flexAnalysis peptide mass fingerprint (PMF) method, which resulted in a peak list in a mass range of between 700 and 5,000 Da. Only peaks with S/N greater than 10 were chosen for MSMS analysis. The selected peaks were fragmented using the LIFT technology to identify the peptides. The laser power and number of shots (2,000 - 4,000) were adjusted by the operator. Monoisotopic masses of annotated peaks were compared to IPI database entries (version 3.68) using the Biotools 3.1 software (Bruker Daltonik) and the MASCOT 2.2 search engine (Matrix Science, London, UK). MASCOT searches were restricted to trypsin or semi-trypsin digestion with one partial cleavage. Carbamidomethylation of cysteine was set as a fixed modification. No variable modifications were taken into account. Mass tolerances were set to 50 ppm for precursor ions and 0.7 Da for fragment ions. Only peptides which were identified by Mascot ion scores that indicated identity or extensive homology with $p < 0.05$ were regarded as valid.

2.9.2. MRM

An Agilent 1260 Infinity HPLC-Chip/MS system, equipped with an 1260 Infinity Capillary and Nanoflow Pump, High Performance Micro Autosampler with Thermostat, Chip Cube MS interface, and an 6400 Series QQQ Mass Spectrometer, was used for nanoLC MRM analysis. For the separation of the peptides a HPLC Chip (Large Capacity Chip (II)) was used instead of a regular HPLC column. MRM data was acquired with Mass Hunter Workstation Acquisition Software and analyzed using Skyline/MacCoss Lab Software.

10 μl of the eluted peptides were transferred from the elution plate into autosampler vials, adequate for following nanoLC analysis with MRM read-out. Table 2.3 shows the chromatographic conditions.

Table 2.3.: Chromatographic conditions

Chromatographic conditions		
Solvent A		H_2O_{dd} with 0.1 % FA
Solvent B		100 % ACN with 0.1 % FA
Injection volume		10 μl
Cap Flow rate		4 μl per min
Nano Flow rate		600 nl per min
Gradient	0 min	5 % B
	7 min	50 % B
	9 min	80 % B
	9.5 min	80 % B
	10 min	5 % B
	15 min	5 % B

Optimum transitions and parameters for collision energy (CE) and fragmentor potential were determined by infusion of a solution of 1 pmol/μl. A minimum of three transitions were selected for monitoring. Typical MS instrument settings included a spray voltage of 1,900 nA and a dwell time of 50 ms for each transition. MRM-transitions and parameters of the targeted peptides are summarized in table 2.4.

Table 2.4.: MRM peptide transitions

Protein name	MW [Da]	Amino acid sequence		Parent ion	Fragment ion	CE	Fragmentor
erbB-2	1333.61	VCYGLGMEHLR	normal	445.6	456.7	8	150
				445.6	538.3	4	150
				445.6	618.3	4	150
				445.6	742.4	12	150
				445.6	912.5	12	150
			SIS	448.9	461.7	8	150
				448.9	543.3	4	150
				448.9	623.3	4	150
				448.9	752.4	12	150
				448.9	922.5	12	150
Complement C3	1125.66	VLLDGVQNLR	normal	563.8	457.8	8	150
				563.8	530.3	20	150
				563.8	686.4	16	150
				563.8	801.4	16	150
				563.8	914.5	16	150
			SIS	568.8	462.8	8	150
				568.8	540.3	20	150
				568.8	696.4	16	150
				568.8	811.4	16	150
				568.8	924.5	16	150
Apolipoprotein B-100	1590.87	VLLDQLGTTISFER	normal	796.4	538.3	16	120
				796.4	752.4	40	120
				796.4	910.5	12	120
				796.4	1,023.6	28	120
				796.4	1,266.6	24	120
			SIS	801.4	548.3	16	120
				801.4	762.4	40	120
				801.4	920.5	12	120
				801.4	1,033.6	28	120
				801.4	1,276.6	24	120
Clusterin	1872.99	LFDSDPITVTVPVEVSR	normal	625.3	490.3	28	90
				625.3	686.4	20	90
				625.3	785.5	16	90
				625.3	886.5	16	90
			SIS	628.7	500.3	28	90
				628.7	696.4	20	90
				628.7	795.5	16	90
				628.7	896.5	16	90
Plasminogen	2495.32	VILGAHQEVNLEPHVQEIEVSR	normal	624.8	490.3	20	150
				624.8	548.8	24	150
				624.8	597.3	12	150
				624.8	661.8	12	150
				624.8	860.5	20	150
			SIS	627.3	500.3	20	150
				627.3	553.8	24	150
				627.3	602.3	12	150
				627.3	666.8	12	150
				627.3	870.5	20	150

2.9.3. Quantification

Stable isotope standards (SIS) were used for the absolute quantification of endogenous peptides. A defined amount of SIS was spiked in the sample before further processing by TXP immunoprecipitation. Exact amounts of the peptides were determined by amino acid analysis (Medical Proteome Centre, Bochum). Dilution series of synthetic tryptic peptides were prepared in 1 % FA without TXP immunoprecipitation and in PBSN and plasma digest with subsequent TXP immunoprecipitation. The ratio of the areas under the curve from peptide to SIS were calculated for quantification. The recovery was determined by setting the initial peptide amount to 100 % and calculating the captured peptide amount in relation to 100 %.

Chapter 3.

Results

3.1. Antibody generation and characterization

Antibodies directed against short peptide sequences (*Triple X*-, TXP-antibodies) were generated by the immunization of rabbits. Two rabbits were immunized per peptide sequence.

The peptides were synthesized containing the TXP sequences → four to five terminal amino acids. The first three to four amino acids are specific for the particular terminus of the selected peptide (*Triple X*), the fourth or fifth amino acid (regarding C-terminus target peptides) is defined by the cleaving site of the used endopeptidase. As trypsin was used in the assays, the fourth, respectively, fifth amino acid is either arginine or lysine. The short peptide sequences contained a cysteine on the N-terminus to couple the peptides onto a carrier protein and a GSG-tag was used as spacer molecules.

The selected peptides are small molecules with a simple structure. Hence the peptides have only low antigenicity to trigger an immune response. For the immunization, the peptides were coupled to a high molecular weight carrier protein to promote the T-helper cell epitope to enhance the immune response. The used carrier protein was *keyhole limpet hemocyanin* (KLH), an extremely large protein found in the hemolymph of the giant keyhole limpet *Megathura crenulata*. This protein has a high antigenicity due to its size and heterogeneous structure, especially of its glycan pattern. Additionally, its phylogenetical distance from mammalian proteins reduces the occurence of false positives in immunoassays of mammalian model organisms. The heterobifunctional coupling reagent sulfo-MBS was covalently coupled by an active ester on the amino group of the carrier protein. The maleimide group of sulfo-MBS reacted with the N-terminal thiol group of the cysteines of the peptide sequences, which led to an accurately defined assembly of the peptide sequences on the carrier protein.

The rabbit immunizations were performed in two series. The targeted epitopes are displayed in Table 3.1.

Table 3.1.: The rabbit immunization was performed in two series. The first set contained only C-terminal peptide sequences, covering peptides derived from proteins in the low and medium abundant range. The second set contained a mixture of N- and C-terminal short peptide sequences, covering peptides derived from proteins in the high abundant range.

Set of antibodies	Terminus	*Triple X* amino acid sequence
Set 1 - low/medium abundant	C-terminal	DAPK
		DTWK
		DYGK
		EGYR
		EHLR
		ESFR
		EVLR
		FPPK
		LDYK
		LEVK
		PIEK
		QGYR
		TPER
		YSAR
Set 2 - high abundant	N-terminal	EQLG
		EVGT
		SLGNV
		TLNQ
		VELED
		VLLD
	C-terminal	AFVK
		VEVSR
		VNASR

The first set of rabbit immunizations targeted only C-terminal peptide termini regarding trypsin cleavage sites. In addition, the second set targeted both C- and N-terminal peptide termini.

The rabbit sera were characterized by microsphere-based arrays for immunization monitoring (antibody binding assays) with regard to binding properties or cross-reactivity. After the establishment of an automated immunoprecipitation step with subsequent MS analysis, the immuno-purified antibodies were further characterized by peptide capture assays using synthetic peptides.

3.1.1. Antibody binding assay for immunization monitoring

Microsphere-based arrays are a highly flexible platform for the simultaneous measurement of up to 500 analytes. As such, this system is perfectly suited to test the different rabbit sera for specific peptide binding. One point of interest was the functionality of the serum antibodies, with regards to binding properties or cross-reactivity with other peptides containing a different TXP-sequence. Another focus was whether the antibodies bind both free as well as blocked termini (mimicking peptides with an internal TXP-sequence). To monitor immunization, sera were characterized after day 41 and 60 using microsphere-based peptide microarrays, so-called antibody binding assays. A combination of S/N values over 100 and little to no cross-reactivity are required for the immunizations to be successful.

The results of two immunizations (one successful, one non-successful) are shown here. Figure 3.1 shows the results of the multiplex array with the serum sample for anti-VEVSR.

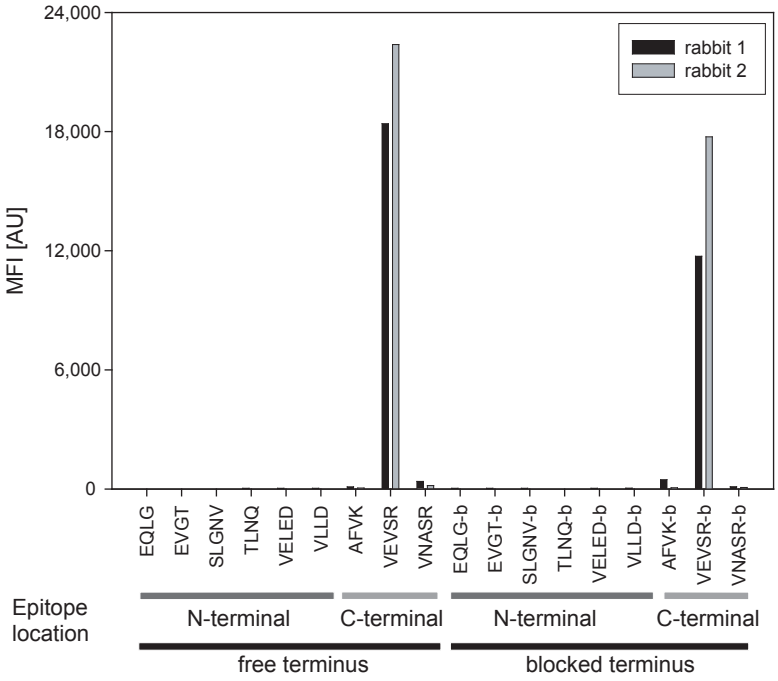

Figure 3.1.: Anti VEVSR antibody binding assay - rabbit sera (2 replicates), immunized against VEVSR peptide (41th day of immunization), were tested for binding activity against a range of free and blocked N- and C-terminal peptides. Serum dilution: 1:10,000.

A very high signal for both serum replicates was observed, following VEVSR immunization. Virtually no cross-reactivity with other short TXP peptide sequences was observed. The anti-VEVSR sera gave also strong signals with the blocked peptides, suggesting that peptides with internal VEVSR sequences will also be recognized by the generated antibodies.

Figure 3.2 shows the reactivity of the anti-VEVSR serum 19 days later, drawn on day 60. The intensities were still high, the signals for the free and the blocked peptides were almost equal. After the rabbits had been sacrificed on day 81 the sera were again tested for specific peptide binding, see figure 3.3.

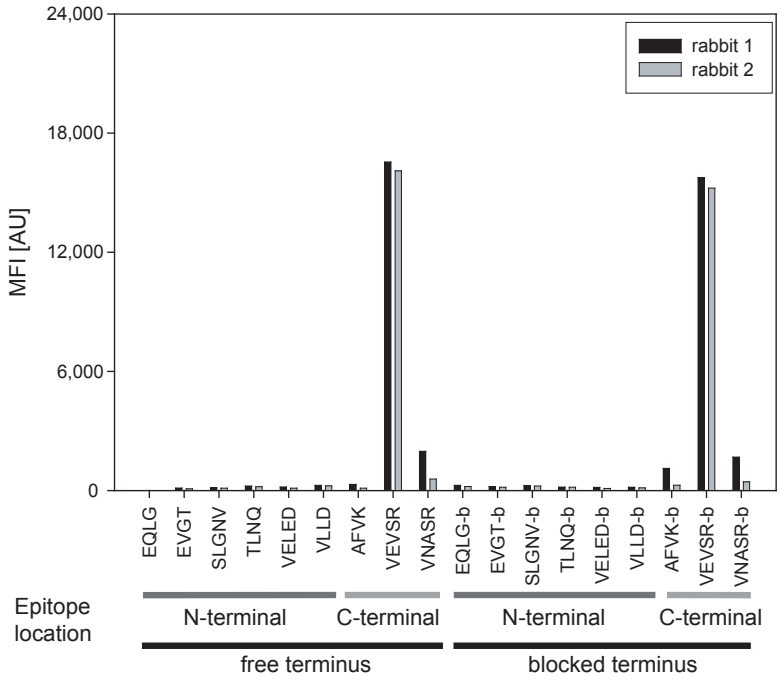

Figure 3.2.: Anti VEVSR antibody binding assay - rabbit sera (2 replicates), immunized against VEVSR peptide (60th day of immunization), were tested for binding activity against a range of free and blocked N- and C-terminal peptides. Serum dilution: 1:10,000.

The signal corresponding to anti-VEVSR decreased slightly from around 18,000 MFI after day 41 to 15,000 MFI after day 81 for the peptides with the free termini. The signal for the blocked peptides however decreased from 12,000 (rabbit 1) and 18,000 (rabbit 2) to less than 5,000 MFI. The cross-reactivity remained negligible.

The antibody binding assay results of the antisera against the N-terminal epitope TLNQ are displayed in figure 3.4. Although the intensities for the capture of the free peptides were high (rabbit 1) the cross-reactivity to the other peptides was substantial. The results for all immunizations are summarized in table 3.2 and 3.3 with normalized signal to noise ratios (S/N). The MFI values of the analyzed sera were normalized to the blank assays.

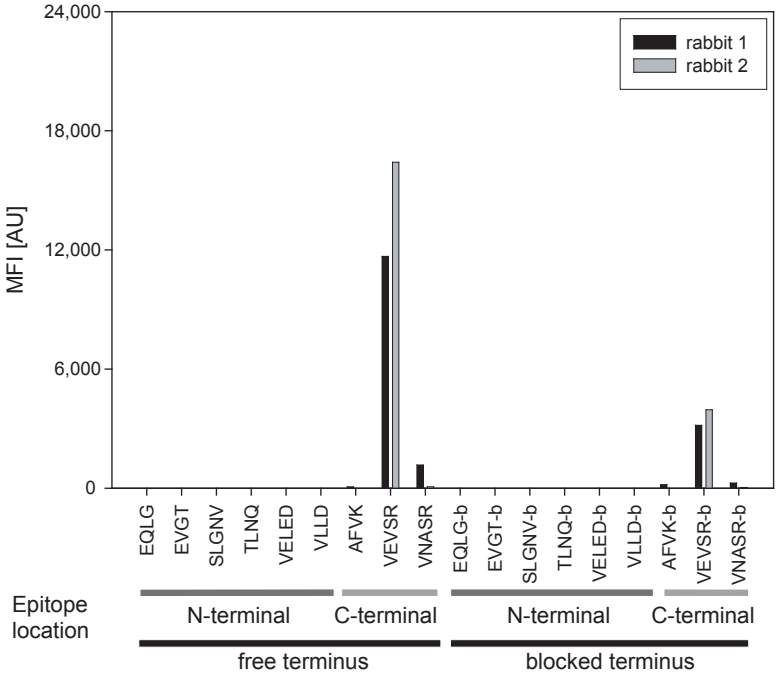

Figure 3.3.: Anti VEVSR antibody binding assay - rabbit sera (2 replicates), immunized against VEVSR peptide (81th day of immunization), were tested for binding activity against a range of free and blocked N- and C-terminal peptides. Serum dilution: 1:20,000.

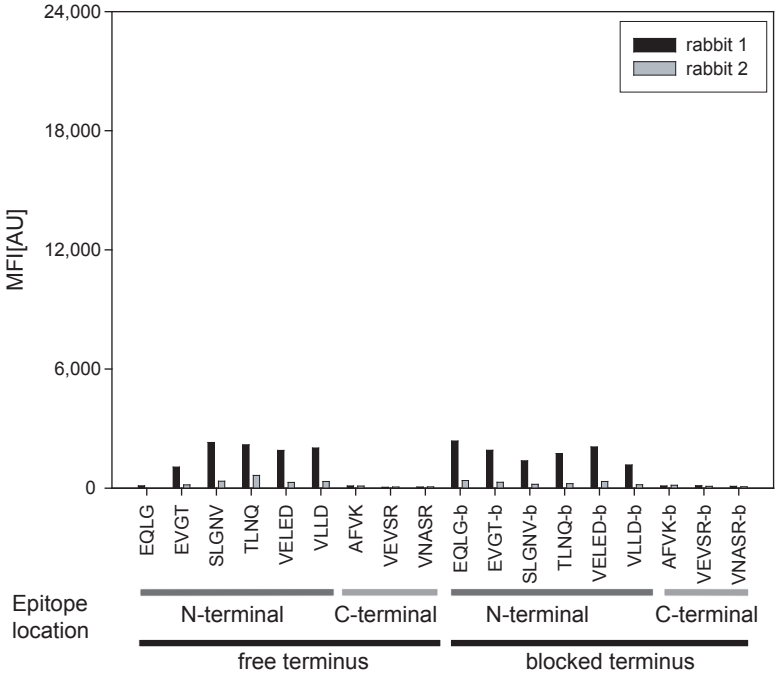

Figure 3.4.: Anti TLNQ antibody binding assay - rabbit sera (2 replicates), immunized against TLNQ peptide (81th day of immunization), were tested for binding activity against a range of free and blocked N- and C-terminal peptides. Serum dilution: 1:20,000.

Table 3.2.: Evaluation of rabbit sera by antibody binding assays - set 1.

TXP tag	Terminus	S/N Free peptides	S/N Blocked peptides	Comment	Succeeded	Antibody purification
DAPK rabbit 1	C	2,518	2,313		yes	yes
DAPK rabbit 2	C	2,727	2,305		yes	yes
DTWK rabbit 1	C	808	345		yes	yes
DTWK rabbit 2	C	1,143	519		yes	yes
DYGK rabbit 1	C	1,501	107		yes	yes
DYGK rabbit 2	C	1,761	79		yes	yes
EGYR rabbit 1	C	238	129		yes	yes
EGYR rabbit 2	C	245	41		yes	yes
EHLR rabbit 1	C	1,405	720		yes	yes
EHLR rabbit 2	C	1,144	484		yes	yes
ESFR rabbit 1	C	1,093	700		yes	yes
ESFR rabbit 2	C	1,283	949		yes	yes
EVLR rabbit 1	C	1,999	538		yes	yes
EVLR rabbit 2	C	2,291	559		yes	yes
FPPK rabbit 1	C	1,667	227		yes	yes
FPPK rabbit 2	C	2,310	1,581		yes	yes
LDYK rabbit 1	C	597	26		yes	yes
LDYK rabbit 2	C	791	39		yes	yes
LEVK rabbit 1	C	1,070	202		yes	yes
LEVK rabbit 2	C	670	116		yes	yes
PIEK rabbit 1	C	1,262	194		yes	yes
PIEK rabbit 2	C	1,159	87		yes	yes
QGYR rabbit 1	C	1,659	150		yes	yes
QGYR rabbit 2	C	1,105	19		yes	yes
TPER rabbit 1	C	412	63		yes	yes
TPER rabbit 2	C	1,022	156		yes	yes
YSAR rabbit 1	C	312	11		yes	yes
YSAR rabbit 2	C	755	6		yes	yes

Table 3.3.: Evaluation of the rabbit sera by antibody binding assays - set 2.

TXP tag	Terminus	S/N Free peptides	S/N Blocked peptides	Comment	Succeeded	Antibody purification
EQLG rabbit 1	N	367	1,893	no specific reaction	failed	no
EQLG rabbit 2	N	59	777	no specific reaction	failed	no
EVGT rabbit 1	N	489	1,088	no specific reaction	failed	no
EVGT rabbit 2	N	258	703	no specific reaction	failed	no
SLGNV rabbit 1	N	2,838	940	no specific reaction	failed	no
SLGNV rabbit 2	N	2,686	448	no specific reaction	failed	no
TLNQ rabbit 1	N	1,344	874	no specific reaction	failed	no
TLNQ rabbit 2	N	395	113	no specific reaction	failed	no
VELED rabbit 1	N	2,888	992	cross-reactivity	+-	yes
VELED rabbit 2	N	4,391	1,591	cross-reactivity	+-	yes
VLLD rabbit 1	N	5,062	1,294	cross-reactivity	+-	yes
VLLD rabbit 2	N	4,486	605	cross-reactivity	+-	yes
AFVK rabbit 1	C	animal died				
AFVK rabbit 2	C	7,982	1,286		yes	yes
VEVSR rabbit 1	C	9,340	1,582		yes	yes
VEVSR rabbit 2	C	13,135	1,977		yes	yes
VNASR rabbit 1	C	9,891	4,202		yes	yes
VNASR rabbit 2	C	6,572	4,432		yes	yes

All tested antibodies of the first set showed good binding properties to peptide antigens carrying free termini (TXP sequence). Some of the antisera showed a strong binding to the blocked peptides. The resulting antibodies were expected to capture not only peptides with a terminal TXP sequence, but also peptides containing an internal TXP sequence. Altogether, all antisera showed the required combination of S/N values over 100 and little to no cross-reactivity. Hence the whole of set 1 was immuno-purified.

The results of set 2 were not as consistent as for set 1. The antisera generated against C-terminal peptides showed good antigen (TXP sequence) binding to the free peptides. Five of them also revealed strong binding to the blocked peptides. For the most part, the antisera generated against N-terminal peptides showed insufficient to no functionality. The required selection criteria for immuno-purification were not achieved. Eight of them were abandoned. However, the anti-VELED and anti-VLLD sera were purified, because the cross-reactivity was lower than in the residual antisera generated against N-terminal TXP sequences. The graphs of all antibody binding assays are found in the supplementals, see figure A.1 to A.21.

Based on these results a total of 39 rabbit antisera were immunopurified.

3.1.2. Establishment of an automated immunoprecipitation step using magnetic microspheres

The purified antibodies were tested in a peptide capture assay with subsequent MALDI MS read-out. Automated immunoaffinity enrichment assays were established using magnetic protein G microspheres (Dynabeads, Invitrogen) in a magnetic microspheres handler (KingFisher System, ThermoFisher Scientific). After incubation of the TXP-antibodies with a complex peptide mixture, magnetic protein G microspheres were used to capture the peptide-antibody complexes out of the complex mixture. The magnetic microspheres and the complex were washed by being transferred from microtiterplate to microtiterplate filled with washing solution. This microsphere transfer reduced sample carryover to a minimum.

After incubation of the samples with the antibodies and the magnetic protein G microspheres, five washing steps were added. The first two washing steps were conducted in PBS. PBS, with a pH of 7.4 and physiological salt content compared to blood plasma, was used to remove non-specific bound molecules in a physiological environment. The last three washing steps were conducted with ammonium bicarbonate (ABC) buffer, adjusted to pH 7.4, to desalt the captured peptides, before they were eluted in 1% formic acid. High concentrations of salts can affect or even prohibit the co-crystallization of analyte and matrix, which leads to decreased sensitivity (Lottspeich *et al.*, 2006). Matrix cluster formation causes peaks in the range below 1,200 m/z, which may interfere with targeted peptides in that range. Hence, it was necessary to remove alkali salts

originating from the digested plasma and the PBS. ABC was chosen due to its properties as "MS-friendly" buffer with no high amounts of salts, that can be disturbing in subsequent MS analysis. The three desalting steps using ABS buffer were sufficient to remove most of the alkali salts in the precipitated peptides, which was proved with MS analysis (data not shown).

The magnetic field strength of the KingFisher System is too small to overcome the surface tension of the aqueous solutions used. Therefore, it was necessary to employ a surfactant in the aqueous solutions to avoid loss of microspheres between the individual plate changes. Low levels of a non-ionic detergent, e.g. n-Octyl-ß-D-glucopyranosid (NOG), up to 1 %, emerged to be tolerable in MALDI MS analysis, as already reported by Zhang and Li (2004). However, analysis showed that even a small amount of 0.1 % NOG in the elution buffer decreased the intensity of the peptide peaks (data not shown). For that reason, NOG was omitted in the elution buffer of the TXP immunoprecipitations. To prevent the microspheres from being spotted on the MALDI targets, the elution plate was placed on a plate magnet while pipetting the elutions on the PAC targets.

3.1.3. Peptide capture assay

The applicability of the purified TXP antibodies to an immunoprecipitation method was demonstrated in the following. The question was answered if the TXP antibodies are able to capture their target peptide without cross-reactivity to other peptides, containing different terminal epitopes? In addition, their ability to capture more than one peptide target was evaluated, based on the theoretical presumption, that those antibodies should be capable of capturing both standard peptides (given that two standard peptides containing the same TXP terminus were present within the same sample).

Different synthetic peptides were generated containing triple X epitopes. The synthetic peptides were selected according to their plasma concentration. The range of the selected peptides spans from high abundant proteins like albumin with 41 mg/ml plasma concentration down to low abundant proteins like the tumor necrosis factor receptor superfamily member 11B present at only 35 pg/ml plasma protein concentration. This results in a total range of 9 orders of magnitude. Peptides from low to middle abundant proteins are displayed in table 3.4, peptides from high abundant peptides are displayed in table 3.5. The amino acid cystein is marked with an asterisk as a sign of carbamidomethylated cysteins. Carbamidomethylation was necessary to inhibit the formation of disulfide bonds. In contrast to peptide-specific antibodies, which are normally able to bind only one peptide, TXP antibodies were generated to capture several target peptides with the same terminal epitope. To demonstrate this capability for several antibodies, two different peptides were chosen and synthesized (see table 3.5).

Table 3.4.: Synthetic peptides from middle to low abundant plasma proteins → the TXP sequence is marked in red.

Peptide sequence including TXP part	Monoisotopic weight (Da)	Protein name	Protein abundance [pg/ml]	Reference
IYHSHIDAPK	1,179.61	Ceruloplasmin	2.80 x 10^8	Kim *et al.* (2002)
LDGLDLVDTWK	1,273.66	Alkaline phosphatase, tissue-nonspecific isozyme	4.07 x 10^4	Polanski and Anderson (2007)
EPC*VESLVSQYFQTVTDYGK	2,349.07	Apolipoprotein A-II	2.44 x 10^8	Luo and Liu (1994)
NIPGDFEC*EC*PEGYR	1,841.70	Vitamin K-dependent protein S	2.10 x 10^7	Kalafatis and Mann (1997)
VC*YGLGMEHLR	1,333.61	Receptor tyrosine-protein kinase erbB-2	1.10 x 10^4	Wu (2002)
APTAQVESFR	1,104.56	Tenascin	1.00 x 10^6	Schienk *et al.* (1995)
IFFYDSENPPASEVLR	1,882.92	Serum paraoxonase/ arylesterase 1	5.93 x 10^7	Kujiraoka *et al.* (2000)
WTTQETFPPK	1,233.61	Tumor necrosis factor receptor superfamily member 11B	3.50 x 10^1	Kyrtsonis *et al.* (2004)
C*DENILWLDYK	1,467.66	Pyruvate kinase isozymes M1/M2	1.50 x 10^7	Lueftner *et al.* (2000)
ALEAANGELEVK	1,242.65	Keratin, type I cytoskeletal 19	2.40 x 10^3	Hasholzner *et al.* (1994)
YYIHDHFIPIEK	1,573.80	Leptin receptor	4.80 x 10^3	Schulze *et al.* (2003)
DAGMQLQGYR	1,137.53	Aspartate aminotransferase, mitochondrial	not known	
TFLTVYWTPER	1,411.72	Intercellular adhesion molecule 1	2.14 x 10^5	Lei and Johnson (2000)
SDAIYSAR	881.43	Low-density lipoprotein receptor-related protein 1	6.00 x 10^6	Quinn *et al.* (1997)

Table 3.5.: Synthetic peptides from high abundant plasma proteins → the TXP sequence is marked in red. Except of the VNASR peptide all TXP sequences are represented in duplicates of different peptides.

Peptide sequence including TXP part	Monoisotopic weight (Da)	Protein name	Protein abundance [pg/ml]	Reference
EQLGPVTQEFWDNLEK	1,931.93	Apolipoprotein A-I	1.40 x 10^9	Glowinska *et al.* (2003)
EQLGEFYEALDC*LR	1,741.78	Alpha-1-acid glycoprotein 1	6.90 x 10^8	Polanski and Anderson (2007)
EVGTPHGIILDSVDAAFIC*PGSSR	2,497.21	Hemopexin	7.60 x 10^8	Anderson (2005)
EVGTVLSQVYSK	1,308.70	Apolipoprotein B-100	7.30 x 10^8	Glowinska *et al.* (2003)
SLGNVIMVC*R	1,147.57	Complement factor H	5.00 x 10^8	Esparza-Gordillo *et al.* (2004)
SLGNVNFTVSAEALESQELC*GTEVPSVPEHGR	3,412.60	Alpha-2-macroglobulin	1.80 x 10^9	Polanski and Anderson (2007)
TLNQSSDELQLSMGNAMFVK	2,212.06	Alpha-1-antichymotrypsin	4.20 x 10^7	Anderson (2005)
TLNQPDSQLQLTTGNGLFLSEGLK	2,573.34	Alpha-1-antitrypsin	1.40 x 10^9	Polanski and Anderson (2007)
VELEDWNGR	1,116.53	Fibrinogen gamma chain	2.72 x 10^9	Glowinska *et al.* (2003)
VELEDWAGNEAYAEYHFR	2,197.98	Fibrinogen alpha chain	2.72 x 10^9	Glowinska *et al.* (2003)
VLLDGVQNLR	1,125.66	Complement C3	1.30 x 10^9	Polanski and Anderson (2007)
VLLDQLGTTISFER	1,590.87	Apolipoprotein B-100	7.30 x 10^8	Glowinska *et al.* (2003)
DAVEKPQEFTIVAFVK	1,819.98	Apolipoprotein B-100	7.30 x 10^8	Glowinska *et al.* (2003)
DGAGDVAFVK	977.49	Transferrin	4.00 x 10^9	Stevens *et al.* (1986)
VPQVSTPTLVEVSR	1,510.84	Serum albumin	4.10 x 10^{10}	Polanski and Anderson (2007)
LFDSDPITVTVPVEVSR	1,872.99	Clusterin	3.70 x 10^8	Hogasen *et al.* (1993)
DTFVNASR	908.44	Plasma protease C1 inhibitor	3.00 x 10^8	Polanski and Anderson (2007)

A synthetic peptide mix was prepared in PBSN at a 100 nM concentration per peptide. This peptide mix was used as sample for the antibody evaluation. 100 μl of the peptide mix was incubated with 1 μg of every TXP antibody and the peptide/antibody complex was captured with magnetic protein G microspheres. 1 μg antibody has a theoretical capacity of 6.6 pmol peptide, therefore with a total amount of 10 pmol peptide in 100 μl the ratio was nearly equimolar.

The results of these assays gave an insight into the antibody performance. Additionally, the assays showed the applicability of the peptides to a MALDI read-out.

Figure 3.5 shows the peptide mixture, which was desalted and concentrated by C18 ZipTips. Most of the peptides were clearly detectable. Few peptides with poor ionization properties were not detectable due to the presence of peptides with strong ionization properties in the same sample. Peptides in the mass range of the alpha-Cyano-4-Hydroxy-Cinnamic acid matrix peaks (CHCA) were also not detectable. CHCA is considered to be the matrix of choice for peptides (Gobom *et al.*, 2001) and is incorporated on the pre-spotted anchor chips (PAC). It provides good sensitivity, but gives comparatively strong background peaks up to 1,200 Da (Keller and Li, 2000), especially when the concentration of the sample is low.

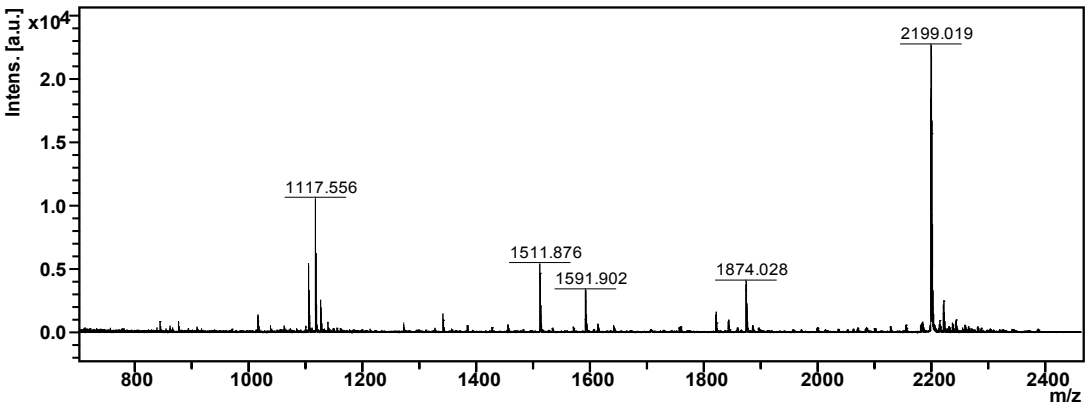

Figure 3.5.: MALDI mass spectrum of a peptide mix containing 24 synthetic peptides from set 1 and 2 each at 100 nM concentration, reflecting a protein concentration of 10 μg/ml (assuming a mean MW of 100,000 Da). 0.25 μl of the ziptipped peptide mix sample was spotted.

After the immunoaffinity enrichment via TXP immunoprecipitation, the MALDI read-out exhibits the functionality of the applied TXP antibodies. Figure 3.6 shows the spectrum of a TXP immunoprecipitation elution using the anti-VEVSR antibody. The C-terminal anti-VEVSR was able to capture both of its antigen target peptides:

- Tryptic peptide from serum albumin: VPQVSTPTLVEVSR
- Tryptic peptide from clusterin: LFDSDPITVTVPVEVSR

No cross-reactivity with other peptides in the peptide mix was observed at all. The intensity and S/N of the target peptides was improved following antibody enrichment,

compared to the same peptides for the non antibody purified mixture. The signal of the albumin peptide increased about fivefold.

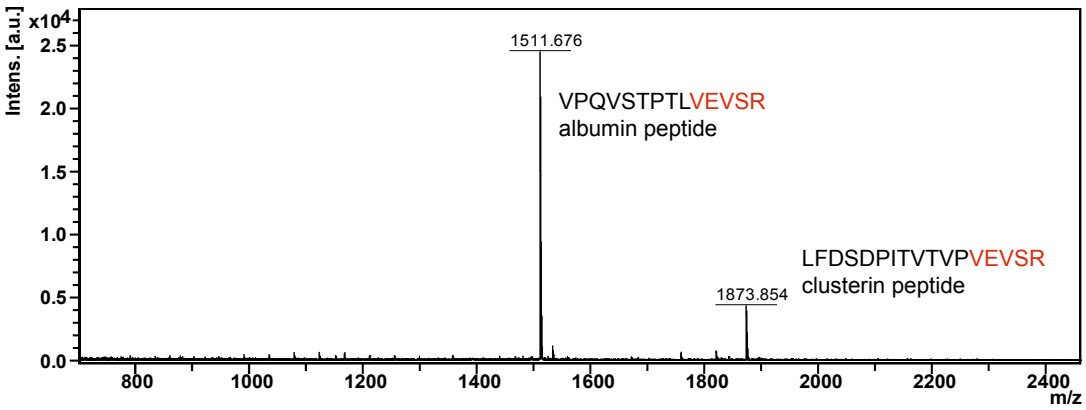

Figure 3.6.: MALDI mass spectrum of a TXP immunoprecipitation using the C-terminal anti-VEVSR antibody. The TXP antibody is capable of capturing both targeted standard peptides: VPQVSTPTLVEVSR→ serum albumin peptide and LFDSDPITVTVPVEVSR→ clusterin peptide.

Figure 3.7 shows a MALDI mass spectrum following TXP immunoprecipitation using the N-terminal anti-VLLD antibody. Again both target peptides were captured:

- Tryptic peptide from complement C3: VLLDGVQNLR
- Tryptic peptide from apolipoprotein B-100: VLLDQLGTTISFER

Again no cross-reactivity with other TXP target containing peptides was observed. Both peaks showed improvements in the signal to noise values compared to the the read-out of the peptide mix. Although the results for the anti-VLLD antiserum in the antibody binding assays (see section 3.1.1) were poor, the antibody showed good functionality in the peptide capture assay. Similar results were obtained with the other N-terminal antibody anti-VELED.

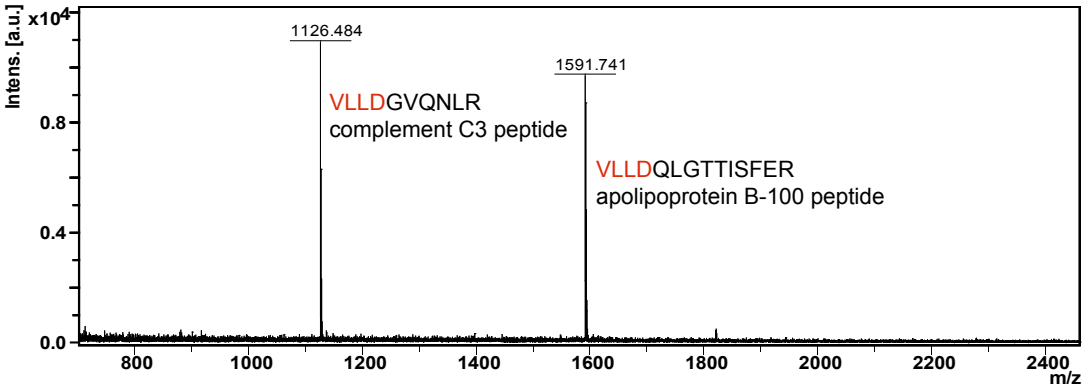

Figure 3.7.: MALDI read-out of a TXP immunoprecipitation using the N-terminal anti-VLLD antibody. The TXP antibody is capable of capturing both targeted standard peptides: VLLD GVQNLR → complement C3 peptide and VLLDQLGTTISFER → apolipoprotein B-100 peptide.

A control assay was carried out where the peptide mixture was incubated with magnetic protein G microspheres with no antibodies attached. Here, no synthetic peptides were detected in the mass spectrum, see figure 3.8.

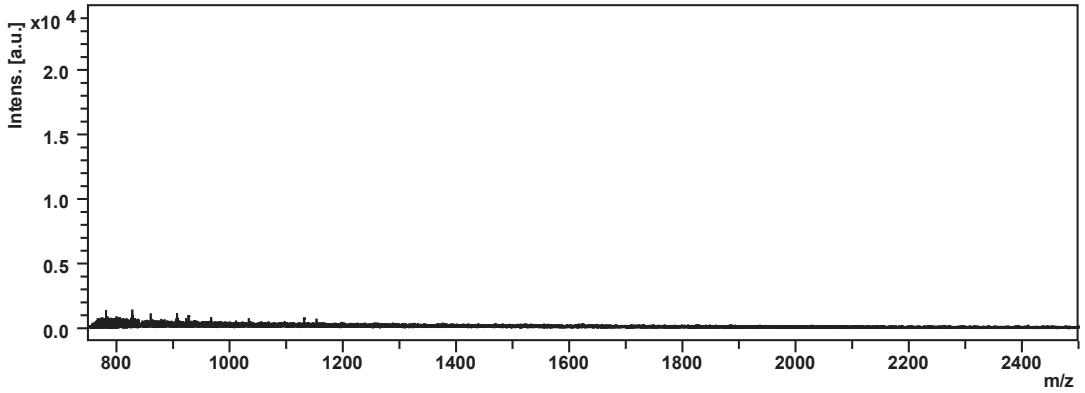

Figure 3.8.: MALDI read-out of an automatic assay without antibodies, using only magnetic protein G microspheres. No peptides were detected.

Table 3.6 shows an overview of all peptide capture assays, conducted with the corresponding TXP antibodies. Only peptides were used in the immunoaffinity enrichment assays, when the corresponding antibody was purified. The S/N of two replicate measurements are displayed. S/N values below 10 were excluded and the corresponding antibody not further used. Using this selection criteria, 34 of 38 purified antibodies were considered as successful in the peptide capture assays. Of the four failed antibodies, the anti-LEVK antibody failed in both rabbit immunizations, whereas the anti-YSAR and anti-VELED worked for at least one rabbit immunization. The second standard peptide for AFVK (977.49 Da) was not detected in the assay. Possible reasons for that could be suppression by other peptides or matrix peaks. Due to the fact that one of two standard peptides (1,819.98 Da) was captured by the anti-AFVK antibody, the antibody was considered as applicable.

Table 3.6.: Evaluation of purified antibodies *via* peptide capture assay. The signal to noise ratios were used for validation, n.d. = not determined; n.i. = not identified.

Peptide sequence inlcuding TXP sequence	Monoisotopic [Da]	S/N rbt 1	S/N rbt 2	Succeeded
IYHSHIDAPK	1,179.61	215.15	283.15	yes
LDGLDLVDTWK	1,273.66	209.60	393.95	yes
EPCVESLVSQYFQTVTDYGK	2,349.07	83.90	11.15	yes
NIPGDFECECPEGYR	1,841.70	703.65	365.85	yes
VCYGLGMEHLR	1,333.61	491.10	823.65	yes
APTAQVESFR	1,104.56	506.90	677.65	yes
IFFYDSENPPASEVLR	1,882.92	1,023.75	1,038.25	yes
WTTQETFPPK	1,233.61	67.45	244.30	yes
CDENILWLDYK	1,467.66	255.90	32.95	yes
ALEAANGELEVK	1,242.65	n.i.	n.i.	no
YYIHDHFIPIEK	1,573.80	29.45	249.35	yes
DAGMQLQGYR	1,137.53	453.45	559.10	yes
TFLTVYWTPER	1,411.72	164.20	1,056.25	yes
SDAIYSAR	881.43	n.i.	18.80	only rbt 2
VELEDWNGR	1,116.53	106.95	18.40	yes
VELEDWAGNEAYAEYHFR	2,197.98	248.25	n.i.	only rbt 1
VLLDGVQNLR	1,125.66	164.80	13.10	yes
VLLDQLGTTISFER	1,590.82	172.55	22.30	yes
DAVEKPQEFTIVAFVK	1,819.98	rbt2 75.0	rbt3 289.40	yes
DGAGDVAFVK	977.49	n.d.	n.d.	no
VPQVSTPTLVEVSR	1,510.84	656.10	481.1	yes
LFDSDPITVTVPVEVSR	1,872.99	140.55	58.75	yes
DTFVNASR	908.44	12.20	11.50	yes

The antibodies, fulfilling the selection criteria, were used in further assays, using trypsin digested human plasma as sample. The unsuccessful immunization anti-LEVK was nevertheless tested in a plasma TXP immunoprecipitation, as the corresponding peptide used for immunization had possibly poor ionization qualities and may therefore not have been detectable by MALDI mass spectrometry. The same also applied for the second AFVK-peptide with the m/z 977.49. The antibody with the best target

peptide capture abilities (rbt 1 or 2) was used in the following assays. In total, 19 TXP antibodies were applied to plasma analysis.

3.2. Immunoaffinity enrichment using TXP antibodies

One important goal for successful mass spectrometric plasma analysis is the reduction of sample complexity. In the following section, TXP antibodies were evaluated for their ability to reduce plasma sample complexity by capturing peptides with the same terminus. Plasma digest, processed only by C18-purification (ZipTip), was spotted on a PAC target to demonstrate the complexity of the sample, see figure 3.9. Most of the dominating peaks present are peptides from serum albumin. They are marked with an asterisk. High abundant proteins like serum albumin and IgG can constitute up to 80 % of the total serum proteins. The presence of these highly abundant peptides obscured the detection of lower abundant peptides in the spotted sample making their detection and identification unfeasable. The application of TXP antibodies could represent one means to deplete high abundant proteins like albumin through the selective enrichment of lower abundant targeted peptides.

Besides plasma proteins, some plasma lipids were also detectable (marked with two asterisks, 758.597 m/z → figure 3.9). The plasma lipid profile was characterized by Pynn *et al.* (2010). Like many peptides derived from high-abundant proteins, plasma lipids, especially phosphatidylcholines, are easily ionizable and therefore potential suppressing agents regarding targeted peptide ionization.

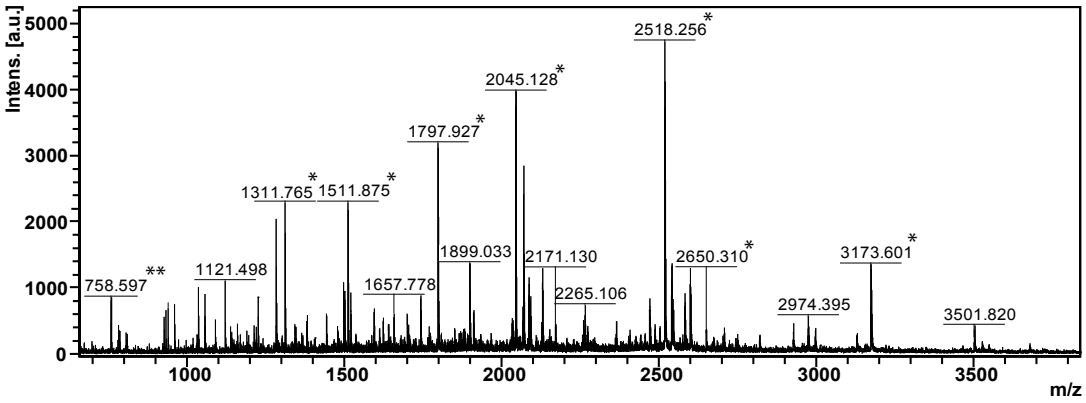

Figure 3.9.: Digested plasma, processed by C18 purification. Annotated peaks marked with an asterisk represent serum albumin peptides. The annotated peak marked with two asterisks represents a plasma phospholipid molecular species.

Figure 3.10 displays a spectrum of a TPX immunoprecipitation, carried out with the TXP antibody anti-EGYR, which was incubated with non-lyophilized digested human plasma (5 μl original plasma amount). Compared to figure 3.9, showing a very complex spectrum, the spectrum generated from an immunoprecipitated digested plasma sample contained only a few intense peaks.

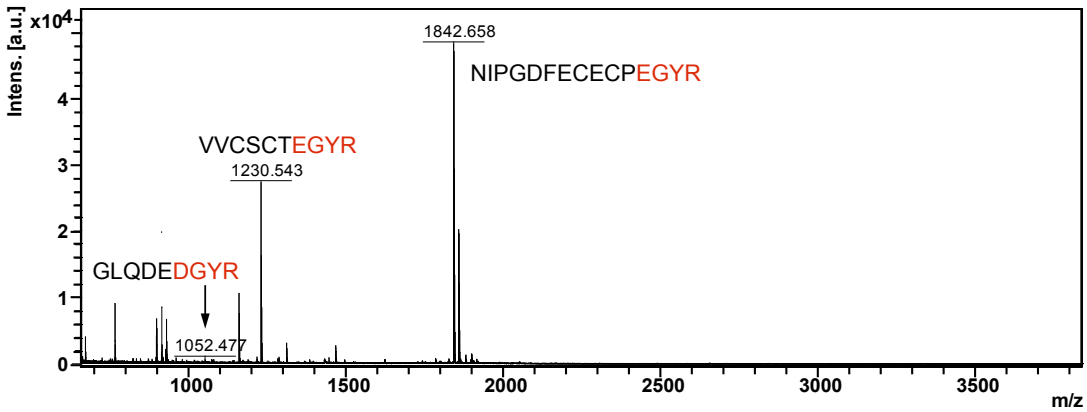

Figure 3.10.: Analysis of a TXP immunoprecipitate with anti-EGYR antibody. Three peptides containing the TXP tag were identified, whereas two of them had the exact tag EGYR and one peptide was identified with the C-terminal ending DGYR.

Most of the peaks could be identified by MSMS, e.g. the MSMS spectrum for the peak (with an m/z value of 1,842.658) is displayed in figure 3.11. Database searches using the MASCOT search engine identified a tryptic peptide from the protein: vitamin K dependent protein S.

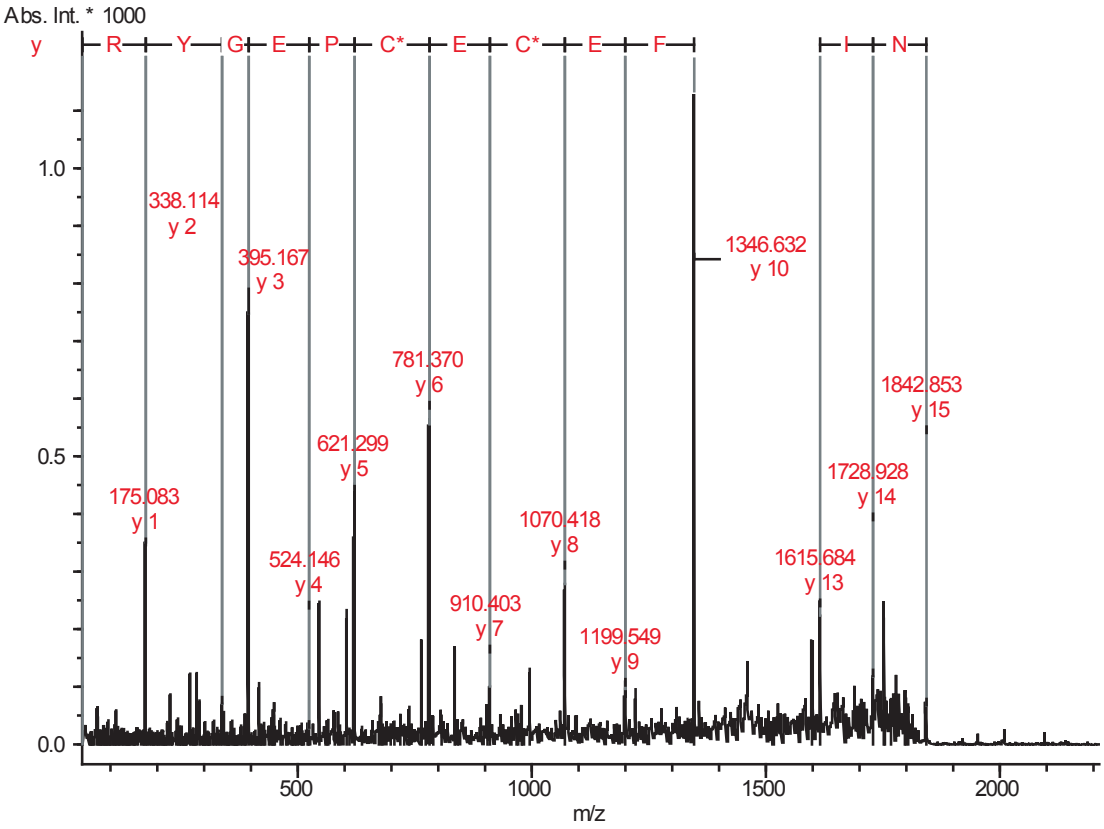

Figure 3.11.: MSMS spectrum of a tryptic peptide derived from vitamin K dependent protein S containing the TXP tag EGYR at the C-terminus. The spectrum shows the y-ion amino aid series (red). All y-ions could be identified apart from two, resulting in a very credible MASCOT identification with a score of 77. The asterisk on the C indicates a carbamidomethylation of the cysteine residue.

The spectrum shows the identification using the y-ion series (red). For that peptide

almost every related fragment peak could be assigned to the corresponding amino acid, resulting in a positive protein identification with a MASCOT score of 77 (for the displayed identification, the following parameters evaluate the identification: Individual ion scores > 27 indicate peptides with significant homology. Individual ion scores > 32 indicate identity or extensive homology, $p<0.05$). The asterisk labeling the C indicates a carbamidomethylation, resulting from the alkylation process during sample preparation before digest. The identified peptide from Vitamin K dependent protein S was the same peptide, that was used for antibody characterization in the peptide capture assay. The other masses displayed in the spectrum were also fragmented and two further peptides could be identified containing the targeted TXP tag EGYR. One peptide was identified containing the C-terminus DGYR. The MSMS spectra of the peptides, captured with the EGYR-antibody, are found in the supplementals (figure A.39 and A.40). The presence of single amino acids not matching the TXP tag can be referred to the polyclonality of the purified antibody.

In table 3.7 all identified peptides containing the corresponding tag EGYR (plus one mismatched AA position) are listed.

Table 3.7.: Captured peptides using TXP antibody anti-EGYR with corresponding plasma levels.

Protein	Amino acid sequence	m/z	Normal plasma level
Complement C4-A	GLQDEDGYR	1,052.477	2.1 mg/ml
Coagulation Factor IX	VVCSCTEGYR	1,230.543	4.2 μg/ml
Vitamin K dependent Protein S	NIPGDFECECPEGYR	1,842.658	42 μg/ml

Captured peptides covered a concentration range of about four orders of magnitude, capturing beside a tryptic peptide from the high abundant complement C4-A with a plasma concentration of 2.1 mg/ml (Lee *et al.*, 2006) and the vitamin K dependent protein S with a plasma level of 42 μg/ml (Polanski and Anderson, 2007) also a tryptic peptide from the protein coagulation Factor IX with a plasma level of 4.2 μg/ml (Thompson, 1977).

Besides the peptides with the targeted TXP terminus, some peptides derived from high abundant proteins were also identified, see figure 3.12, showing a detailed spectra in a m/z range from 800 to 2,000. Additional masses were also processed by MSMS analysis and database search revealed the masses as peptides derived from high abundant proteins like albumin (m/z 1,311.750) or alpha-1-acid glycoprotein 2 (m/z 1,160.616). The peaks marked with two asterisks result from synthetic peptides used in the antibody purification process.

Using 5 μl initial plasma amount used in the sample plate and an elution volume of 20 μl in the elution plate, the sample is purified but four times diluted. To avoid dilution and to try to increase the sensitivity of the TXP immunoprecipitation, more

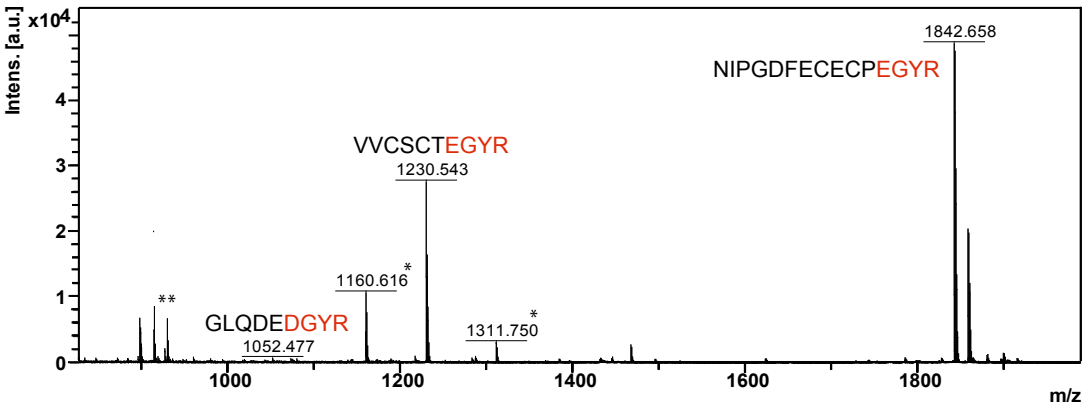

Figure 3.12.: Detail perspective - IP anti-EGYR. The peaks marked with an asterisk are tryptic peptides from high abundant proteins like albumin (m/z 1,311.750) or alpha-1-acid glycoprotein 2 (m/z 1,160.616). The peaks marked with two asterisks represent antibody purification artefacts.

plasma was used as initial sample (20 μl plasma, lyophilized and reconstituted). Whilst the peak intensities of the resulting targeted peptides were increased, more non-specific peptides derived from high abundant proteins were detected. This problem is further addressed in section 3.5.

3.3. Assay performance

To assess the assay performance of the TXP immunoprecipitation combined with mass spectrometric read-out, precision and accuracy were compared using two different ionization methods: matrix-assisted laser desorption/ionization (MALDI) with TOF detection and electrospray ionization (ESI), conducted as MRM with triple quadrupole analysis. Additionally, the limit of detection (LOD) and the limit of quantification (LOQ) were determined. LOD was defined as the lowest concentration of a peptide dilution series with S/N higher than ten.

According to the Guidance for Industry, Bioanalytical Method val, LOQ was defined as the lowest concentration of the dilution series, which can be measured with S/N over ten. In addition, the data should be identifiable, discrete and reproducible with a precision of 20 % and an accuracy of 80-120 %. The accuracy was determined by using isotopic labeled standard peptides, which were spiked into the digest before the TXP antibodies had been added.

With MALDI TOF analysis the intra-assay variation was determined in three TXP immunoprecipitation assays, which were carried out on the same day. The same applies for the analysis with MRM QQQ. In addition, an inter-assay variation was also determined in three TXP immunoprecipitation assays, which were carried out on three consecutive days.

For the determination of the parameters precision, accuracy, LOD and LOQ, a tryptic peptide of the erB-2 Protein was used: VCYGLGMEHLR with a normal plasma abundance of 11 ng/ml (Wu, 2002). It was diluted in a tryptic plasma digest (1,000 nM to 0.05 nM) and a TXP immunoprecipitation was carried out using 2 μg of the corresponding anti-EHLR TXP antibody. Synthetic isotope standard (SIS) VCYGLGMEHLR* with the m/z of 1343.68, which is 10 Da heavier than the non-isotopic peptide (due to the isotopic labels C_{13} and N_{15} in R), was added in three different concentrations. The amount of peptide was calculated by forming the ratio between the areas of normal and SIS peptide.

3.3.1. Quantification using MALDI MS

The area under the peak in the MALDI MS spectra was used for absolute quantification. Following assays were all carried out in triplicates to determine intra-assay variation. Pre-tests were carried out using dilution series of the VCYGLGMEHLR peptide with 10 nM SIS in 1 % formic acid. The peptide dilutions were spotted directly on the MALDI target to assess the quantitative character of the MALDI read-out. Figure 3.13 displays the accuracy of the calculated peptide amount in comparison to 100 % accuracy. For higher concentrations an over-quantification was observed, whereas with lower concentrations an under-quantification was found in addition to high standard deviation (see figure 3.13), indicating low precision. The three lowest peptide amounts were not detectable. No accurate quantification was possible using this procedure.

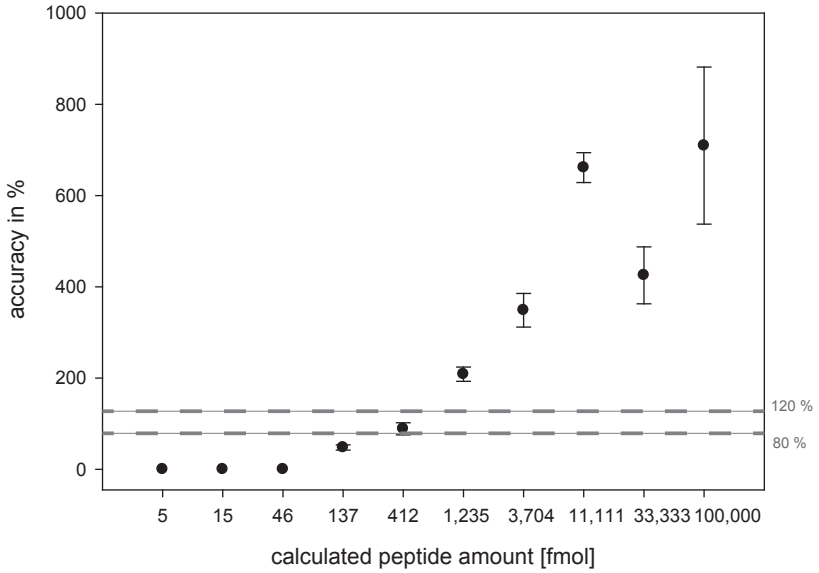

Figure 3.13.: Peptide quantification by MALDI MS using stable isotope labeled standards - Accuracy 1 amount of SIS. The dilution series of the VCYGLGMEHLR peptide in 1 % FA was spiked with 10 nM SIS and directly spotted on a PAC target. Quantification was enabled by forming the ratio of the area under the peak from isotopic and non-isotopic labeled peptide. 20 % deviation (plus minus) is marked by the two dashed gray lines.

To improve accuracy, three different SIS amounts were spiked in the diluted peptide solutions: 100 nM, 10 nM or 1 nM (10,000 fmol, 1,000 fmol and 100 fmol in 100 μl). Table 3.8 displays the dilution pattern and the corresponding SIS spike-in. The amount of SIS was chosen to be in the dynamic range of one order of magnitude according to the corresponding peptide dilution.

Table 3.8.: Peptide dilution series and SIS spike-in

Theoretical plasma protein concentration erbB-2 [ng/ml]	Peptide [nM]	SIS peptide [nM]
137,910.00	1,000.00	100
45,970.00	333.33	100
15,323.33	111.11	100
5,107.78	37.04	100
1,702.59	12.35	10
567.53	4.12	10
189.18	1.37	1
63.06	0.46	1
21.02	0.15	1
7.01	0.05	1

Figure 3.14 shows the accuracy of the dilution series spiked with three different SIS quantities. Only peaks with S/N higher than ten were taken into account. Compared to the experiment with only one concentration of SIS (see figure 3.13), an improvement regarding precision and accuracy was achieved. The values for 33,333 fmol, 11,111 fmol and 3,704 fmol were within a 20 % range. For the rest of the peptide concentrations an under-quantification was observed. The lowest three peptide amounts were not detectable.

To determine precision and accuracy of the quantification within a TXP immunoprecipitation assay, a dilution series of the VCYGLGMEHLR peptide + SIS (same dilution as shown in table 3.8) was prepared in PBSN and 2 μg anti-EHLR antibody was added. After elution the amount of captured peptide was calculated. Figure 3.15 displays the accuracy for the immunoprecipitated peptides.

For most of the captured peptides an under-quantification was observed. Only the two highest peptide concentrations were detected to be in the 100 % range accuracy. Nevertheless, using the immunoprecipitation a huge improvement of consistency of detection and quantification can be monitored. All peptide concentrations were detected with a S/N higher than ten. The accuracy values were increasing with peptide concentration. Although no accurate quantification was possible, high precision of the quantification values was observed.

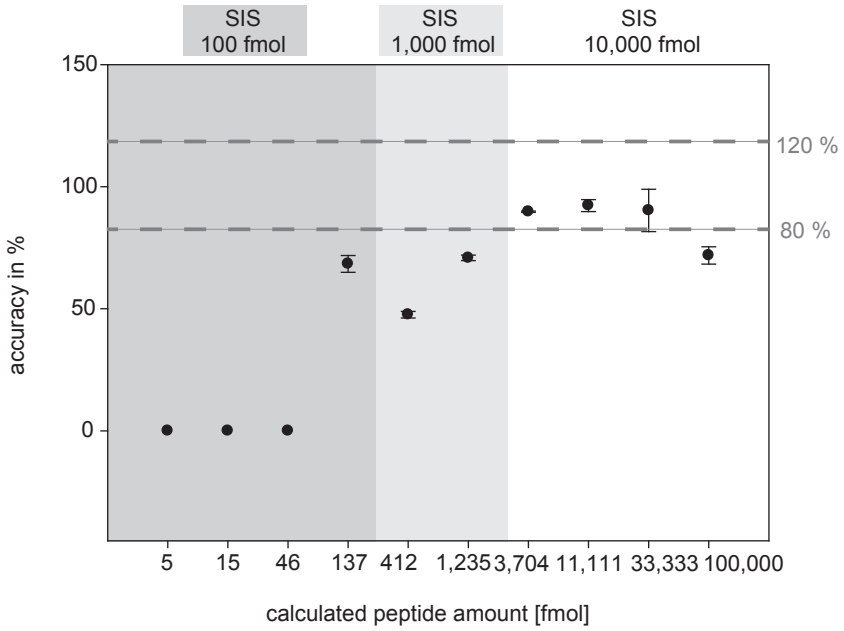

Figure 3.14.: Accuracy of peptide quantification by MALDI MS using three amounts of SIS. The dilution series of the VCYGLGMEHLR peptide in 1 % FA was spiked with three different amounts of SIS and directly spotted on a PAC target. Only peaks with a S/N over ten were taken into account. The two dashed gray lines represent 80 % to 120 % accuracy. The amounts of SIS employed are shaded.

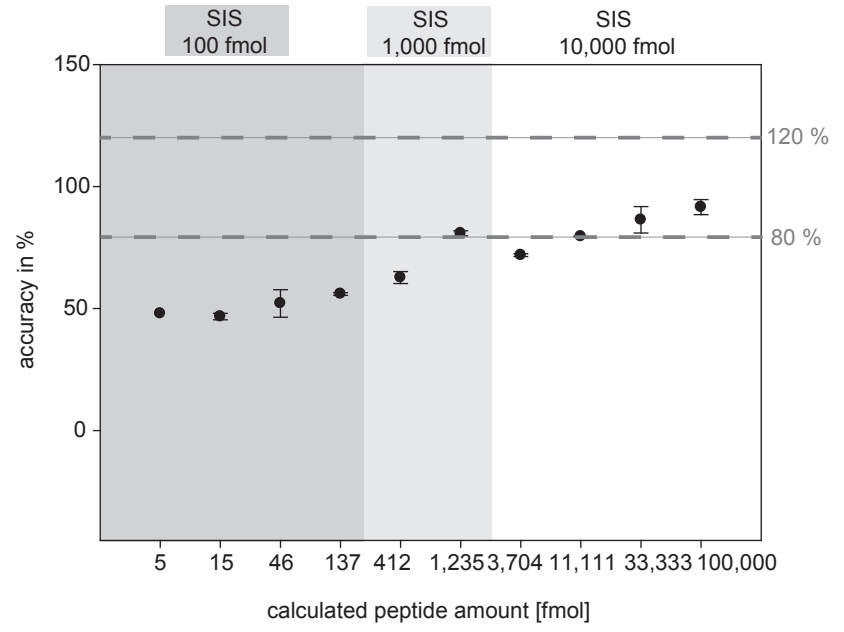

Figure 3.15.: Accuracy of peptide quantification by MALDI MS. A dilution series of the VCYGLGMEHLR peptide in PBSN was prepared and an IP using anti EHLR antibody was carried out. The eluted peptides were analyzed with MALDI MS and the amount of peptide was calculated using the ratio peptide/SIS. The two dashed gray lines represent 80 % to 120 % accuracy. The amount of SIS is marked by the shaded quadrants. A consistent decline of the accuracy can be monitored from the upper peptide dilution down the the lower ones.

Determination of precision and accuracy was repeated in a human plasma digest to test the quantification via isotopic labeled standards and MALDI in a biological sample. The linearity of this assay is displayed in figure 3.16 with a coefficient of determination $R^2 = 0.99689$ and a slope of 1.99. According to the accuracy shown in figure 3.17 the slope is too high for a constant accuracy of 100 % which would be represented by a slope of 1. 15 fmol and 5 fmol were not detectable ($S/N < 10$).

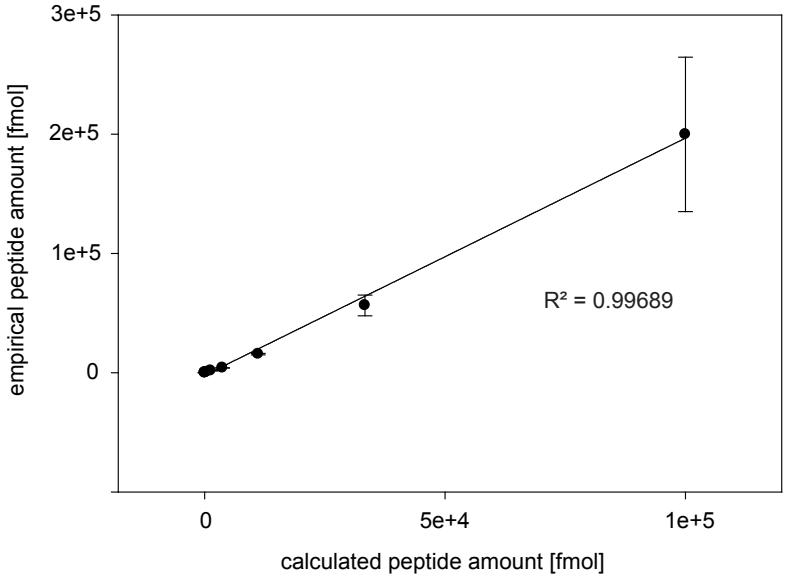

Figure 3.16.: Linearity of peptide quantification by MALDI MS. A dilution series of the VCYGLGMEHLR peptide in plasma and a TXP immunoprecipitation was carried out. The elutions were analyzed with MALDI MS and the amount of peptide was calculated using the ratio peptide/SIS. The assay shows a linearity with a coefficient of determination $R^2 = 0.99689$. The slope of the curve is 1.99. 15 fmol and 5 fmol were not detectable.

Figure 3.17 displays the accuracy for the quantification of the diluted peptide. Using plasma as matrix for the synthetic erbB2 peptide, three quantification values were found in the range of +-20 % variation around 100 % accuracy. Especially, in the concentration range, where the amount of peptide matched the amount of SIS, the quantification was found to be accurate. The quantification was precise except of the two highest peptide amounts. Similar to the dilution in PBSN, a decline of the accuracy values was observed.

Table 3.9 shows a summary of accuracy values in all conducted MALDI quantification experiments. In those, a decline in accuracy was observed. However, the sensitivity improved by a factor of 27 using the immunoprecipitation assays (five-fold concentration after IP, from 100 μl $\rightarrow$ 20 μl). In addition, the accuracy of peptide quantification was improved after immunoprecipitation.

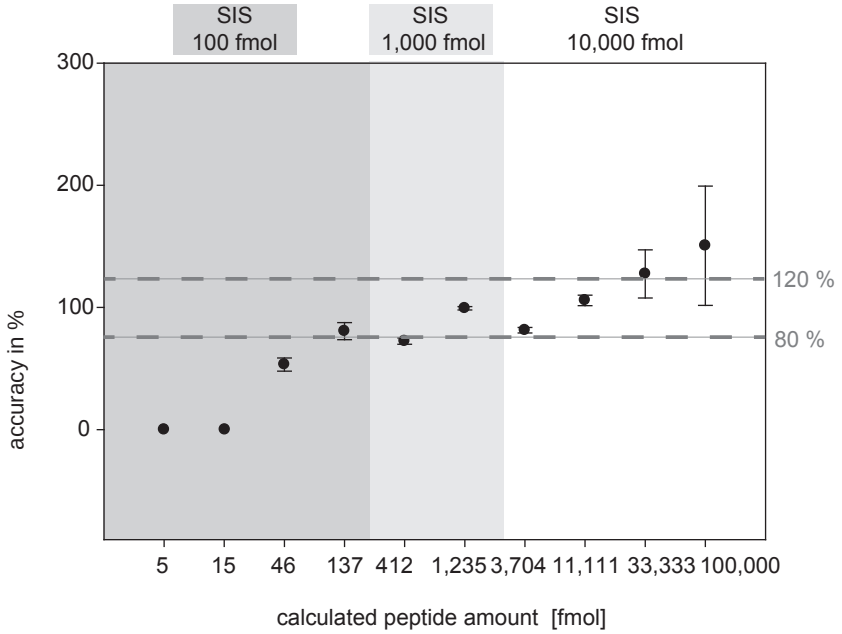

Figure 3.17.: Accuracy of peptide quantification by MALDI MS - Immunoprecipitation in plasma. A dilution series of the VCYGLGMEHLR peptide in plasma and a TXP immunoprecipitation was carried out. The elutions were analyzed with MALDI MS and the amount of peptide was calculated using the ratio peptide/SIS. The amount of SIS is marked by the shaded quadrants. A consistent decline of the accuracy can be monitored from the upper peptide dilution down the the lower ones. 15 fmol and 5 fmol could not be detected.

Table 3.9.: Accuracy - MALDI read-out

	Accuracy [%]			
	without IP		with IP	
concentration [nM]	FA [%] 1 SIS	FA [%] 3 SIS	PBSN [%] 3 SIS	plasma digest [%] 3 SIS
1,000.00	709	72	92	151
333.33	425	90	86	127
111.11	661	82	80	106
37.04	349	90	72	81
12.35	208	71	81	99
4.12	89	48	63	72
1.37	48	68	56	81
0.46	0	0	52	53
0.15	0	0	47	0
0.05	0	0	48	0

3.3.2. Quantification using MRM MS

Due to the limited dynamic range of the MALDI TOF/TOF read-out, corresponding plasma spike-in experiments were carried out with MRM MS using a triple quadrupole mass spectrometer.

For the determination of the parameters precision, accuracy, LOD and LOQ the tryptic peptide of the erB-2 Protein (amino acid sequence: VCYGLGMEHLR) was diluted in a tryptic plasma digest (1,000 nM to 0.05 nM) and a TXP immunoprecipitation was carried out using 2 μg of the corresponding anti-EHLR TXP antibody. Quantification was enabled by the spike-in of three different amounts of the synthetic isotopic labeled standard (SIS) VCYGLGMEHLR* with the m/z of 1,343.68, which is 10 Da heavier than the non-isotopic peptide (due to the isotopic labels C_{13} and N_{15} in R). The amount of SIS was adapted to the used dilution of the standard peptide. SIS was spiked in quantities, that did not exceed the ten-fold range of the standard peptide, to prevent suppression effects in the MS read-out. The peptide amount was calculated using the area under the curve ratios of standard peptide and SIS.

To determine the intra-assay performance characteristics of the TXP immunoprecipitation in human plasma digest, the TXP immunoprecipitation using the anti-EHLR TXP antibody and the dilution series from 100,000 down to 5 fmol in 100 μl sample (1,000 nM to 0.05 nM) of the corresponding standard peptide was carried out in triplicates on the same day. For the determination of the inter-assay variation the assay was performed on three consecutive days.

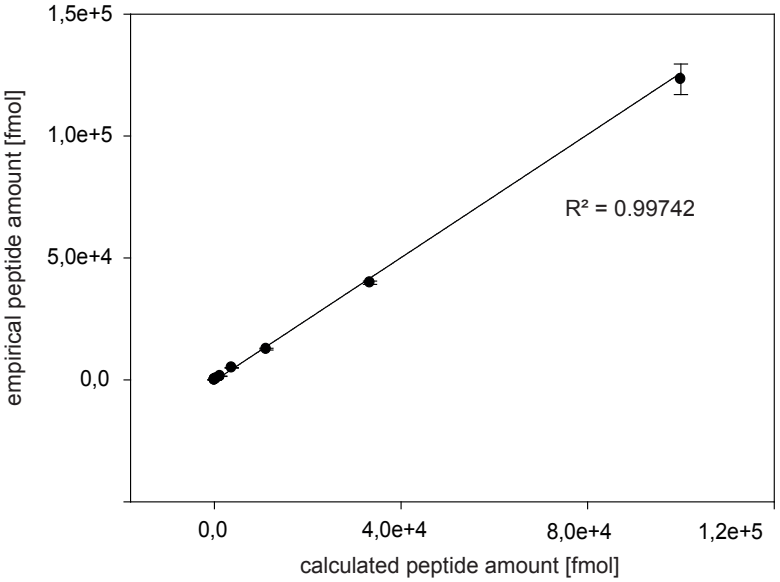

Figure 3.18.: Linearity of peptide quantification by MRM MS - intra-assay variation. Quantification of the peptide VCYGLGMEHLR in a plasma digest, captured with the anti-EHLR antibody. The mean values and the standard deviations are calculated from three assays carried out on the same day. The results show a linear regression with $R^2 = 0.99742$ and a slope of 1.22. 5 fmol was below detection limit.

The linearity of the TXP immunoprecipitation with the anti-EHLR TXP antibody is shown in figure 3.18. The assay was carried out in triplicates on the same day to determine the intra-assay variation. The coefficient of determination was $R^2 = 0.99742$, which indicates a good linearity of the assay. The slope of the regression was 1.22, which is a large improvement compared to MALDI TOF, where the slope of the regression was 1.99.

Figure 3.19 displays the accuracy of the assay. The values are within the range of +- 20 % except of two values outside the range → 128 % (3,704 fmol) and 138 % (137 fmol).

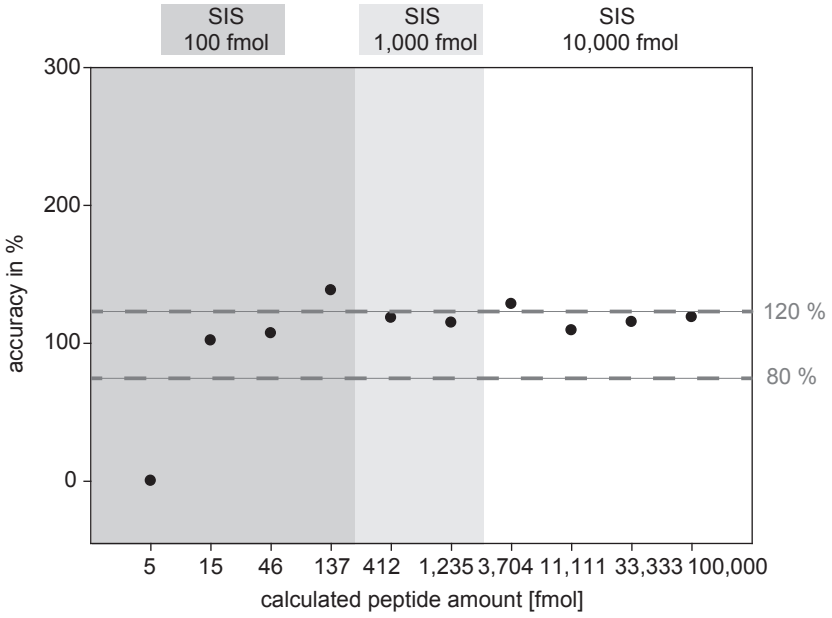

Figure 3.19.: Accuracy of peptide quantification by MRM MS - intra-assay variation. Quantification of the peptide VCYGLGMEHLR in a plasma digest, captured with the anti-EHLR antibody. The elutions were analyzed with MRM MS and the amount of peptide was calculated using the ratio peptide/SIS. The amount of SIS is marked by the shaded quadrants. 5 fmol was below detection limit.

Inter-assay variance of the IP with subsequent MRM read-out (n=3) is shown in figure 3.20. The coefficient of determination $R^2 = 0.99973$ indicates a good linearity of the assay. The slope with 1.07 indicates accurate quantification.

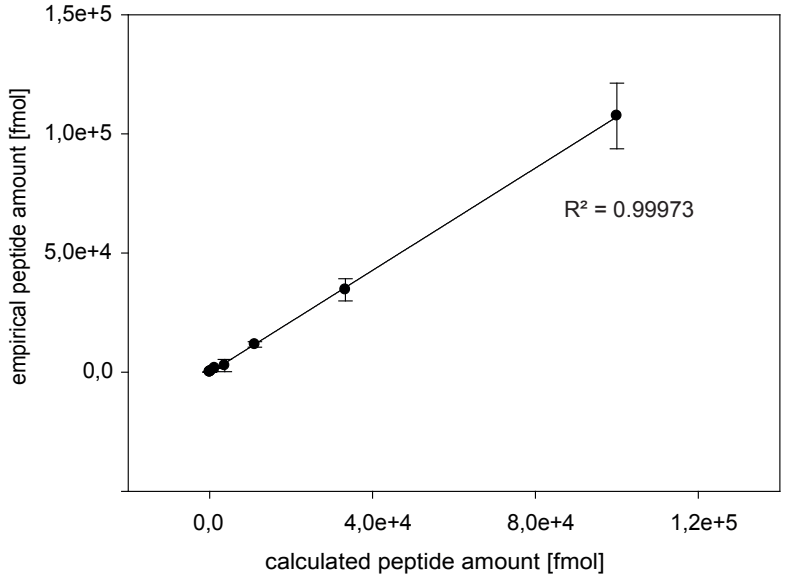

Figure 3.20.: Linearity of peptide quantification by MRM MS - inter-assay variation. Quantification of a dilution series of the peptide VCYGLGMEHLR in plasma digest, captured with the anti-EHLR antibody. The mean values and the standard deviations are calculated from single assay values carried out on three consecutive days. A regression fit of the assay with $R^2 = 0.99973$ and a slope of 1.07 was calculated for the assay.

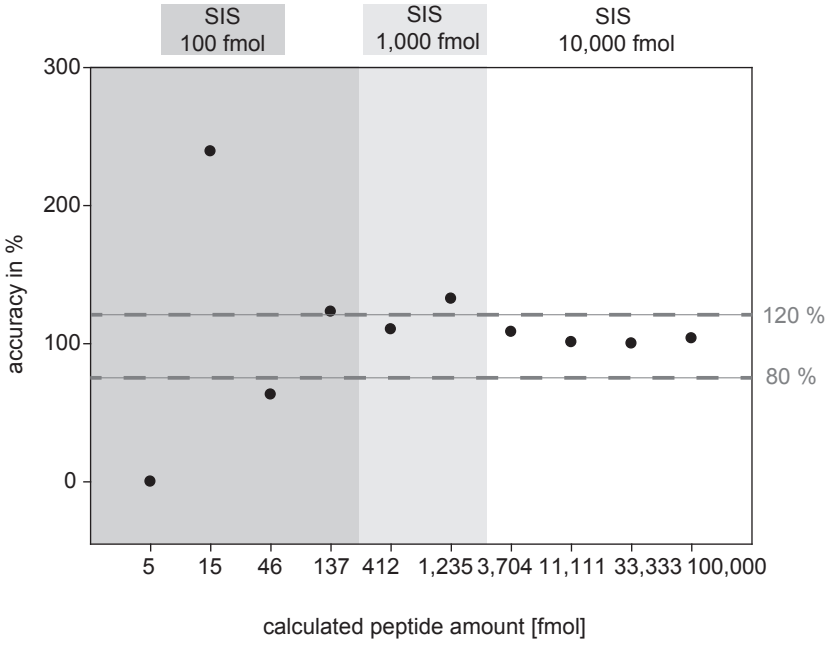

Figure 3.21.: Accuracy of peptide quantification by MRM MS - inter-assay variation. Quantification of the peptide VCYGLGMEHLR in a plasma digest, captured with the anti-EHLR antibody. The experiment was carried out on three consecutive days. The elutions were analyzed with MRM MS and the amount of peptide was calculated using the ratio peptide/SIS. The amount of SIS is marked by the shaded quadrants. 5 fmol was below detection limit.

Figure 3.21 displays the accuracy of the inter-assay analysis. The accuracy for 137 to 100,000 fmol peptide were within 80 % to 120 %. Values for 137 fmol and 1,235 fmol were outside this range. Accuracy values for 46 fmol showed an under-quantification with more than 20 % deviation. In contrast, the 15 fmol quantification was a huge outlier with more than 240 %. 5 fmol was not detectable. Table 3.10 displays precision and accuracy in detail regarding intra- and inter-assay variation.

Table 3.10.: Intra- and inter-assay variation TXP plasma assay (intra- and inter-assay variation was calculated with n=3). Precision is expressed as relative S.D. (standard deviation): (S.D./mean) x 100. Accuracy is expressed as percent difference:((empirical peptide amount - calculated peptide amount)/calculated peptide amount) x 100 + 100.

	Intra-assay variation (n=3)				Inter-assay variation (n=3)			
Calculated peptide amount [fmol]	Empirical peptide amount [fmol]		Precision [%]	Accuracy [%]	Empirical peptide amount [fmol]		Precision [%]	Accuracy [%]
	mean	S.D.			mean	S.D.		
100,000	118,864	6,039	5	119	103,711	13,285	13	104
33,333	38,434	660	2	115	33,332	4,481	13	100
11,111	12,145	368	3	109	11,222	1,115	10	101
3,704	4,756	139	3	128	4,017	1,172	29	108
1,235	1,418	75	5	115	1,636	146	9	132
412	487	32	7	118	454	10	2	110
137	190	52	27	139	169	37	22	123
46	49	34	69	107	29	10	34	63
15	16	11	69	107	36	27	75	240
5	0	0	-	-	0	0	-	-

Calculated from three assay replicates, carried out on one day, the intra-assay mean precision ranged between 2 and 7 % from 412 to 100,000 fmol, whereas accuracy ranged between 109 and 128 % (table 3.10). The precision of the lowest detectable three peptide amounts ranged between 27 and 69 %, therefore 412 fmol (representing 568 ng/ml theoretical plasma protein concentration) was determined as limit of quantification (LOQ). As 5 fmol could not be detected, the limit of detection (LOD) was determined to 15 fmol, representing 21 ng/ml plasma protein concentration, for this assay. The corresponding theoretical plasma protein concentrations are found in table 3.8.

The inter-assay precision ranged between 2 and 29 % from 137 to 100,000 fmol with two values slightly higher than 20 % for 3,704 fmol (29 %) and for 137 fmol (22 %), see table 3.10. The accuracy ranged between 100 and 132 % from 137 to 100,000 fmol. The two lowest detectable peptide amounts were found to be out of range for a precise quantification (precision > 20 %, accuracy not in the range from 80 to 120 %). Therefore, LOQ was determined to 137 fmol (representing 189 ng/ml theoretical plasma protein concentration). As again 5 fmol could not be detected, the limit of detection (LOD) was determined to 15 fmol, representing 21 ng/ml plasma protein concentration.

3.4. Dynamic range of multiplex immunoaffinity enrichment

Due to the capability of the TXP antibodies to capture several target peptides, the multiplex dynamic range was investigated. More precisely, are the antibodies able to capture lower abundant target peptides in the presence of high abundant target peptides in the sample? How large is the range from low abundant target peptides to high abundant target peptides being captured by one antibody?

To determine the dynamic range of the TXP antibodies two TXP antibodies were chosen. TXP antibodies were chosen, where two different synthetic standard peptides were available (anti-VLLD and anti-VEVSR, see table 3.5) and the peptides were adequate for nanoLC MRM MS analysis regarding ionization properties. Since the used TXP antibodies also target peptides from high abundant proteins, the experiment was carried out in an artificial setup.

One standard peptide was used as matrix peptide with a constant high concentration of 333.33 nM (33 pmol in 100 μl). The second peptide was diluted in the peptide matrix from 1,000 nM down to 0.05 nM (100 pmol to 5 fmol in 100 μl). The second peptide was also diluted without the matrix peptide. Figure 3.22 shows the peptide concentration setup.

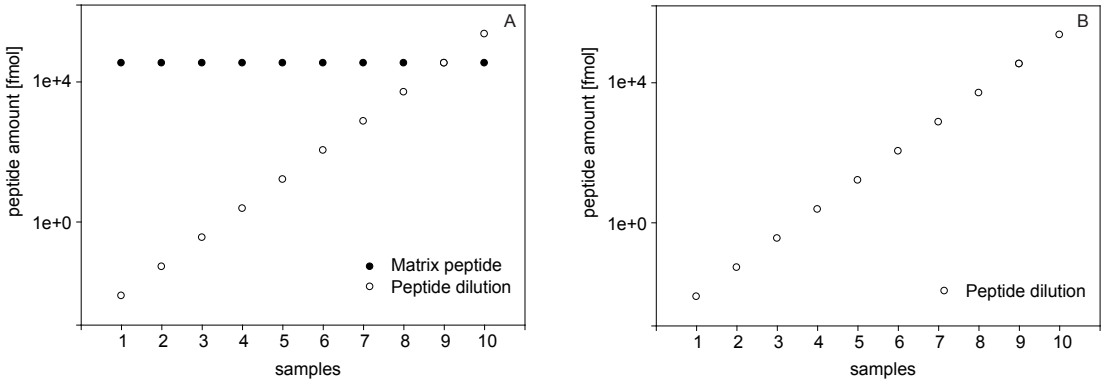

Figure 3.22.: Setup of dynamic range experiment of TXP antibodies. The concentration of the matrix peptide was kept constant at 333.33 nM (33,333 fmol in 100 μl). The second peptide was diluted in the matrix **(A)** and without the matrix peptide **(B)** from 1,000 nM down to 0.05 nM (100,000 fmol to 5 fmol in 100 μl).

Four target peptides of the tested two TXP antibodies were mixed in the accordant concentrations with the corresponding SIS peptides (in three different SIS concentrations, see section 3.3). In a TXP immunoprecipitation, 2 μg of the antibody captured the peptides and they were quantified according to peak area ratio to their corresponding SIS. Due to previous results, MRM MS read-out was used for these experiments.

Table 3.11 shows the calculated precision and accuracy for the TXP immunoprecipitation of anti-VLLD capturing a tryptic peptide from apolipoprotein B-100 (VLLDQLGTTISFER, see table 3.5). The precision of the intra-assay variation ranged between 2

Table 3.11.: Intra- and inter-assay variation - anti-VLLD, without matrix peptide (intra- and inter-assay variation was calculated with n=3). Precision is expressed as relative S.D. (standard deviation): (S.D./mean) x 100. Accuracy is expressed as percent difference:((empirical peptide amount - calculated peptide amount)/calculated peptide amount) x 100 + 100.

	Intra-assay variation (n=3)				Inter-assay variation (n=3)			
Calculated peptide amount [fmol]	Empirical peptide amount [fmol]		Precision [%]	Accuracy [%]	Empirical peptide amount [fmol]		Precision [%]	Accuracy [%]
	mean	S.D.			mean	S.D.		
100,000	128,710	2,305	2	129	138,716	11,975	9	139
33,333	40,361	2,828	7	121	41,453	7,440	18	124
11,111	14,139	576	4	127	13,574	1,275	9	122
3,704	4,438	778	18	120	4,458	698	16	120
1,235	1,391	120	9	113	1,402	250	18	114
412	526	112	21	128	556	47	8	135
137	170	55	32	124	211	118	56	154
46	43	7	16	93	23	12	53	50
15	55	31	57	360	136	112	82	893
5	17	23	134	338	66	63	96	1,316

and 32 % from 46 to 100,000 fmol with two values over 20 % for 412 fmol and 137 fmol. Accuracy ranged from 93 to 129 % from 46 to 100,000 fmol. The lower peptide amounts (15 and 5 fmol) had precision values higher than 50 %, accuracy values were higher than 300 %.

The inter-assay precision ranged between 8 and 18 % from 412 to 100,000 fmol. The peptide amounts from 5 to 137 fmol had precision values over 50 %. Similar to the precision, the accuracy showed at least 50 % deviation and very high deviation for the lower two peptide amounts. LOD was found to be at 5 fmol. Based on the results for the inter-assay precision and accuracy, LOQ was determined to 412 fmol peptide.

Table 3.12 shows the calculated precision and accuracy for the TXP immunoprecipitation capturing a tryptic peptide from apolipoprotein B-100 (VLLDQLGTTISFER, see table 3.5) with the anti-VLLD antibody out of a PBSN buffer in presence of a matrix peptide (VLLDGVQNLR, see table 3.5) with 333.33 nM concentration. Both peptides carry the TXP target sequence VLLD.

Table 3.12.: Intra- and inter-assay variation- dynamic range anti-VLLD, with matrix peptide (intra- and inter-assay variation was calculated with n=3). Precision is expressed as relative S.D. (standard deviation): (S.D./mean) x 100. Accuracy is expressed as percent difference:((empirical peptide amount - calculated peptide amount)/calculated peptide amount) x 100 + 100.

	Intra-assay variation (n=3)				Inter-assay variation (n=3)			
Calculated peptide amount [fmol]	Empirical peptide amount [fmol]				Empirical peptide amount [fmol]			
	mean	S.D.	Precision [%]	Accuracy [%]	mean	S.D.	Precision [%]	Accuracy [%]
100,000	159,791	28,707	18	160	162,143	27,686	17	162
33,333	37,086	3,221	9	111	44,663	3,777	8	134
11,111	12,827	2,684	21	115	18,366	4,807	26	165
3,704	3,808	349	9	103	5,052	1,192	24	136
1,235	1,568	260	17	127	1,234	823	67	100
412	773	146	19	188	558	375	67	136
137	413	381	92	301	281	253	90	205
46	263	416	158	575	27	17	62	59
15	39	28	72	257	2,244	3,831	171	14,720
5	16	20	125	326	18	23	129	354

The precision of the intra-assay variation ranged between 9 and 21 % for the concentrations from 46 to 100,000 fmol with one value over 20 % for 11,111 fmol. For the four lower peptide concentrations precision values were greater than 50 %. Good accuracy values (less than 20 % devation) were only found for three out of ten values.

Calculated from three assay replicates, carried out on three consecutive days, the inter-assay precision ranged between 8 and 26 % for the peptide concentrations from 3,704 to 100,000 (table 3.12). The precision values for the concentrations from 5 to 1,235 fmol were higher than 50 %. Again, the accuracy values were very high for many of the peptide amounts (nine out of ten). LOD was found to be at 5 fmol. No LOQ could be determined due to insufficient accuracy.

The quantification of the matrix peptide was also evaluated, which was present in the assay (Complement C3, VLLDGVQNLR, see table 3.5) in a constant high concentration of 33,333 fmol. Table 3.13 shows the calculated precision and accuracy for the quantification of the matrix peptide. The precision of the intra-assay ranged between 5 and 86 %. The accuracy ranged between 72 and 243 %, resulting in high inaccuracy for the quantification of the matrix peptide. Calculated from three assay replicates, carried out on three consecutive days, the inter-assay precision ranged between 9 and 40 %, showing better precision compared to the intra-assay variation. The accuracy

ranged between 93 and 168 %, which also showed inaccurate quantification for 5 of 10 measurements.

Table 3.13.: Intra- and inter-assay variation- matrix peptide anti-VLLD (intra- and inter-assay variation was calculated with n=3). Precision is expressed as relative S.D. (standard deviation): (S.D./mean) x 100. Accuracy is expressed as percent difference:((empirical peptide amount - calculated peptide amount)/calculated peptide amount) x 100 + 100.

	Intra-assay variation (n=3)				Inter-assay variation (n=3)			
Calculated peptide amount [fmol]	Empirical peptide amount [fmol]		Precision [%]	Accuracy [%]	Empirical peptide amount [fmol]		Precision [%]	Accuracy [%]
	mean	S.D.			mean	S.D.		
33,333	81,001	17,866	22	243	42,221	16,032	38	127
33,333	34,365	15,733	46	103	31,042	12,554	40	93
33,333	41,494	2,157	5	124	52,618	7,371	14	158
33,333	35,039	21,577	62	105	55,836	5,933	11	168
33,333	53,176	5,238	10	160	33,328	5,924	18	100
33,333	60,660	51,956	86	182	35,013	3,249	9	105
33,333	38,859	3,905	10	117	35,274	9,838	28	106
33,333	36,342	18,269	50	109	46,053	7,963	17	138
33,333	43,161	8,105	19	129	43,887	8,499	19	132
33,333	24,113	8,526	35	72	39,620	10,742	27	119

The results for the anti-VEVSR TXP immunoprecipitation are also displayed in detail. Table 3.14 shows the calculated precision and accuracy for the TXP immunoprecipitation capturing a tryptic peptide from plasminogen (LFDSDPITVTVPVEVSR, see table 3.5) out of PBSN buffer. The precision of the intra-assay variation ranged between 7 and 28 % from 46 to 100,000 fmol with two values over 20 % for 3,704 fmol and 137 fmol. Precision values for the lower peptide amounts (15 and 5 fmol) were over 37 %. Accuracy values were found to be in an acceptable range from 80 % to 120 % in between 11,111 to 412 fmol.

Calculated from three assay replicates, carried out on three consecutive days, the inter-assay precision ranged between 7 and 26 % from 137 to 100,000 fmol. Peptide amounts from 5 to 46 fmol had precision values over 29 %. Accuracy values were found to be in an acceptable range from 80 % to 120 % in between 33,333 to 412 fmol.

LOD for both intra- and inter-assay variations was found to be at 5 fmol. LOQ was determined to 412 fmol, which was the lowest peptide concentration quantified with acceptable precision and accuracy in both intra- and inter-assay analysis.

Table 3.15 shows the calculated precision and accuracy for the TXP immunoprecipitation capturing the plasminogen peptide (VILGAHQEVNLEPHVQEIEVSR, see table 3.5) with the anti-VEVSR antibody out of a PBSN buffer in presence of a matrix peptide in a constant high amount of 33,333 fmol. The precision of the intra-assay variation ranged between 1 and 13 % from 412 to 100,000 fmol. The lower peptide amounts had precision values higher than 80 %.

Table 3.14.: Intra-and inter-assay variation - anti-VEVSR, without matrix peptide (intra- and inter-assay variation was calculated with n=3). Precision is expressed as relative S.D. (standard deviation): (S.D./mean) x 100. Accuracy is expressed as percent difference:((empirical peptide amount - calculated peptide amount)/calculated peptide amount) x 100 + 100.

	Intra-assay variation (n=3)				Inter-assay variation (n=3)			
Calculated peptide amount [fmol]	Empirical peptide amount [fmol]		Precision [%]	Accuracy [%]	Empirical peptide amount [fmol]		Precision [%]	Accuracy [%]
	mean	S.D.			mean	S.D.		
100,000	158,617	23,849	15	158	132,906	16,062	12	133
33,333	43,719	3,533	8	131	38,903	6,427	17	117
11,111	13,167	884	7	119	12,290	1,050	9	111
3,704	3,670	811	22	99	3,568	931	26	96
1,235	1,466	170	12	119	1,332	248	19	108
412	393	28	7	95	377	27	7	91
137	196	55	28	143	194	24	12	141
46	81	7	9	175	53	29	55	116
15	24	9	37	162	24	7	29	159
5	47	26	55	940	17	17	97	342

Calculated from three assay replications, carried out on three consecutive days, the inter-assay precision ranged between 2 and 24 % from 46 to 100,000 fmol. The bottom two peptide amounts had precision values over 50 %. Accuracy was found to be out of the range of 80 to 120 % in most of the quantified peptide amounts. Therfore no LOQs could be determined.

Table 3.15.: Intra-and inter-assay variation - anti-VEVSR, with matrix peptide (intra- and inter-assay variation was calculated with n=3). Precision is expressed as relative S.D. (standard deviation): (S.D./mean) x 100. Accuracy is expressed as percent difference:((empirical peptide amount - calculated peptide amount)/calculated peptide amount) x 100 + 100.

	Intra-assay variation (n=3)				Inter-assay variation (n=3)			
Calculated peptide amount [fmol]	Empirical peptide amount [fmol]		Precision [%]	Accuracy [%]	Empirical peptide amount [fmol]		Precision [%]	Accuracy [%]
	mean	S.D.			mean	S.D.		
100,000	165,473	22,248	13	165	165,343	8,662	5	165
33,333	44,346	3,876	9	133	45,409	5,826	13	136
11,111	13,793	1,168	8	124	14,085	319	2	127
3,704	4,483	539	12	121	4,765	261	5	129
1,235	1,368	11	1	111	1,414	80	6	114
412	401	22	5	97	473	43	9	115
137	128	113	88	94	246	60	24	180
46	72	65	89	157	45	9	20	97
15	47	39	85	314	49	28	56	329
5	60	21	34	1,194	147	199	135	2,950

As 5 fmol peptide was still detectable (LOD = 5 fmol) in the presence of 33.3 pmol

matrix peptide, the dynamic range of the used TXP antibody anti-VEVSR was hence about 7,000 fold the amount of 5 fmol. 2 μg of the anti-VEVSR antibody was able to capture different peptides from low fmol peptide amounts to double-digit pmol amounts.

Table 3.16 shows the calculated precision and accuracy for the TXP immunoprecipitation capturing a tryptic peptide from clusterin (LFDSDPITVTVPVEVSR, see table 3.5) of a constant concentration of 33,333 fmol.

	Intra-assay variation (n=3)				Inter-assay variation (n=3)			
Calculated peptide amount [fmol]	Empirical peptide amount [fmol]				Empirical peptide amount [fmol]			
	mean	S.D.	Precision [%]	Accuracy [%]	mean	S.D.	Precision [%]	Accuracy [%]
33,333	25,038	3,211	13	75	34,533	14,324	41	104
33,333	23,374	1,515	6	70	30,054	5,244	17	90
33,333	27,599	9,214	33	83	30,358	1,484	5	81
33,333	26,137	412	2	78	29,553	5,365	18	89
33,333	25,947	6,372	25	78	42,184	11,928	28	127
33,333	28,416	7,625	27	85	38,959	9,746	25	117
33,333	30,935	2,439	8	93	35,446	423	1	106
33,333	30,036	5,616	19	90	38,356	11,508	30	115
33,333	31,750	2,800	9	95	36,776	6,566	18	110
33,333	28,524	706	2	85	46,643	17,867	38	140

Table 3.16.: Intra- and inter-assay variation- matrix peptide anti VEVSR (intra- and inter-assay variation was calculated with n=3). Precision is expressed as relative S.D. (standard deviation): (S.D./mean) x 100. Accuracy is expressed as percent difference:((empirical peptide amount - calculated peptide amount)/calculated peptide amount) x 100 + 100.

The precision of the intra-assay variation ranged between 2 and 33 %. The accuracy ranged between 70 and 95 %, showing constant small underquantification for the matrix peptide. Calculated from three assay replicates, carried out on three consecutive days, the inter-assay precision ranged between 1 and 41 %. The accuracy ranged between 89 and 140 %, whereas only two values were out of the range between 80 and 120 %.

Figure 3.23 displays the calculated peptide amounts after the TXP immunoprecipitation with the anti-VEVSR antibody carried out on one day in in three identical assays. **A** shows the peptide amounts of the dilution series of the plasminogen peptide without matrix, captured with the TXP antibody. It was possible to achieve detection limits down to 5 fmol. The quantification of the diluted plasminogen peptide in presence of the clusterin matrix peptide reached the same limit of detection as in the assay without matrix, shown in figure 3.23 **B**.

Figure 3.24 displays the calculated peptide amounts after the TXP immunoprecipitations with the anti-VEVSR antibody carried out on three consecutive days. **A** shows the peptide amounts of the dilution series of the plasminogen peptide without matrix, captured with the TXP antibody. It was possible to achieve detection limits down to 5 fmol. The quantification of the diluted plasminogen peptide in presence of the clus-

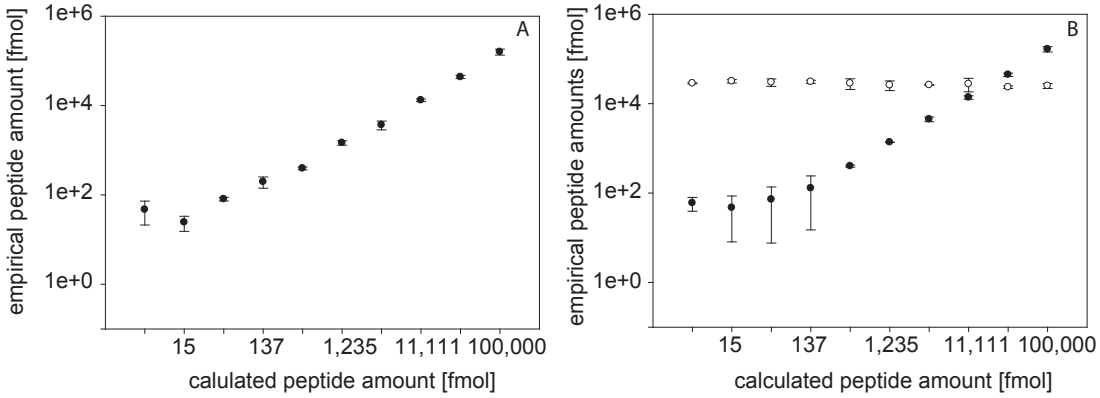

Figure 3.23.: Multiplex dynamic range intra-assay - anti VEVSR. The mean values and the standard deviations are calculated from three assay values carried out on the same day in three identical assays. **A** Quantification of a dilution series of the peptide VILGAHQEVNLEPHVQEIEVSR in PBSN, captured with the anti-VEVSR antibody. **B** Quantification of a dilution series of the peptide VILGAHQEVNLEPHVQEIEVSR in presence of 333.33 nM peptide LFDSDPITVTVPVEVSR in PBSN, captured with the anti-VEVSR antibody.

terin matrix peptide reached the same limit of detection as in the assay without matrix, shown in figure 3.23 **B**.

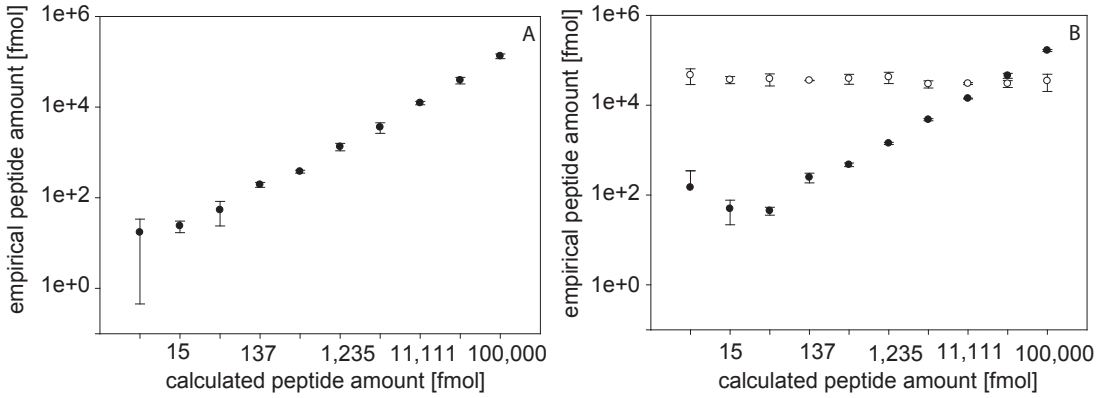

Figure 3.24.: Multiplex dynamic range inter-assay - anti VEVSR. The mean values and the standard deviations are calculated from three assays carried out on three consecutive days. **A** Quantification of a dilution series of the peptide VILGAHQEVNLEPHVQEIEVSR in PBSN, captured with the anti-VEVSR antibody. **B** Quantification of a dilution series of the peptide VILGAHQEVNLEPHVQEIEVSR in presence of 333.33 nM peptide LFDSDPITVTVPVEVSR in PBSN, captured with the anti-VEVSR antibody.

3.5. Non-specific binding of high abundant peptides

Using a combination of isotopic labeled peptide standards and MRM read-out, successful quantification could be achieved using TXP antibodies, see section 3.3. As TXP antibodies are capable of enriching peptide groups, MALDI MS was subsequently used to screen the antibodies for their qualitative capturing abilities. Due to the extremely limited dynamic range of MALDI MS analysis, see Domon and Aebersold (2010), the huge dynamic range of the plasma proteome (over ten orders of magnitude) represents a real challenge for the proteomic analysis. Human serum albumin present at about 41 mg/ml in plasma has to be depleted 100,000-fold to reach sensitivity values in the low ng/ml range, where most of the clinical relevant biomarkers are expected.

20 μl plasma was used in the following assays. In fact, after an immunoaffinity precipitation assay it was expected, that the elution should contain only targeted peptides. Figure 3.25 **A** shows an immunopurification of a plasma digest using the anti-EGYR antibody. Many non-specific peptides from high abundant proteins like albumin are detected. But compared to the plasma digest purification by C18 containing pipette tips (ZipTips), see Figure 3.25 **B**, EGYR-containing peptides were also identified, which could not be detected using C18 purification.

To identify the factors responsible for the presence of the non-targeted peptides, two control assays were carried out. In the first of these the same procedure described above was employed but without the TXP antibodies. The resulting mass spectrum revealed several peptides, most of which were shown to be derived from albumin upon fragmentation and database searching (figure 3.25 **C** and table A.1 in the supplementals). None of the peptides containing the C-terminal EGYR sequence were detected here. In a second control experiment, the assay was repeated without protein G coupled microspheres as well as the antibodies. Remarkably, the non-specific albumin peptides were still clearly visible in the mass spectra, with a five- to ten-fold lower intensity (figure 3.25 **D**). This suggests that, in addition to the protein G microspheres, the disposable plastic components of the magnetic microsphere handler contributed to the presence of the contaminating peptides. This findings led to the idea of introducing an additional separation step capable of separating the antibody-peptide complexes from the excess of tryptic peptides in solution.

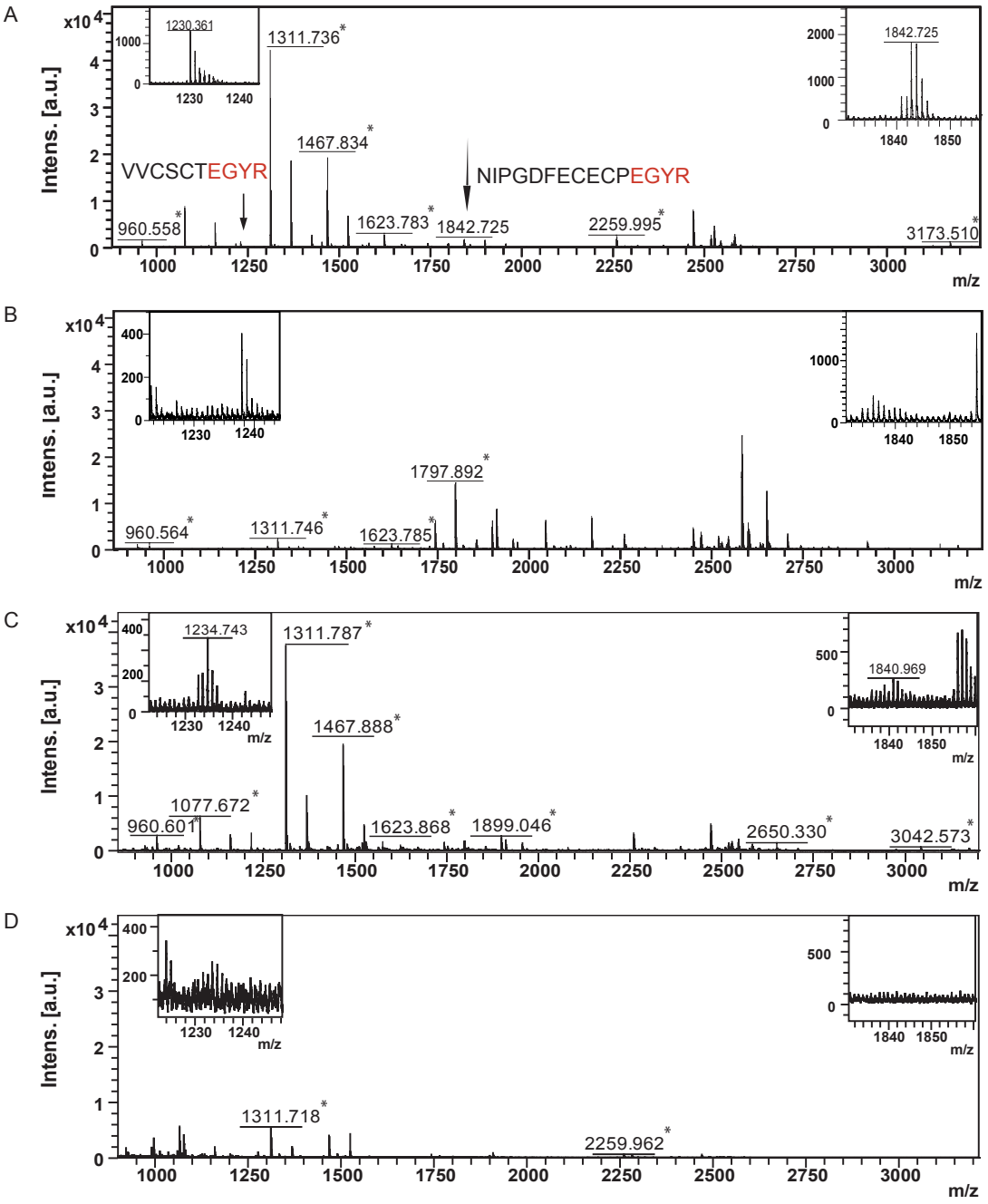

Figure 3.25.: Non-specific binding of peptides from high abundant proteins. Albumin peptides are marked with an asterisk. **A** Spectrum of a TXP immunoprecipitation elution, carried out with 20 μl plasma and the anti-EGYR antibody. The target peptide peaks, containing the TXP tag are displayed in detail. **B** Spectrum of a tryptic plasma digest, processed by C18. **C** Elution spectrum of an assay without the use of antibodies, using protein G microspheres only. **D** Elution spectrum without the use of an antibody or magnetic microspheres.

3.5.1. Depletion columns

Since many peptides from high abundant proteins were identified in the elutions after the immunoprecipitation (see previous section) a depletion of IgG and human serum albumin was carried out before immunoprecipitaion. In the following section, the depletion kit from Calbiochem was tested for the applicability in an TXP immunoaffinity assay with subsequent MALDI MS read-out. Human plasma from two healthy volunteers (male and female) was first depleted, subsequently digested with trypsin and analyzed in a TXP immunoprecipitation assay with four different C-terminal TXP antibodies:

- anti-EGYR
- anti-EVLR
- anti-QGYR
- anti-VEVSR

Table 3.17 shows the identified peptides in the elution of the TXP immunoprecipitations using the four different antibodies. The gray font in column "epitope concordance" represents amino acids, which are not matching the TXP tag, see section 3.2. The depletion of albumin and IgG turned out to be successful, see also figure A.41 in supplementals. Considering all applied antibodies, no non-specific albumin peptides were detected after the depletion procedure. Instead, some peptides from other high abundant proteins like alpha-1-antitrypsin and alpha-2-macroglobulin appeared, especially with the use of the anti-VEVSR antibody. The elutions of anti-EGYR, anti-EVLR and anti-QGYR antibody TXP immunoprecipitations revealed exactly the same target peptides with or without depletion, additional peptides detected after albumin and IgG depletion were found to originate from other high abundant proteins.

Only in the elution with the anti-VEVSR TXP immunoprecipitation an additional target peptide was found (a tryptic peptide from clusterin), however three non-specific bound peptides were detected compared to the TXP immunoprecipitation using non-depleted plasma. Clusterin is present in human plasma at a concentration of 370 μg/ml (see section 3.1.3), i.e. in high abundance. Hence, the detection of additional peptides from moderate to low abundant proteins was not possible for the four tested TXP antibodies. However, human serum albumin was removed by the columns, which caused most non-specific binding, but peptides from other high abundant proteins were identified instead.

Table 3.17.: Identified peptides without and after albumin/IgG depletion prior to plasma digest. Only one additional TXP motif peptide and three non-specific peptides were found with the depletion procedure prior to TXP immunoprecipitation. The gray font in the match column marks amino acids, which are not matching the TXP tag.

TXP tag	parent	protein	sequence	found without depletion	found after depletion	epitope concordance	IPI human score
EGYR	1,160.63	Alpha-1-acid glycoprotein	WFYIASAFR	-	+	-	70
	1,230.5	Coagulation factor IX	VVCSCTEGYR	+	+	EGYR	19
	1,842.8	Vitamin K-dependent protein S	NIPGDFECECPEGYR	+	+	EGYR	67
EVLR	948.48	Fibrinogen beta chain	ECEEIIR	+	+	EIIR	26
	1,160.63	Alpha-1-acid glycoprotein	WFYIASAFR	-	+	-	70
	1,629.86	Fibrinogen alpha chain	DSHSLTTNIMEILR	+	+	EILR	48
	1,708.81	AMBP protein	EYCGVPGDGDEELLR	+	+	ELLR	60
	1,883.97	Serum paraoxonase/arylesterase 1	IFFYDSENPPASEVLR	+	+	EVLR	76
QGYR	929.39	Dual specificity phosphatase 27	YQAEGYR + Carbamyl (N-term)	+	+	EGYR	26
	1,160.63	Alpha-1-acid glycoprotein	WFYIASAFR	-	+	-	70
	1,330.74	Complement C4-A	LNMGITDLQGLR	+	+	QGLR	36
	1,712.77	Hemopexin	GECQAEGVLFFQGDR	+	+	QGDR	12
	1,840.91	Alpha-2-macroglobulin	AHTSFQISLSVSYTGSR	-	+	-	32
VEVSR	949.46	Afamin	FTFEYSR	+	+	FEYSR	33
	1,160.63	Alpha-1-acid glycoprotein	WFYIASAFR	-	+	-	70
	1,283.6	Apolipoprotein A-I	WQEEMELYR	+	+	-	30
	1,511.87	Albumin	VPQVSTPTLVEVSR	+	+	VEVSR	67
	1,840.91	Alpha-2-macroglobulin	AHTSFQISLSVSYTGSR	-	+	-	32
	1,874.02	Clusterin	LFDSDPITVTVPVEVSR	-	+	VEVSR	127
	1,545.79	Alpha-2-macroglobulin	LVHVEEPHTETVR	+	+	-	14
	2,090.13	Alpha-1-antitrypsin	ELDRDTVFALVNYIFFK	-	+	-	37
	2,496.36	Plasminogen	VILGAHQEVNLEPHVQEIEVSR	+	+	IEVSR	49
	2,799.52	Fibronectin	GLKPGVVYEGQLISIQQYGHQEVTR	+	+	QEVTR	20

3.5.2. Ultracentrifugation coupled to TXP immunoprecipitation

Although the application of the albumin and IgG depletion columns was successful in removing two high abundant proteins (see section 3.5.1), the TXP elutions revealed the presence of other high abundant proteins instead. Because only one additional target peptide was discovered with the application of four tested TXP antibodies, which was also only a high abundant one, the use of depletion columns was not pursued any further.

Another huge drawback in the use of depletion columns is the risk of losing target proteins along with the high abundant proteins. Although depletion kits facilitate the efficient removal of high abundant proteins, other proteins have also been shown to be removed (Ichibangase *et al.*, 2009). Granger *et al.* (2005) showed that the amount of very low abundant proteins, in particular (e.g. cytokines), are significantly reduced after albumin depletion. One possibility to circumvent the loss of proteins of interest would be to carry out depletion procedures after the tryptic digest of the plasma sample. This would prevent the loss of proteins, that are e.g. bound to albumin in its function as a carrier protein.

1933 showed Theodor Svedberg that ultracentrifugation can be used for the separation of molecules with different molecular masses (Svedberg, 1933). Tengerdy and Faust (1971) demonstrated the separation of antigen-antibody complexes and antigens by ultracentrifugation. Based on those results, it should be possible to separate peptide-antibody complexes from a complex tryptic digest using ultracentrifugation. This procedure was inserted in the TXP immunoaffinity workflow to remove non-specific peptides.

3.5.2.1. Assay establishment using a model system

A model system was established using a synthetic biotinylated HA-Peptide (Biotin-Doa-Doa-YPYDVPDYA-NH_2, Intavis, Cologne, Germany) and a monoclonal anti-HA antibody (clone 3F10, provided by Prof. Elisabeth Kremmer, Munich, Germany) to perform a proof-of-principle experiment for the ultracentrifugation procedure. The quantitative read-out of the assays was performed by microsphere-based immunoassays (Luminex), which were established to enable quantification of free peptide, antibody and peptide-antibody-complex.

The assay measuring the synthetic peptide revealed a linear range between 0.04 and 3.33 ng/ml (see figure 3.26 **A**). Similar results were achieved for the HA-antibody (see figure 3.26 **B**). The 4-parametric fitting showed good coefficients of determination → $R^2 = 0.998$ (peptide) and $R^2 = 0.995$ (antibody).

The separation efficiency of the density gradient ultracentrifugation as well as the binding capacity of the antibody were analyzed using the HA-model system. After an

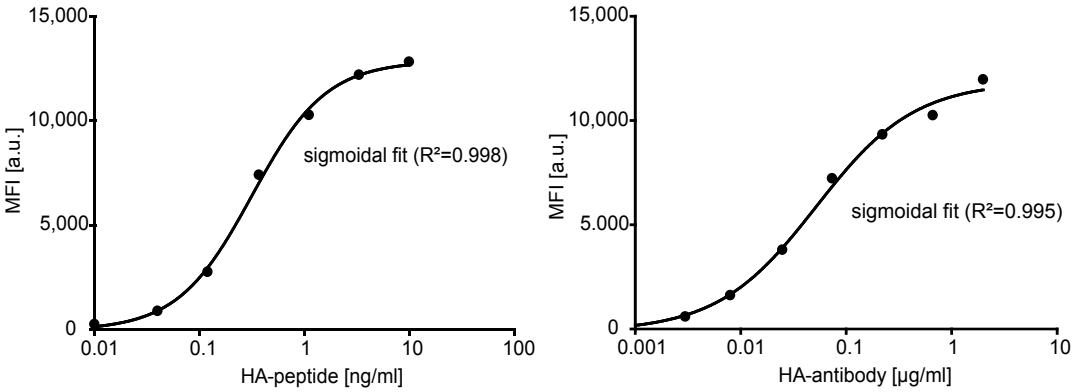

Figure 3.26.: Microsphere-based immunoassays of a dilution series of the biotinylated HA-peptide **A** and the HA-antibody **B**

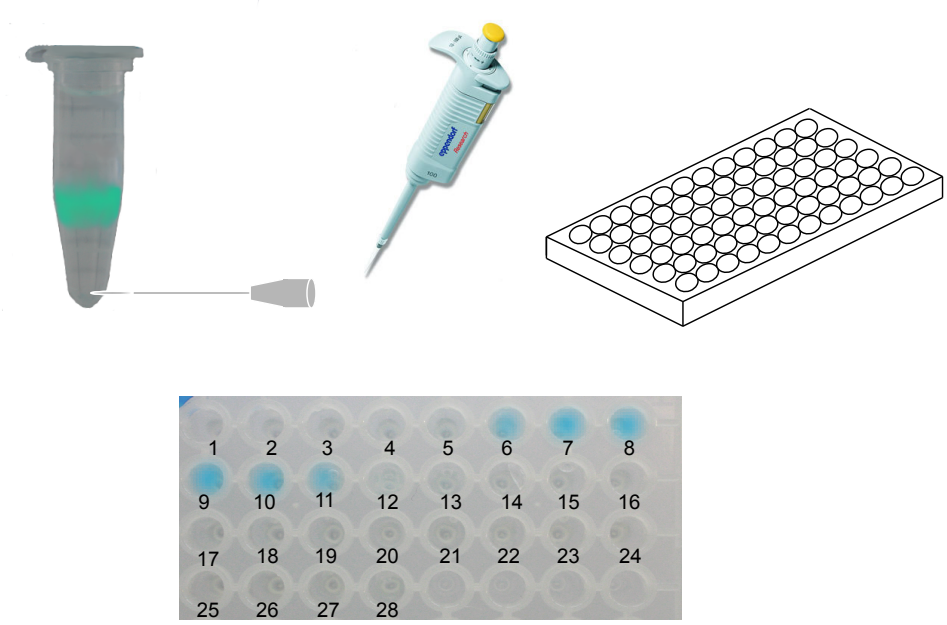

Figure 3.27.: Fractionation after ultracentrifugation using a 20-gauge needle, which was plunged horizontally into the bottom of the centrifugation tube (inlet facing down). Thus, droplets draining out of the needle were collected with a pipette and transferred into a 96 well PCR plate. In fractions 6 to 11 the dye-labeled antibody is visible.

ultracentrifugation run, the complete gradient was fractionated in 27 x 50 μl fractions. Figure 3.27 depicts the fractionation method in detail.

For the fractionation a 20-gauge needle was plunged horizontally into the bottom of the centrifugation tube, whereas the inlet was facing down. The fractions were collected with a pipette and transferred into a 96 well PCR plate. With the use of dye-antibody conjugates (Cy5) a visual control of the antibody location was possible, figure 3.27. In fractions 6 to 11 the dye-antibody conjugate is visible.

Aliquots of each fraction were diluted and analyzed with the corresponding immunoassays for the HA-model. Figure 3.28 shows the analyte distribution after ultracentrifugation. With HA-peptide excess in the sample, the majority of the free peptide

(light gray) was detected at the top of the gradient (fraction 13-28). In contrast, the peptide-antibody-complex (black) and the antibody (dark gray) were mainly detected in the bottom fractions of the centrifugation tube (fraction 1-12).

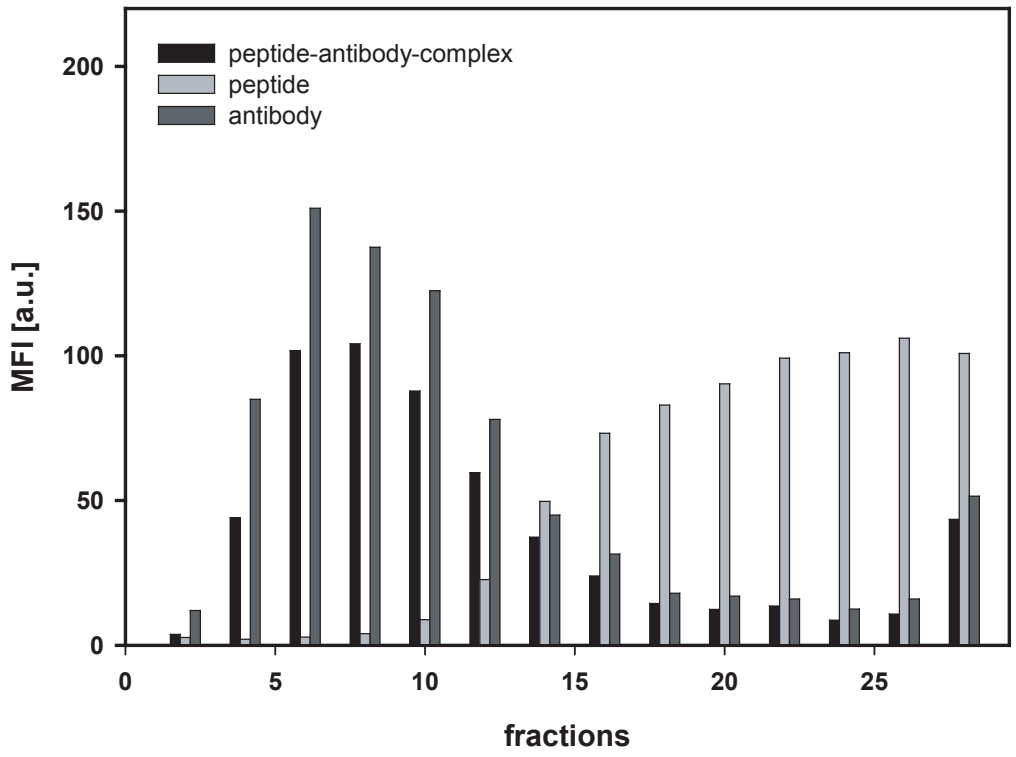

Figure 3.28.: Distribution of free monoclonal rat anti-HA antibody, biotinylated HA peptide and resulting antibody-peptide complex following 15 h sucrose gradient ultracentrifugation. 27 fractions (50 μl each) were collected and analyzed using the Luminex immunoassay platform. Mean fluorescent intensity (MFI) values of each analyte are plotted (ascending numbers from bottom to top of sample tube). For better comparison, MFI values divided by 10 are reported for the antibody-peptide immunocomplex and MFI divided 100 for the peptide.

Over 70 % of the antibody (both free and peptide-bound) were found to be located in the bottom 500 μl of the sucrose gradient, which contained less than 1 % of the unbound peptide, see figure 3.29. Hence, the ultracentrifugation procedure appeared to enable the efficient separation of free HA-peptides from the analyte-antibody-complex.

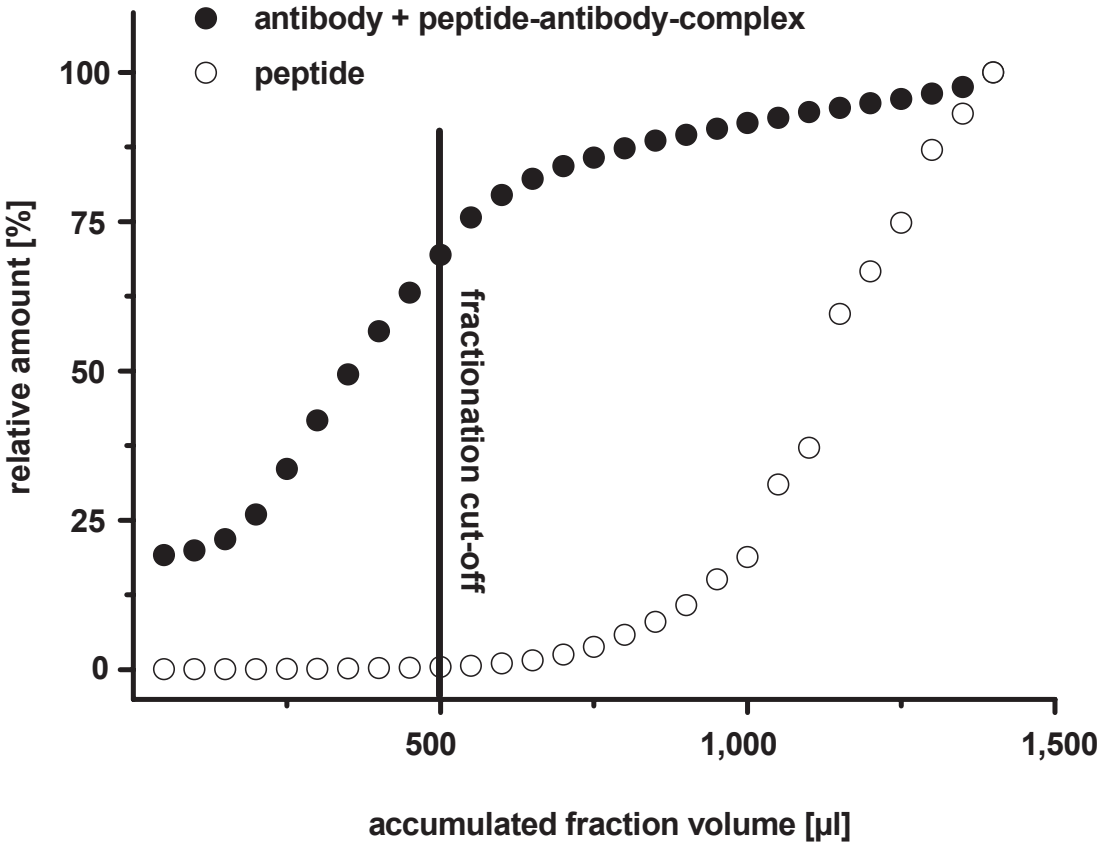

Figure 3.29.: Quantitative analyte distribution after ultracentrifugation. The fraction of the total amount of anti-HA antibody and biotinylated HA peptide accumulated with total collected fraction volume measured from the bottom of the sample tube. The fractionation cut-off represents the volume containing 70 % accumulation of peptide-antibody immunocomplex but less than 0.5 % of the residual free peptide. a.u., arbitrary units.

3.5.2.2. Impact of ultracentrifugation on a TXP immunoprecipitation

Following validation of the ultracentrifugation procedure using HA-peptide and antibody, the procedure was inserted in the plasma TXP immunoprecipitation workflow. The impact of ultracentrifugation on the immunoaffinity workflow was evaluated using anti-EGYR antibodies. The ultracentrifugation step was inserted between the incubation of the plasma digest with the anti-EGYR antibodies and protein G capture with magnetic microspheres.

According to the resolution of the ultracentrifugation validation process 500 μl volume was drawn as a bottom fraction, 400 μl as middle fraction and 300 μl as top fraction in further experiments. Elution after protein G microsphere capture should contain less peptides derived from high abundant proteins compared to the workflow without ultracentrifugation.

Figure 3.30 **B**, **C** and **D** show the MALDI MS read-out of the ultracentrifugation fractions after the protein G microsphere separation procedure. For process control antibody sedimentation was visually assessed by ultracentrifugation of a Cy5-labeled IgG (pictures shown in 3.30 **A**, **B** and **C**).

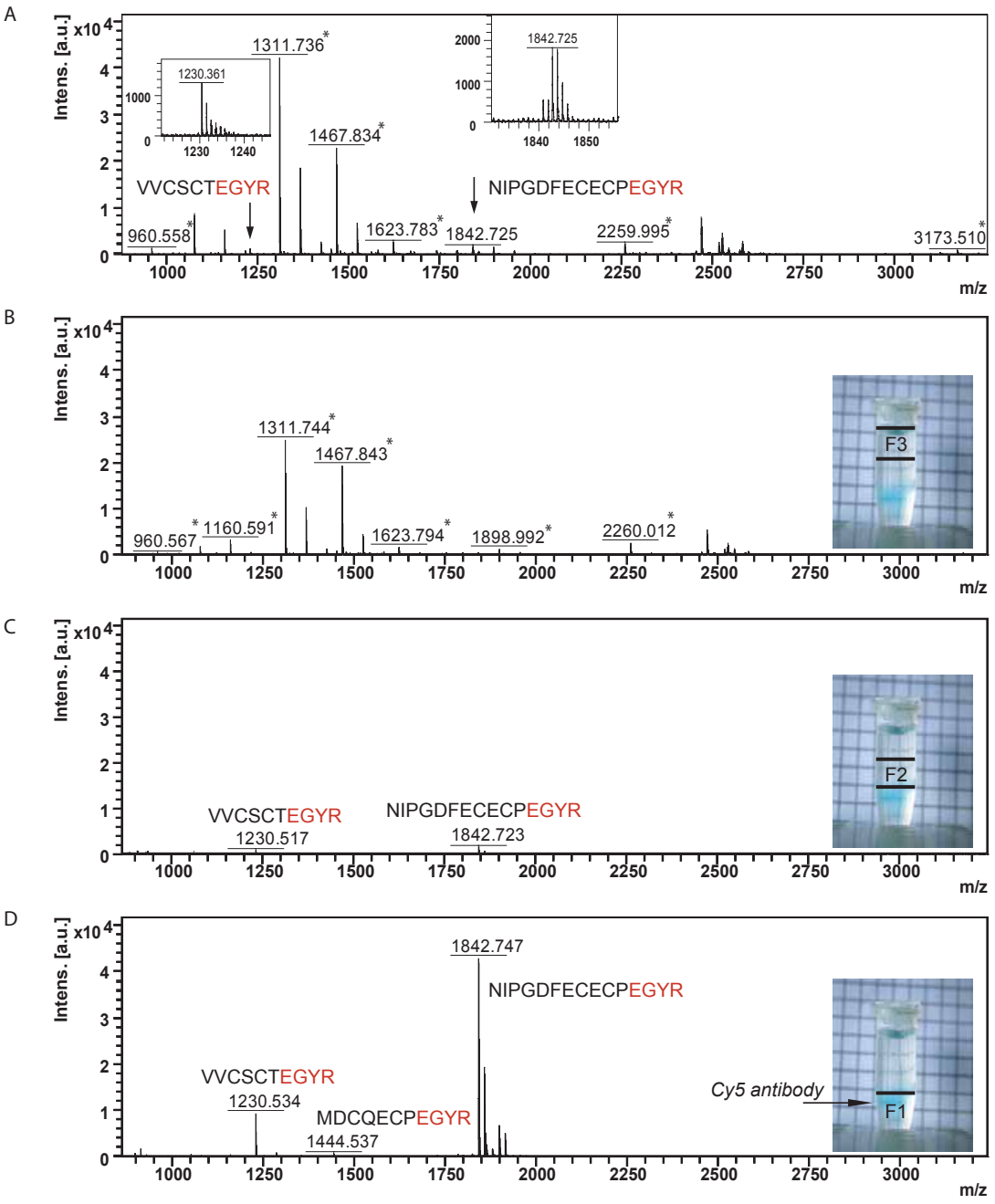

Figure 3.30.: Mass spectra of tryptic plasma peptides enriched using the anti-EGYR TXP antibodies: (A) without sucrose density gradient separation; (B) in the top 300 μl fraction; (C) in the middle 400 μl fraction and (D) in the bottom 500 μl fraction following sucrose density gradient ultracentrifugation. Samples containing antibodies conjugated with the dye Cy5 were added to each ultracentrifuge run to visualize the location of antibodies within the sucrose layers after centrifugation (inserts in figures A, B, C and D). The peptides corresponding to non-targeted high abundant plasma proteins are marked with an asterisk.

In order to obtain some measure of the improved sensitivity gained through the implementation of the ultracentrifugation procedure, the signal-to-noise value of the NIPGDFECECPEGYR target peptide (m/z 1,842.747, Vitamin K-dependent Protein S) was relatively compared with the signal-to-noise values of alpha-1-acid glycoprotein 1 (m/z 1,160.70, WFYIASAFR) and human serum albumin (m/z 1,311.77, HPDYSVVLLLR and m/z 1467.85, RHPDYSVVLLLR), see figure 3.31. Implementation of the ultracentrifugation step resulted in a statistically significant increase in the signal to noise ratio of the EGYR target to non-specific peptide of over 2,000 fold.

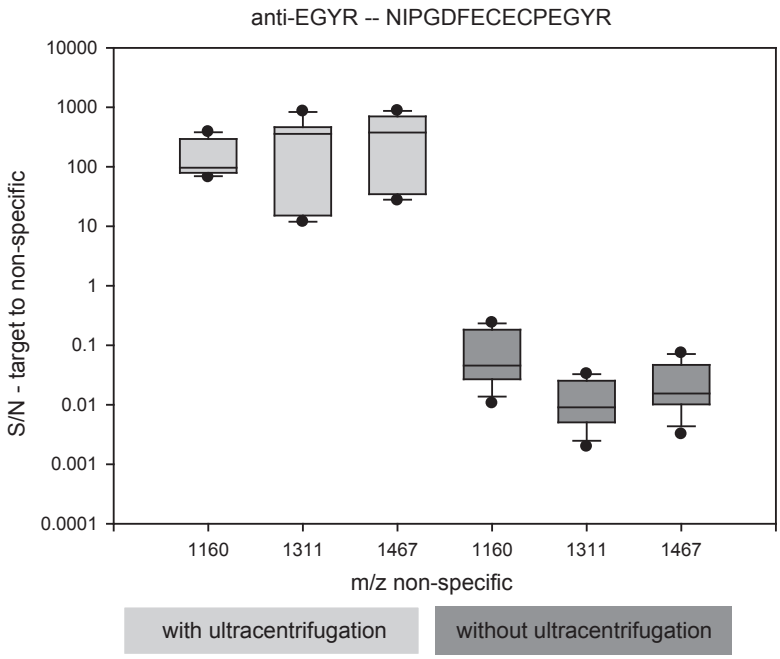

Figure 3.31.: Distribution of signal to noise ratios for target peptide NIPGDFECECPEGYR (m/z 1,842.68, Vitamin K-dependent Protein S) relative to three non-antibody targeted peptides from two different proteins alpha 1-acid glycoprotein 1 (m/z 1,160.70, WFYIASAFR) and two peptides from human serum albumin (m/z 1,311.77, HPDYSVVLLLR and m/z 1,467.85, RHPDYSVVLLLR) comparing the assay with and without the ultracentrifugation step. Data from three assay replicates were included in one box plot. The S/N ratios of the values generated with the ultracentrifugation procedure are significantly higher compared to the respective values of the assays without ultracentrifugation ($P<0.001$). Statistical significances were calculated with Mann-Whitney test using StatistiXL 1.8.

3.6. Qualitative evaluation of a plasma immunoprecipitation assay combined with ultracentrifugation

After demonstrating the feasibility of using ultracentrifugation as pre-step to immunoprecipitation, a larger panel of TXP antibodies was investigated for their capability to capture target peptides out of trypsin-digested human blood plasma. Combining the results from the protocols with and without ultracentrifugation, it was possible to identify 42 plasma digest peptides with only 15 TXP antibodies, see table 3.18, 3.19 and 3.20.

Table 3.18.: Captured peptides part 1. If the exact peptide tag was captured, the tag is marked bold in the peptide. Red marked peptides match the previous synthesized standard peptides.

							UC			no UC		
TXP tag	MW [Da]	sequence	protein	Accession number	Plasma conc. [pg/ml]	Reference	Mascot Score	Identified	Identified in triplicates	Mascot Score	Identified	Identified in triplicates
DAPK	1,180.61	IYHSHI**DAPK**	Ceruloplasmin	P00450	2,80E+08	Polanski and Anderson (2007)	67	X	X	38	X	X
DTWK	1,601.84	VSALLTPAEQTGTWK	Apolipoprotein B-100	P04114	9,15E+08	Hortin *et al.* (2008)	59	X				
DTWK	1,893.89	ASTPNGYDNGIIWATWK	Isoform Gamma-B of Fibrinogen gamma chain	P02679	9,15E+08	Hortin *et al.* (2008)	95	X	X			
DYGK	1,074.54	LDELRDEGK	Serum albumin	P02768	4,10E+10	Polanski and Anderson (2007)				35	X	
DYGK	2,350.13	EPCVESLVSQYFQTVT**DYGK**	Apolipoprotein A-II	P02652	2,44E+08	Polanski and Anderson (2007)	141	X		170	X	X
EGYR	1,230.49	VVCSCT**EGYR**	Coagulation factor IX	P00740	4,50E+06	Hortin *et al.* (2008)	66	X	X			
EGYR	1,444.51	MDCQECP**EGYR**	Isoform 2 of Filamin-A	P21333	3,50E+04	Alper *et al.* (2009)	35	X				
EGYR	1,842.682	NIPGDFECECP**EGYR**	Vitamin K-dependent protein S	P07225	2,50E+07	Hortin *et al.* (2008)	113	X	X	62	X	
EHLR	1,395.782	SSNLIILEEHLK	Complement factor H	P08603	5,00E+08	Hortin *et al.* (2008)	48	X		54	X	X
EHLR	1,545.686	GFMQTYYDDHLR	Apolipoprotein C-IV	P55056	1,00E+06	Hortin *et al.* (2008)	38	X				
EHLR	2,509.049	SCVGETTESTQCEDEEL**EHLR**	Complement component C7	P10643	5,20E+07	Polanski and Anderson (2007)	163	X	X	136	X	X
ESFR	1,126.551	LHVDPENFR	Hemoglobin subunit delta	P68871	3,25E+07	Hortin *et al.* (2008)	56	X	X	78	X	X
ESFR	1,169.510	SSALDMENFR	Inter-alpha-trypsin inhibitor heavy chain H2	P19823	2,10E+08	Hortin *et al.* (2008)	32	X		42	X	X
ESFR	1,519.721	ALYLQYTDETFR	Ceruloplasmin	P00450	2,80E+08	Polanski and Anderson (2007)	108	X	X	98	X	X
ESFR	1,647.816	KALYLQYTDETFR	Ceruloplasmin	P00450	2,80E+08	Polanski and Anderson (2007)	59	X		70	X	X
ESFR	1,927.919	SLAELGGHLDQQVEEFR	Apolipoprotein A-IV	P06727	1,90E+08	Hortin *et al.* (2008)	52	X		80	X	X
ESFR	2,707.100	HQPQEFPTYVEPTNDEICEAFR	Vitamin D-binding protein	P02774	5,50E+08	Hortin *et al.* (2008)	128	X	X	148	X	X

Table 3.19.: Captured peptides part 2. If the exact peptide tag was captured, the tag is marked bold in the peptide. Red marked peptides match the previous synthesized standard peptides. n.k. - not known

							UC			no UC		
TXP tag	MW [Da]	sequence	protein	Accession number	Plasma conc. [pg/ml]	Reference	Mascot Score	Identified	Identified in triplicates	Mascot Score	Identified	Identified in triplicates
EVLR	774.415	ECEELLR	Sterile alpha and TIR motif-containing protein 1	Q6SZW1	n.k.	-	31	X				
EVLR	1,290.698	SLTTNIMEILR	Fibrinogen alpha chain	P02671	1,25E+09	Hortin *et al.* (2008)	72	X	X			
EVLR	1,629.811	SLTTNIMEILR	Fibrinogen alpha chain	P02671	1,25E+09	Hortin *et al.* (2008)	139	X	X	51	X	
EVLR	1,883.895	IFFYDSENPPAS**EVLR**	Serum paraoxonase/ arylesterase1	P27169	5,93E+07	Polanski and Anderson (2007)	145	X	X	42	X	
EVLR	2,199.098	YNPVVIDFEMQPIH**EVLR**	Complement component C8 alpha chain	P07357	4,70E+07	Hortin *et al.* (2008)	68	X	X			
FPPK	1,492.652	TPSCGDICN**FPPK**	C4b-binding protein alpha chain	P04003	3,65E+08	Hortin *et al.* (2008)	70	X	X			
FPPK	2,619.280	THTCPPCPAPELLGGPSVFL**FPPK**	Anti-RhD monoclonal T125 gamma1 heavy chain precursor	P01857	4,30E+09	Hortin *et al.* (2008)	116	X	X			
LEVK	1,419.718	VQFELHYQEVK	Inter-alpha-trypsin inhibitor heavy chain H2	P19823	2,10E+08	Hortin *et al.* (2008)	50	X		75	X	
PIEK	824.482	GLPA**PIEK**	Ig gamma-2 chain C region	P01859	2,84E+09	Hortin *et al.* (2008)	55	X	X	53	X	X
PIEK	838.487	ALPA**PIEK**	Ig gamma-1 chain C region	P01857	4,30E+09	Hortin *et al.* (2008)	66	X	X	64	X	X
PIEK	1,266.737	VSNKALPA**PIEK**	Ig gamma-1 chain C region	P01857	4,30E+09	Hortin *et al.* (2008)				36	X	

Table 3.20.: Captured peptides part 3. If the exact peptide tag was captured, the tag is marked bold in the peptide. Red marked peptides match the previous synthesized standard peptides.

						UC			no UC		
TXP tag	MW [Da]	sequence	protein	Accession number	Plasma conc. [pg/ml]	Reference	Mascot Score	Identified	Identified in triplicates	Mascot Score	Identified	Identified in triplicates
QGYR	1,022.546	ATVVYQGER	Beta-2-glycoprotein 1	P02749	2,25E+08	Hortin *et al.* (2008)	39	X	X	47	X	X
QGYR	1,110.543	STTPDITGYR	Fibronectin	P02751	3,00E+08	Hortin *et al.* (2008)				32	X	
QGYR	1,330.735	LNMGITDLQGLR	Complement C4-A	P0C0L4	1,00E+08	Hortin *et al.* (2008)				40	X	
QGYR	1,712.790	GECQAEGVLFFQGDR	Hemopexin	P02790	8,25E+08	Hortin *et al.* (2008)	88	X	X	89	X	X
VLLD	1,110.567	**VLLD**GVQNPR	Complement C3	P01024	1.3E +09	Polanski and Anderson (2007)	63	X		71	X	
VLLD	1,591.863	**VLLD**QLGTTISFER	Apolipoprotein B-100	P04114	9,15E+08	Hortin *et al.* (2008)	85	X		59	X	
VLLD	1,702.787	VFLDCCNYITELR	Complement C3	P01024	1.3E +09	Polanski and Anderson (2007)				57	X	
VELED	1,117.530	**VELED**WNGR	Isoform Gamma-B of Fibrinogen gamma chain	P02679	9,15E+08	Hortin *et al.* (2008)	64	X	X	64	X	
VELED	2,198.953	**VELED**WAGNEAYAEYHFR	Isoform 1 of Fibrinogen alpha chain	P02671	1,25E+09	Hortin *et al.* (2008)	80	X		55	X	X
AFVK	978.466	DGAGDV**AFVK**	Serotransferrin	P02787	4,00E+09	Polanski and Anderson (2007)	30	X				
AFVK	1,152.576	QPSSAFA**AFVK**	Complement C3	P01024	1.3E +09	Polanski and Anderson (2007)	45	X		66	X	
VEVSR	1,511.856	VPQVSTPTL**VEVSR**	Serum albumin	P02768	4,10E+10	Polanski and Anderson (2007)	127	X	X	112	X	X
VEVSR	1,639.947	KVPQVSTPTL**VEVSR**	Serum albumin	P02768	4,10E+10	Polanski and Anderson (2007)	125	X	X			
VEVSR	1,873.994	LFDSDPITVTVP**VEVSR**	Clusterin	P10909	1.0E +08	Hortin *et al.* (2008)	25	X				

A maximum of three peptides sharing the exact C-terminal TXP tag sequence were observed in immunoprecipitates of one antibody (anti-EGYR). TXP antibodies also captured peptides which harbored one other amino acid compared to the used TXP antigen. Generally, the other amino acids were similar in structure to those in the TXP antigen. Accepting this specificity, a maximum of six peptides were captured by one TXP antibody at the same time (anti-EVLR and anti-ESFR). In most cases, at least two peptides, in which a maximum of one amino acid was replaced within the TXP epitope, could be captured by one antibody and identified. Only one peptide could be identified with anti-DAPK and anti-LEVK antibodies. For four antibodies (anti-DTWK, anti-ESFR, anti-LEVK and anti-QGYR) only peptides containing one mismatch in the TXP target sequence could be identified. This implies that TXP antibodies targeting a short 4-5 amino acid sequence can be applied for peptide enrichment from plasma digest samples. With the introduction of an ultracentrifugation step it was possible to identify 37 peptides in at least one out of three technical replicate experiments. 57 % of 37 peptides could be identified in all three replicates. In comparison, 29 peptides were identified without ultracentrifugation. Of these, only 55 % could be identified in all three replicates. Thus, with the use of the ultracentrifugation method, more peptides containing the respective target sequence (including peptides with one mismatch in the epitope) were identified.

Similarly as shown in figure 3.31, a comparison of the enrichment of target peptide to non-specific peptides was performed for conditions with and without ultracentrifugation. The signal to noise values of one target peptide per antibody were compared with signal to noise values of each of three non-specifically detected peptides. With 10 out of 15 TXP antibodies, a significantly improved signal to noise ratio was achieved for the target peptide with the ultracentrifugation step (figure 3.31, Supplemental figures A.43 to A.56). For four antibodies anti-AFVK, anti-DYGK, anti-LEVK, anti-QGYR and anti-VELED, the ratio did not improve. Hence, for the majority of the tested TXP antibodies, a significant improvement of the target peptide signal to noise ratio was achieved by applying an ultracentrifugation procedure to the assay procedure.

In order to evaluate the assay, lists of tryptic peptides were compiled that should have been detected by the TXP antibodies. Based on two empirical plasma proteome databases, the Peptide Atlas Plasma (Build May 2010 containing 16,987 entries, Deutsch *et al.* (2008)) and the database created by the HUPO Plasma Proteome Project (Omenn *et al.*, 2005), the experimental results are compared in tables 3.21, 3.22 and 3.23.

Table 3.21.: Plasma proteome database - TXP peptides 1. Comparison of peptide sequences identified in TXP immunoaffinity enriched fractions (underlined) versus peptide sequences found in empirical databases representing the subset of tryptic peptides experimentally shown to be detectable by mass spectrometry.

Sequence	Molecular mass [Da]	Uniprot reference	Protein Atlas Human Plasma	HUPO Plasma Proteome Project
IYHSHIDAPK	1,179.6087	P00450 Ceruloplasmin	PAp00044520	IPI00017601.1
FFQYDTWK	1,133.5233	P01344 Insulin-like growth factor II	PAp00137404	
EPCVESLVSQYFQTVTDYGK	2,349.0667	P02652 Apolipoprotein A-II	PAp00024985	IPI00021854.1
VVCSCTEGYR	1,229.4792	P00740 Coagulation factor IX	PAp00378430	IPI00296176.1
DDGSWEVIEGYR	1,424.6259	P00367 Glutamate dehydrogenase 1, mitochondrial; P49448 Glutamate dehydrogenase 2, mitochondrial	PAp00064702	
MDCQECPEGYR	1,443.4840	P21333 Filamin A	PAp00026827	
NIPGDFECECPEGYR	1,841.6970	P07225 Vitamin K-dependent protein S		IPI00294004.1
VVNSTTGPGEHLR	1,365.7050	P07996 Thrombospondin-1	PAp00415875	
SCVGETTFESTQCEDEELEHLR	2,508.0000	P10643 Complement component C7	PAp00027646	IPI00296608.1
APTAQVESFR	1,104.5615	P24821 Tenascin	PAp00091921	
APEENTAAIVYVENGESENQESFR	2,682.2094	Q8TEP8 Centrosomal protein of 192 kDa		IPI00181475.1
TDMELEVLR	1,104.5537	P12955 Xaa-Pro dipeptidase	PAp00094413	IPI00257882.1
FLEEHPGGEEVLR	1,510.7467	P00167 Cytochrome b5	PAp00185870	
LLNYNPEDPPGSEVLR	1,811.9102	Q15166 Serum paraoxonase/lactonase 3	PAp00093392	IPI00217446.1
IFFYDSENPPASEVLR	1,882.9151	P27169 Serum paraoxonase/arylesterase 1	PAp00025909	IPI00218732.1
MEGDSVLLEVDGEEVLR	1,888.9138	P04278 Sex hormone-binding globulin	PAp00044875	IPI00023019.1
YNPVVIDFEMQPIHEVLR	2,198.1243	P07357 Complement component C8 alpha chain	PAp00039195	IPI00011252.1

Table 3.22.: Plasma proteome database - TXP peptides 2. Comparison of peptide sequences identified in TXP immunoaffinity enriched fractions (underlined) versus peptide sequences found in empirical databases representing the subset of tryptic peptides experimentally shown to be detectable by mass spectrometry.

Sequence	Molecular mass [Da]	Uniprot reference	Protein Atlas Human Plasma	HUPO Plasma Proteome Project
TPSCGDICNFPPK	1,491.6106	P04003 C4b-binding protein alpha chain	PAp00060583	IPI00021727.1
THTCPPCPAPELLGGPSVFLFPPK	2,618.2640	P01857 Ig gamma-1 chain C region	PAp00061684	IPI00152302.1
EASHVLEVK	1,010.5449	Q9Y5S2 Serine/threonine-protein kinase MRCK beta		IPI00005689.2
IDDIWNLEVK	1,243.6499	P04114 Apolipoprotein B-100	PAp00025874	IPI00022229.1
ALEEANADLEVK	1,300.6562	P13646 Keratin, type I cytoskeletal 13; P02533 Keratin, type I cytoskeletal 14; P19012 Keratin, type I cytoskeletal 15; P08779 Keratin, type I cytoskeletal 16	PAp00039444	IPI00179358.1 IPI00218819.1
ALEEANTELEVK	1,344.6824	Q04695 Keratin, type I cytoskeletal 17	PAp00032389	IPI00244103.1
VFGAPEVLENLEVK	1,542.8344	Q8TEM1 Nuclear pore membrane glycoprotein 210		IPI00291755.1
LSQSGEVGEPAGTDPGLDDLDVALSNLEVK	3,024.4817	Q86UX7 Fermitin family homolog 3	PAp00074141	
GLPAPIEK	823.4854	P01859 Ig gamma-2 chain C region	PAp00062066	IPI00004608.1
ALPAPIEK	837.5011	P01857 Ig gamma-1 chain C region; P01860 Ig gamma-3 chain C region	PAp00029028	IPI00004617.1 IPI00152302.1 IPI00168728.1
VSNKALPAPIEK	1,265.7393	P01857 Ig gamma-1 chain C region; P01860 Ig gamma-3 chain C region	PAp00028553	IPI00004617.1 IPI00152302.1 IPI00168728.1
DAGMQLQGYR	1,137.5287	P00505 Aspartate aminotransferase, mitochondrial	PAp00131640	
TDGCQHFCLPGQESYTCSCAQGYR	2,881.0500	P22891 Vitamin K-dependent protein Z	PAp00445892	IPI00027843.1
VELEDWNGR	1,116.5252	P02679 Fibrinogen gamma chain	PAp00045733	IPI00021891.3
VELEDFNGNR	1,191.5572	O75636 Ficolin-3		IPI00293925.1
VELEDWAGNEAYAEYHFR	2,197.9756	P02671 Fibrinogen alpha chain	PAp00149457	

Table 3.23.: Plasma proteome database - TXP peptides 3. Comparison of peptide sequences identified in TXP immunoaffinity enriched fractions (underlined) versus peptide sequences found in empirical databases representing the subset of tryptic peptides experimentally shown to be detectable by mass spectrometry.

Sequence	Molecular mass [Da]	Uniprot reference	Protein Atlas Human Plasma	HUPO Plasma Proteome Project
VLLDQLR	855.5229	Q9HDC9 Adipocyte plasma membrane-associated protein		IPI00031131.2
VLLDGVQNPR	1,109.6243	P01024 Complement C3	PAp00028461	IPI00164623.2
VLLDGVQNLR	1,125.6556		PAp00138495	
VLLDQLGTTISFER	1,590.8665	P04114 Apolipoprotein B-100	PAp00028462	IPI00022229.1
VLLDWINDVLVEER	1,711.9195	Q9HBI1 Beta-parvin	PAp00139400	
GDVAFVK	734.4015	P02787 Serotransferrin; P02788 Lactotransferrin; P08582 Melanotransferrin	PAp00161845	IPI00022463.1
DGAGDVAFVK	977.4869	P02787 Serotransferrin	PAp00024622	IPI00022463.1
QPSSAFAAFVK	1,151.6026	P01024 Complement C3	PAp00027449	IPI00032257.1 IPI00164623.2
CLAEGAGDVAFVK	1,335.6329	P08582 Melanotransferrin	PAp00001121	
CLAENAGDVAFVK	1,392.6544	P02788 Lactotransferrin	PAp00064486	
DAVEKPQEFTIVAFVK	1,819.9769	P04114 Apolipoprotein B-100	PAp00024585	IPI00022229.1
GYTQQLAFRQPSSAFAAFVK	2,216.1425	P01024 Complement C3	PAp00025622	
TIELLGQEVSR	1,243.6822	Q6UXH0 Hepatocellular carcinoma-associated protein TD26	PAp00139634	
VPQVSTPTLVEVSR	1,510.8404	P02768 Serum albumin	PAp00028510	IPI00022434.1
KVPQVSTPTLVEVSR	1,638.9353	P02768 Serum albumin	PAp00026329	IPI00022434.1
LFDSDPITVTVPVEVSR	1,872.9881	P10909 Clusterin	PAp00026453	IPI00291262.1
VILGAHQEVNLESHVQEIEVSR	2,485.2973	P08519 Apolipoprotein(a)	PAp00094707	IPI00029168.1
VILGAHQEVNLEPHVQEIEVSR	2,495.3180	P00747 Plasminogen	PAp00045765	IPI00019580.1
EDSTALVMNSTTESNTVFSSVSLDAATEVSR	3,247.5083	Q8WXI7 Mucin-16		IPI00103552.2
DTFVNASR	908.4404	P05155 Plasma protease C1 inhibitor	PAp00024775	IPI00291866.1

To date, a total of 53 peptides were listed in one or both databases containing the epitopes of the antibodies used here. 21 of these peptides were identified with ultracentrifugation and 14 without by the use of 15 antibodies.

Chapter 4.

Discussion

4.1. Plasma proteome analysis using mass spectrometry

The vast library of organo-specific, disease-related information contained within blood plasma, combined with its availability and ease of sampling, makes it the most significant clinical sample for biomarker discovery to date. In the last ten years plasma proteome analysis has seen massive improvements in the analytical methodologies employed. There are nevertheless still challenges to be faced. The biggest of these is the high complexity of the plasma proteome with a concentration range spanning more than ten orders of magnitude (Masaki *et al.*, 2006). Peptides from high abundant proteins can mask signals of peptides from low abundant proteins due to ionization suppression, rendering the mass spectrometer blind to the low abundant but often more clinical relevant components (Jessome and Volmer, 2006; Aebersold and Mann, 2003; Cologna *et al.*, 2010). Hence depletion or removal of the highly abundant proteins is an important goal in human plasma proteomics. Keshishian *et al.* (2009) and Fortin *et al.* (2009a) used depletion columns to remove the high abundant proteins in plasma to detection limits in the low ng/ml range. The endoprotease trypsin generates peptides in a suitable mass range for mass spectrometry (around 500 - 5,000 Da) and is therefore commonly used as proteolytic agent, see Hillenkamp and Peter-Katalinic (2007). Mass spectrometry based proteome analysis is mostly performed with tryptically digested peptides due to their adequate size and ionization properties for a mass spectrometric read-out.

In this thesis, an immunoaffinity-based method was established for the enrichment of groups of peptides sharing a common N-terminal or C-terminal 4-5 amino acid motif from tryptically digested human plasma using so-called TXP antibodies.

4.2. Evaluation TXP immunoprecipitation assays for plasma analysis

The current gold standard for the analysis of the plasma proteome including biomarker validation are immunoassays like radioimmunoassays (RIA) and enzyme-linked im-

munosorbent assays (ELISA). In particular, *sandwich* ELISAs enable direct quantification of target analytes in a complex plasma sample down to low pg/ml (Lequin, 2005). A huge limitation in the establishment of ELISA assays is the marginal availability of appropriate protein-specific antibodies. To circumvent the complex generation of reliable protein-specific antibodies, immunoaffinity MS can be used for proteome analysis. Anderson *et al.* (2004) described a method for the quantification of peptides in a complex protein digest using immunoprecipitation by peptide-specific antibodies and stable isotope standards with subsequent LC MS read-out → SISCAPA (Stable Isotope Standards and Capture by Anti-Peptide Antibodies).

To reduce the number of peptide-specific antibodies, that would otherwise be required, antibodies were generated against short C- or N-terminal peptide sequences → triple X antibodies (*TXP*). The concept of using one antibody for multiple analytes and consequently applying a group-specific enrichment was introduced by Rush *et al.* (2005) and Wingren *et al.* (2009) and for the TXP antibodies Poetz *et al.* (2009). The application of these TXP antibodies has been previously described by Hoeppe *et al.* (2010), for the capture of groups of peptides from tryptically digested biological samples. The TXP immunoaffinity workflow bears several advantages over other methods currently applied to targeted proteomics. The use of the TXP algorithms for antibody selection (Planatscher *et al.*, 2010) enables a more efficient use of resources as the number of antibodies required for a set of proteins is minimized. The estimation of target antigens can be determined for whole proteomes as well as for a targeted selection of analytes.

Rabbit sera, which were immunized against the synthesized short peptide sequences, were evaluated for specificity and cross-reaction using peptide arrays. These antibody binding tests showed good selectivities regarding antigen binding to free peptides for most of the tested antisera (table 3.1). While the antisera from the C-terminal peptides showed good antigen binding properties, the N-terminal antisera revealed insufficient functionality. Some of the antisera also caused a strong reaction against the blocked peptides, which were intended to mimic "internal sequences" of e.g. not completely digested protein samples or even complete proteins. Based on the results of the antibody binding assays, the TXP antibodies were purified by fast protein liquid chromatography (FPLC).

An immunoprecipitation assay was established using the immuno-purified TXP antibodies to capture signature peptides derived from groups of trypsin-digested plasma proteins. To increase sample throughput and assay reproducibility, an automated system using magnetic microspheres was incorporated into the assay procedure (Whiteaker *et al.*, 2007a). The assays were carried out using a magnetic microsphere handling system (KingFisher, Thermo Scientific), providing high washing efficiency. High washing efficiency was achieved by the microsphere handling procedure, transferring magnetic microspheres from microtiterplate to microtiterplate, instead of liquid. Transferring the liquid would run the high risk of leaving residual liquid in the plates, which leads to

sample loss and carry-over of non-specific molecules.

However, although such automated liquid handling techniques increase throughput and reproducibility, they require the need for detergents to guarantee a loss-free microsphere transfer. Without detergent, the magnetic force between the sampling rods and the microspheres is not strong enough to overcome the surface tension of the aqueous solutions employed. Finding an appropriate detergent was critical for assay establishment as most of the common surfactants are not compatible with mass spectrometry.

Ionic detergents should particularly be avoided (e.g. SDS) because they affect the formation of analyte-matrix crystals during sample preparation on the MALDI targets. PEG-(polyethylene glycol)containing surfactants like Triton or Tween 20 are easily ionizable and produce very intense signals with a molecular weight distribution from 400-1,200 Da, the region where many tryptic peptides are expected. Low levels of non-ionic detergents, e.g. n-Octyl-ß-D-glucopyranosid, up to 1 %, can be tolerated by MALDI MS. No significant effect was observed regarding peptide detection according to Zhang and Li (2004). N-Octyl-ß-D-glucopyranosid (NOG) is considered to be a MS-compatible surfactant and was therefore used in the following assays.

High concentrations of salts can affect or even prohibit the co-cristallization of analyte and matrix, which leads to decreased sensitivity (Lottspeich *et al.*, 2006). To desalt the sample without additional subsequent purification over hydrophobic surfaces (C18 respectively ZipTips) a so called "MS-friendly" washing buffer was used: ammoniumbicarbonate buffer with a pH adjusted to 7.4 to guarantee the physiological pH, if a physiological salt content is not maintained. The washing steps of the two PBS washing plates were shown to be efficient in terms of removing non-specifically bound peptides when a synthetic peptide mixture was investigated. Using a plasma digest sample, the unspecific bound peptides from high abundant proteins like albumin were not completely removed after the washing steps, especially when larger quantities of plasma were used (20 μl lyophilized plasma). Unfortunately, increasing the wash steps did not reduce the appearance of non-specific peptides in the TXP immunopurification elutions.

The desalting steps using ABC-buffer proved to be very efficient in removing interfering salts. Very few to no salt originating peaks were detected in the MALDI mass spectra. Altogether, the developed TXP immunoaffinity assay was considered to be efficient in enriching group-specific peptides with the simultaneous depletion of peptides from high abundant proteins (when 5 μl plasma was used) and without the need of additional C18 purification.

To test the purified antibodies for the application in an immunoaffinity assay with subsequent MALDI analysis the TXP antibodies were incubated with a synthetic peptide mix using the established immunoprecipitation assay, and the eluates of this TXP IP were analyzed. Except for one antibody against LEVK, all antibodies showed good

functionality in the peptide capture assays. Most of the captured peptides showed high S/N values and no or very little cross-reactivity was detected. Many analytes were not detectable without immunoprecipitation (see section 3.1.3). Two peptides, having lysine as C-terminal amino acid, were not detected in the MALDI MS analysis without immunoprecipitation. This observation could be explained by the fact that C-terminal lysine containing peptides are not as easily ionized compared to C-terminal arginine peptides which possess basic guanidino functionality (arginine side chain) leading to preferred ionization (Krause *et al.*, 1999).

Anti-VELED and anti-VLLD, which failed in the antibody binding assays, revealed excellent antigen capture properties. Very good S/N values were achieved and no cross-reactivity with other peptides was observed in the MS read-out for the synthetic peptide mix, see figure 3.7.

In contrast to the results of the antibody binding assays, showing that the TXP antibodies also bind internal sequences to a certain degree (e.g. figure A.1), no peptide carrying an internal tag was identified in all tested TXP immunoprecipitations using digested plasma samples (tables 3.18, 3.19, 3.20). The digest was considered to be efficient, as no masses higher than 14 kDa could be detected in a SDS gel, see supplementals figure A.41.

4.2.1. Quantitative evaluation of the immunoaffinity workflow using TXP antibodies - targeted approach

The sensitivity, precision and accuracy of TXP immunoprecipitation were quantitatively evaluated by preparing a dilution series of a synthetic peptide in a human plasma digest. The synthetic peptide used was a tryptic peptide of the erB-2 protein (VCYGLGMEHLR). The receptor tyrosine-proteinkinase erbB-2 has been reported at 11 ng/ml (Wu, 2002).

The quantification capabilities of the immunoaffinity MALDI MS assay was evaluated by preparing a dilution series in 1 % FA containing SIS peptide (10 nM) which was subsequently spotted onto a MALDI target and directly analyzed by MALDI MS without IP. The quantification was carried out by comparing the ratio between the normal and the SIS peptide area under the curve. The accuracy values of the experiment, shown in figure 3.13, revealed a constant decline in accuracy with decreasing peptide amount. Due to the limited dynamic range of the MALDI TOF analyzer (Domon and Aebersold, 2010), three different amounts of SIS were spiked in the dilution series. 100 nM for the upper range (1,000 nM to 37.04 nM), 10 nM for the medium range (12.35 nM to 4.12 nM) and 1 nM for the lower range (1.37 nM to 0.05 nM). Except for the lower range, the amount of SIS was selected to be in the range of one order of magnitude. Although using comparable amounts of SIS standard improved precision and accuracy, a decline of the accuracy values was still present. The quantification strategy was also tested

with an immunoprecipitation assay using the anti-EHLR antibody for the capture of the diluted peptide and the corresponding SIS.

In an artificial system using PBSN as dilution matrix, a constant decline in the accuracy values was still detectable. The same applied for a tryptic plasma digest as the dilution matrix. In addition, the lowest two peptide concentrations were no longer detectable. However, the detection limits in the IP-assays increased by more than a factor of 25. It should be noted that a 5-fold concentration of the peptides was built into the assay due to the elution in 20 μl elution buffer, compared to the 100 μl starting volume. Also precision and accuracy were improved after the IP compared to the quantification without IP. A possible reason for this observation could also be the sample concentration in the elution procedure.

Comparing the accuracy of all tested experimental setups with or without IP using MALDI TOF as read-out, a constant decline in accuracy was observed. One potential explanation could be non-specific peptide adherence to plastic surfaces. If the peptides (normal and SIS) adhere to the plastics in equal amounts, it is possible, that the concentration interspace of the peptides amounts is increasing, which leads to an over-quantification of the higher peptide amounts, where the peptide amount is higher than the SIS. In contrast, it leads to an under-quantification where the SIS amount is higher than the diluted peptide amount. Given that TOF analyzers are known for their small dynamic range (Domon and Aebersold, 2010), it is more likely, that the decline is originated in the MALDI TOF read-out. In these experiments, quantification was only possible within a dynamic range of one order of magnitude at most with MALDI TOF.

In contrast to the small dynamic range of the MALDI TOF analysis, Kuhn *et al.* (2009) and Hoofnagle *et al.* (2008) described quantification with a dynamic range of four orders of magnitude using immunoaffinity purification of peptides out of a tryptic plasma digest with subsequent LC MRM read-out. Consequently MRM was used for the quantification of the TXP immunoprecipitations. Due to the fact that, in addition to the retention time, the triple quad mass spectrometer monitors both the intact peptide and specific fragments ions of the same peptide, ambiguities in peptide identification and quantification can practically be excluded.

The dilution series of the erbB-2 peptide was prepared in plasma digest and captured with the anti-EHLR antibody. The elutions were analyzed by nanoLC MRM. Compared to the MALDI read-out, where only 1 μl could be spotted onto a MALDI target, 10 μl elutions could be applied in the nanoLC MRM read-out on the LC MS chip (10 μl "on column").

Regarding the results of the MRM analysis the detection limit was found to be 3-fold lower, at 15 fmol, representing 21 ng/ml plasma protein concentration, whereas with MALDI TOF the detection limit in the plasma assay was at 46 fmol, representing 63 ng/ml plasma protein concentration. This is thought to be a result of the increase of

sample amount loaded onto the nanoLC MS chip (10 μl compared to 1 μl being spotted on the MALDI target). The accuracy values of the TXP MRM read-out did not decline with decreasing peptide amounts as observed with MALDI MS detection. Comparing the slopes of the intra-assay regression curves of the MALDI TOF and the LC MRM analysis, the slope of the MALDI TOF analysis with values around 2 represents a poor accuracy. The slope of the MRM analysis with 1.22 showed a much better performance in terms of accurate quantification.

The calculated precision for the intra-assay was lower than 10 % from 412 to 100,000 fmol, showing high robustness for the this range. In addition, accuracy was within the 80 and 120 % range with only one exception. As 412 fmol peptide reflects 568 ng/ml theoretical plasma protein concentration (table 3.8), LOQ was determined to 568 ng/ml. For the inter-assay, the LOQ would be about three-fold lower at 137 fmol (189 ng/ml theoretical plasma protein concentration) due to high precision and accuracy values for peptide amounts between 137 and 100,000 fmol (189 ng/ml to 138 μg/ml theoretical plasma protein concentration).

Kuhn *et al.* (2009) and Hoofnagle *et al.* (2008) described LODs for immunoprecipitation assays using peptide-specific antibodies and subsequent MRM read-out between 1 to 10 ng/ml plasma protein concentration. With 21 ng/ml the LODs of the TXP immunoprecipitation with MRM read-out are comparable.

However, Kuhn *et al.* (2009) also described LOQs of 1 to 10 ng/ml resulting in a dynamic range of four orders of magnitude, characterized in a range from 1.5 ng/ml to 5,000 μg/ml, though they applied only one amount of SIS standard (1 nM). With the TXP immunoprecipitations and MRM read-out a dynamic range of over three orders of magnitude was achieved, characterized in a range of 568 ng/ml and 138 μl/ml, using three different amounts of SIS. Further investigations would be necessary to improve sensitivity in the immunoprecipitation assay to keep up with the LOQ of those achieved by Kuhn *et al.* (2009).

Due to the multispecific nature of the TXP antibodies, groups of target peptides are captured in a complex biological sample like a plasma digest. The TXP antibody anti-EHLR, capturing the tryptic peptide from erbB-2 (applied in the plasma quantification assays in this thesis) also captures other peptides within the plasma digest, some of which are present at much higher concentrations, see table 3.18. Complement factor H, with a normal plasma level of 500 μg/ml and complement component C7 with a normal abundance of 52 μg/ml, are also targeted by the anti-EHLR antibody and can influence the capture of the lower concentrated erbB-2 peptide.

The multiple dynamic range of two TXP antibodies (anti-VLLD and anti-VEVSR) was investigated in a quantitative MRM assay with stable isotope standard peptides. To work under controlled conditions and to prevent further peptides being captured of the antibodies, an artificial buffer system was used (PBSN) instead of a tryptic plasma

digest. One of the two available standard peptides per antibody was diluted in the PBSN buffer in presence of a high concentration (333.33 nM) of the other standard peptide. The ability of the TXP antibodies to capture lower abundant target peptides in present of high abundant target peptides was evaluated. 5 fmol peptide were still detectable in presence of 33.3 pmol matrix peptide, which is a 7,000-fold higher concentration. Hence, the evaluated TXP antibodies were able to capture peptides in a 7,000-fold dynamic range. However, the dynamic range is potentially much bigger (5 fmol was the lowest tested peptide concentration). Accurate quantification was difficult, due non-sufficient accuracy values for the diluted peptide and also for the "high-abundant" matrix peptide. One possible reason for this result can be the synthetic buffer system (PBSN) used. Without a complex mixture of peptides in a sample (like plasma digest), there is a huge risk of peptides binding to plastic surfaces used in the TXP immunoprecipitation. Another reason could be the complex design of the assay to determine the dynamic range of multiplex immunoaffinity enrichment. A bulk of different dilution steps was necessary for sample preparation, which could also result in inaccurate quantification results.

Of course, there could be differences in the single TXP antibodies, resulting in specific dynamic range for each TXP antibody. As a consequence, every TXP antibody used in future immunoprecipitations has to be evaluated regarding its ability to capture targets present at different concentrations.

4.2.2. Qualitative evaluation of the immunoaffinity workflow using TXP antibodies - discovery approach

To achieve a higher sample throughput and to detect and identify all peptides, that are captured with TXP antibodies, a MALDI TOF/TOF read-out was performed for the analyses of all applied TXP antibodies. Herefore, 20 μl plasma (lyophilized and reconstituted) was used. The efficacy of the TXP approach for the identification of plasma peptides was initially confirmed using an antibody specific for the epitope EGYR, an amino acid sequence common amongst the termini of tryptically digested moderately abundant plasma proteins. Although specific peptides were identified, the mass spectra were dominated by peaks corresponding to non-specifically captured peptides, derived from high abundant proteins. The detrimental effects of these, upon the detection of the targeted low abundant peptides, are well documented (Knochenmuss and Zenobi, 2003).

Two tryptic plasma peptides using a TXP antibody specific for the short C-terminal EGYR sequence originating from coagulation factor IX and vitamin K dependent protein S were isolated. The detection of these two proteins, which are present at 4 and 25 μg/ml in plasma was not possible, when peptides were enriched only by using C18

reversed-phase ZipTip pipette tips. This was to be expected - however, given the concentration range and breadth of the plasma proteome and the matrix and analyte ion suppression effects characteristic of the MALDI (along with the electrospray) ionization techniques (Knochenmuss and Zenobi, 2003; Kratzer *et al.*, 1998). Nevertheless, the domination of non-targeted peptides derived from high-abundant proteins following anti-EGYR antibody immunoprecipitation was unexpected. Control experiments revealed that their presence could be traced back to their non-specific binding to the large surface of the protein G microspheres (3.25 **C**). Non-specific peptide binding to disposable plastic components of the automated assay was also observed (3.25 **D**) in accordance with data reported by Anderson and co-workers, see Anderson *et al.* (2009b).

Depletion columns, removing albumin and IgG prior to plasma digestion, were evaluated to test if sensitivity could be improved. In the TXP immunoprecipitation elutions of all applied antibodies, peptides from albumin or IgG were no longer detectable with the use of depletion colums. Instead, some peptides from other high abundant proteins like alpha-1-antitrypsin and alpha-2-macroglobulin appeared. Even though tryptic peptides from albumin or IgG were removed, only minor improvements were observed compared to TXP immunoprecipitations without depletion (section 3.5.1). Therefore, it would be necessary to remove more than only two of the highest abundant proteins in plasma, like for example shown by Keshishian *et al.* (2009) with the use of so-called MARS columns (Multiple Affinity Removal System) for the removal of seven high abundance plasma proteins (albumin, IgG, IgA, transferrin, fibrinogen, alpha-1-antitrypsin, and haptoglobin). However, there is a high risk of losing target proteins along with high abundant proteins during the depletion procedure. Although depletion kits facilitate the efficient removal of high abundant proteins, other proteins have also been shown to be removed (Ichibangase *et al.*, 2009). In addition, very low abundant proteins, e.g. cytokines, can be significantly reduced after the use of depletion columns (Granger *et al.*, 2005). If low abundant proteins are bound to albumin, in its function as a carrier protein, they are also lost after an albumin depletion.

Those facts and the evaluation of depletion columns in combination with TXP immunoprecipitation assays led to the result, that no further depletion procedures were used in more TXP immunoprecipitation assays.

An alternative method for depleting peptides from high abundant proteins, would be to remove the high abundant peptides instead of the proteins after the plasma digest. The insertion of more washing steps in the automated TXP immunoprecipitation did not reduce non-specific binding of high abundant peptides. Control experiments revealed that their presence could be mainly traced back to their non-specific binding to both the large surface of the protein G microspheres and the plastic components of the magnetic microsphere handler, see figure 3.25. These problems have been reported by other groups as well (Kuhn *et al.*, 2009; Anderson *et al.*, 2009b). Therefore, a solid-phase free washing step was to be found to reduce the presence of those contaminating peptides.

Svedberg (1933) demonstrated the use of ultracentrifugation to separate molecules with different molecular masses. Tengerdy and Faust (1971) further developed the procedure by proving that antigen-antibody complexes can be separated from residual antigens using ultracentrifugation. Based on those results, an ultracentrifugation procedure was established to remove non-specific peptides from the antigen-antibody complex to be inserted into the TXP immunoprecipitation procedure. A model system was set up to separate free peptides and peptide-antibody complexes (section 3.5.2.1). In the model system, over 70 % of the antibody and the peptide-antibody complex were located in the bottom 500 μl, while less than 1 % of the unbound peptide were found in the same lower fraction. Thus, this lower fraction was used in subsequent using assays plasma digest.

The centrifugation purification step was subsequently tested using a TXP immunoprecipitation assay targeting tryptic plasma peptides containing the C-terminal EGYR sequence. After ultracentrifugation, the sucrose gradient was fractionated in three volumes (500, 400 and 300 μl) which were then processed using protein G coated magnetic microspheres. Analysis of the gradient fractions by MALDI mass spectrometry revealed a dramatic reduction in background signal arising from non-targeted peptides, derived from high abundant proteins, in the bottom 500 μl fraction (figure 3.30 **D**). For the targeted vitamin K-dependent Protein S-derived peptide, this resulted in an increased S/N of over 2,000 relative to the non-specifically bound high abundant peptides (see figure 3.31). Moreover, the ultracentrifugation step led to the detection of the peptide MDCQECPEGYR derived from filamin A. High signals of peptides derived from high abundant proteins were detected in the top fraction (figure 3.30 **B**), where unbound peptides were expected after the ultracentrifugation procedure. Compared to the depletion procedure using depletion columns, to remove albumin and IgG before plasma digestion, no peptides derived from other high abundant proteins were cumulatively detected.

Further 14 TXP antibodies were evaluated comparing the workflows with and without ultracentrifugation. The workflow incorporating the ultracentrifugation step yielded 37 peptides versus 29 without (tables 3.18, 3.19 & 3.20). This can be explained by the improved S/N of targeted to non-specifically bound peptides which was observed for most of the antibodies (Supplemental figures A.43 to A.56). This resulted in an improvement in the sensitivity and robustness of the assay shown by the increase from 16 to 21 peptide identifications in all three triplicates following ultracentrifugation purification (Tables 3.18, 3.19 & 3.20).

It must be noted, that for 5 of the 15 antibodies, the signal to noise ratios did not improve after ultracentrifugation (Supplemental figures A.43 to A.56). This can be either explained by little to no non-specific binding of peptides derived from high abundant proteins to the antibody - even without ultracentrifugation. Furthermore, off-kinetics of the target peptide to the corresponding antibody can decrease the total peptide con-

centration in the environment of the antibody-peptide immunocomplex. In contrast, the precipitation of the peptide-antibody immunocomplexes in a solution containing a lower concentration of free peptides inherently leads to a significant reduction of non-specific binding of peptides to the surface of the protein G microspheres. Both effects are peptide- and antibody-dependent which might lead to differences in the purification efficiency of the ultracentrifugation separation of immunocomplexes.

On the whole, only target peptides from proteins with a plasma abundance in the lower μg/ml range were identified (tables 3.18, 3.19 & 3.20). However, filamin A which is reported to be present at a concentration of 40 ng/ml (Alper *et al.*, 2009) was also detected. This is comparable to current reports using peptide-immunoprecipitation combined with multiple reaction monitoring (MRM) techniques where current LODs in the lower ng/ml range (using 10μl plasma) have been achieved (Whiteaker *et al.*, 2010; Keshishian *et al.*, 2007; Stahl-Zeng *et al.*, 2007).

It was nevertheless surprising that the assay did not prove to be more sensitive after removal of non-specific peptides. This discrepancy in observed sensitivity however, might be explained by the limitations of the mass spectrometry method employed. Using MALDI-TOF mass spectrometry, only a small dynamic range can be covered with one ionization event as a result of the limited range of the multi channel plate detector and the limited analyte-to-matrix ratio required for successful ion generation in the MALDI process. In the shown experiments, tryptic peptides derived from proteins covering concentrations which differed by a factor of between 200-1,000 were detected with one single antibody. This is well in line with the reported dynamic detection range of MALDI mass spectrometry. As TXP antibodies typically capture at least one peptide present in the higher μg/ml range, ng/ml sensitivity is probably unachievable using MALDI MS. Therefore, it is important to consider this fact for the future design of TXP target antigens and epitopes.

The comparison of the results described in this thesis and the compiled lists of already detected tryptic peptides (see tables 3.21, 3.22 & 3.23) showed that out of a total of 53 peptides, 21 peptides could be detected with ultracentrifugation purification and only 14 without. However, with some antibodies, only peptides containing one amino acid mismatch in the epitope sequence could be identified although these antibodies have been shown to capture synthetic peptides containing the precise respective TXP targeted epitope. This difference in predicted and observed peptides might be explained by the fact that results stored in both databases were obtained from different labs using a variety of protocols and mass spectrometric systems. Thus, TXP immunoaffinity enrichment in combination with electrospray ionization might lead to the identification of additional predicted peptides. In addition, imperfect tryptic digestion could also contribute to the missing peptides.

TXP immunoprecipitations included peptides, where one amino acid did not match the original four amino acid antigen. This result appears reasonable when structurally

similar amino acids are recognized, e.g. Ser for Thr or Val for Ile. For some amino acid replacements however, the reason for this mismatch was not so obvious. Further investigations are needed to determine the underlying causes for this cross-reactivity. It has to be clarified whether the amino acid acceptance in epitope binding can be attributed to the polyclonal character of the antibodies or to a real interaction with one paratope. The use of monoclonal antibodies should help to determine whether or not this is a general feature of antibodies recognizing very short epitopes.

In summary, the data shows that the targeting of short terminal epitopes for the enrichment of tryptically digested group-specific peptides using single TXP antibodies is suitable for probing plasma protein-derived peptides. Four proteins present in lower μg/ml range were directly detectable by MALDI MS and MS/MS following rapid immunoprecipitation. Insertion of an additional ultracentrifugation purification step prior to immunoprecipitation led to a substantial reduction in non-specific high abundant protein-derived peptides including serum albumin. As a result more peptides could be detected with improved consistency.

Importantly, the TXP workflow demonstrates the ability to detect plasma proteins present at ng/ml concentrations without the requirement for chromatography columns. Moreover, the TXP workflow can be automated and parallelized to increase throughput, a significant bottleneck limiting the throughput of systems where sophisticated chromatography has to be applied.

A limitation of the TXP workflow with combined ultracentrifugation purification is the time needed for the ultracentrifugation step and the limited capacities of ultracentrifuge rotors. A maximum of 12 samples can be applied at the same time with the rotor used in this study requiring a total of 24 hours from sample preparation to data output. There are also some improvements to be made regarding the manual fractionation procedure. To guarantee reproducibility, an automated procedure using pipetting robotics would be necessary to avoid manual handling and human-related imprecision. However, considering the complexities associated with nano-liquid chromatography procedures, ultracentrifugation offers a relatively straightforward and robust alternative.

In conclusion, the application of TXP antibodies demonstrates the feasibility of enriching several peptides from non-depleted tryptic plasma digests using TXP antibodies targeting groups of peptides sharing a common short (4-5 amino acids) motif. The in-solution purification of TXP antibody-peptide immunocomplexes from excess non-targeted peptides from whole plasma digests is possible using ultracentrifugation. Incorporation of this additional separation step improved the number of identifiable peptides and increased the sensitivity of the assay to that comparable to current MRM-based immunoassays without the requirement for complex chromatographic separation.

4.2.3. TXP immunoprecipitation for plasma proteome analysis

The applicability of TXP immunoprecipitation was evaluated for a targeted (quantitative, using MRM MS) and a discovery approach (qualitative, using MALDI MS).

The quantitative aspect of the TXP immunoprecipitation assay was performed using stable isotope standards and MRM read-out, due to the high dynamic range of the MRM, enabling precise quantification. Quantification experiments showed good precision and accuracy in the range of three orders of magnitude (138 μg/ml to 189 ng/ml protein concentration) of a TXP immunoprecipitation in a human plasma digest (section 3.3.2). Additionally, the TXP antibodies were able to capture peptides in a dynamic range of 7,000 (5 fmol of peptide 1 was still detectable in presence of 33,333 fmol peptide 2).

The qualitative aspect of the TXP immunoprecipitation revealed reproducible enrichment and detection of group-specific peptides captured with TXP antibodies. A maximum of three peptides sharing the exact C-terminal TXP tag sequence were observed precipitating at the same time using one single antibody (section 3.6). Accepting peptides with one amino acid mismatch within the TXP tag sequence, a maximum of six peptides were captured by one TXP antibody at the same time (anti-EVLR and anti-ESFR). Consequently, TXP antibodies targeting a short 4-5 amino acid sequence can be used to enrich peptides from plasma digest samples. With the introduction of an ultracentrifugation step to remove non-specific bound peptides derived from high abundant proteins, more peptides (37 peptides) with higher S/N values could be identified compared to the procedure without ultracentrifugation (29 peptides), see section 3.5.2.2.

The application of TXP antibodies in an immunoprecipitation assay coupled to mass spectrometric read-out enabled multiplexed plasma protein analysis for the identification and quantification of plasma proteins. Furthermore, significantly fewer antibodies are required for the plasma proteome analysis, due to the group-specific enrichment capabilities of the TXP antibodies.

For further TXP immunoprecipitation assays, more TXP antibodies have to be evaluated regarding their dynamic range to capture target peptides from high to low abundant targets to enable more specific and selective peptide enrichment. In addition, existing TXP antibodies capture typically at least one peptide present in higher abundant proteins, which leads to decreased sensitivity to capture peptides derived from low abundant proteins. This fact is to be considered in the future design of TXP target antigens and epitopes. Regarding accurate quantification of the TXP immunoprecipitation eluates some improvements of the assay are necessary to achieved detection and quantification limits in the low ng/ml range like shown by e.g. (Whiteaker *et al.*, 2010) and others.

TXP antibodies can be considered as comparable, but cheaper alternative to peptide-specific antibodies in SISCAPA workflows. With different ionization methods, like electrospray ionization, additional peptides might be identified. Moreover, it might be also of interest whether ultracentrifugation of antibody-peptide complexes can also be beneficial to address the issue of unspecific binding for existing SISCAPA workflows.

Summary

Blood plasma, the largest human proteome is readily accessible and can be minimal-invasively sampled making it a valuable source of potential biomarkers. However, its analysis is complicated by its complexity and the huge dynamic concentration range of its constituents. Automated assays were established using magnetic microspheres and customized group-specific triple X proteomics (TXP) antibodies. These antibodies are directed against short N- or C-terminal epitope motifs for the immunoprecipitation of signature peptides derived from groups of trypsin-digested plasma proteins. The introduction of these antibodies led to a very efficient enrichment of the targeted analytes and a reduction in sample complexity similar to the SISCAPA (Stable Isotope Standards and Capture by Anti-Peptide Antibodies) approach introduced by Anderson *et al.* (2004).

The quantitative evaluation as targeted approach, via nano liquid chromatography multiple reaction monitoring and stable isotopes peptide standards revealed limits of detection of 21 ng/ml and limits of quantification of 189 ng/ml in a tryptic plasma digest assay. Two peptides with the same TXP tag were simultaneously captured with one TXP antibody in a multiplex dynamic range of about 7,000 (5 fmol peptide were still detectable in presence of 33.3 pmol matrix peptide).

The qualitative evaluation as discovery approach, of a tryptic plasma digest assay via matrix-assisted laser desorption/ionization time of flight (MALDI TOF) analysis revealed the presence of TXP tag-specific peptides captured by the used TXP antibodies. Their analysis, however, was compromised by peptide peaks from non-targeted high abundant proteins. Sucrose gradient ultracentrifugation showed a 99 % depletion of non-targeted peptides. Further investigations with a total of 14 TXP antibodies enabled the detection of targeted TXP peptides and a significant reduction in the intensity of non-specific peptides.

TXP Proteomics by peptide group-specific immunoprecipitation coupled to mass spectrometry read-out allowed reproducible multiplexed plasma protein analysis without the requirement for demanding liquid chromatography separation techniques. Furthermore, the application of TXP antibodies requires significantly fewer antibodies for immuno-affinity mass spectrometry based plasma proteome analysis compared to the use of anti-peptide antibodies.

Zusammenfassung

Blutplasma ist das größte menschliche Proteom. Es kann schnell durch einen minimal invasiven Eingriff gewonnen werden und stellt dadurch eine wertvolle Quelle für potentielle Biomarker dar. Die Analyse jedoch ist kompliziert, bedingt durch die Komplexität des Plasmas und den enormen dynamischen Konzentrationsbereich der beinhalteten Proteine. In dieser Arbeit wurde eine automatisierte Probenbearbeitung mit magnetischen Partikeln und gruppenspezifischen "Triple X Proteomics" (TXP)-Antikörpern etabliert. Diese sind gegen kurze N- oder C-terminale Epitop-Motive von Peptiden gerichtet um diese gruppenweise aus tryptisch verdauten Plasma anzureichern. Die Anwendung dieser führte zu einer sehr effektiven Anreicherung der Zielanalyten und folglich zu einer Reduktion der Komplexität ähnlich dem Konzept SISCAPA (Stable Isotope Standards and Capture by Anti-Peptide Antibodies)von Anderson *et al.* (2004).

Die quantitative Evaluierung mittels nano-Flüssigkeitschromatographie *Multiple Reaction Monitoring* und stabilen Isotopen-Standards zeigte Detektionsgrenzen von 21 ng/ml und Quantifizierungsgrenzen von 189 ng/ml in tryptischem Plasmaverdau. Der multiplexe dynamische Bereich eines TXP-Antikörper lag bei 7,000 (5 fmol Peptid waren in Gegenwart von 33,3 pmol Matrixpeptid noch detektierbar), wobei zwei Peptide mit derselben TXP-Sequenz simultan mit einem TXP-Antikörper gebunden werden konnten.

Die qualitative Evaluierung eines Plasma-Experiments mittels Matrix-unterstützter Laser-Desorption/Ionisation (MALDI) mit Flugzeitanalyse (time of flight, TOF) zeigte die Präsenz von TXP-spezifischen Peptiden, die von den benutzten TXP-Antikörpern gebunden wurden. Die Analyse dieser wurde allerdings beeinträchtigt durch Peptidpeaks von unerwünschten, hoch abundanten Plasmaproteinen. Mittels Dichtegradientenzentrifugation wurden 99 % der unerwünschten Peptide abgereichert. Mit insgesamt 14 TXP-Antikörpern wurden gezielt Peptide mit TXP-Sequenz angereichert. Gleichzeitig konnte eine signifikante Reduktion von unspezifischen Peptiden ohne TXP-Sequenz erreicht werden.

Die Proteomanalyse mit TXP-Antikörpern (gruppenspezifische Immunpräzipitation von Peptiden gekoppelt mit massenspektrometrischer Analyse) erlaubte die reproduzierbare, multiplexe Analyse von Plasmaproteinen ohne zusätzliche, anspruchsvolle LC-Trennungsmethoden. Im Gegensatz zu der Applikation peptidspezifischer Antikörper werden mit TXP-Antikörpern erheblich weniger Antikörper für die Plasma-Proteom-Analyse bei der Immunaffinitätschromatographie benötigt.

Bibliography

(2001). Guidance for industry bioanalytical method validation guidance for industry bioanalytical method validation. *Veterinary Medicine*, **2010**(May), 1–25.

Ackermann, B. L. and Berna, M. J. (2007). Coupling immunoaffinity techniques with MS for quantitative analysis of low-abundance protein biomarkers. *Expert Review of Proteomics*, **4**(2), 175–186.

Adkins, J. N., Varnum, S. M., Auberry, K. J., Moore, R. J., Angell, N. H., Smith, R. D., Springer, D. L., and Pounds, J. G. (2002). Toward a human blood serum proteome: analysis by multidimensional separation coupled with mass spectrometry. *Molecular & Cellular Proteomics: MCP*, **1**(12), 947–955.

Aebersold, R. and Mann, M. (2003). Mass spectrometry-based proteomics. *Nature*, **422**(6928), 198–207.

Aggarwal, K., Choe, L. H., and Lee, K. H. (2006). Shotgun proteomics using the iTRAQ isobaric tags. *Briefings in Functional Genomics & Proteomics*, **5**(2), 112–120.

Alper, O., Stetler-Stevenson, W. G., Harris, L. N., Leitner, W. W., Ozdemirli, M., Hartmann, D., Raffeld, M., Abu-Asab, M., Byers, S., Zhuang, Z., Oldfield, E. H., Tong, Y., Bergmann-Leitner, E., Criss, W. E., Nagasaki, K., Mok, S. C., Cramer, D. W., Karaveli, F. S., Goldbach-Mansky, R., Leo, P., Stromberg, K., and Weil, R. J. (2009). Novel anti-filamin-A antibody detects a secreted variant of filamin-A in plasma from patients with breast carcinoma and high-grade astrocytoma. *Cancer Science*, **100**(9), 1748–1756.

Anderson, L. (2005). Candidate-based proteomics in the search for biomarkers of cardiovascular disease. *The Journal of Physiology*, **563**(Pt 1), 23–60. PMID: 15611012.

Anderson, L. and Anderson, N. G. (1977). High resolution two-dimensional electrophoresis of human plasma proteins. *Proceedings of the National Academy of Sciences of the United States of America*, **74**(12), 5421–5425.

Anderson, L. and Hunter, C. L. (2006). Quantitative mass spectrometric multiple reaction monitoring assays for major plasma proteins. *Molecular & Cellular Proteomics: MCP*, **5**(4), 573–588.

Anderson, N. L. (2010). The clinical plasma proteome: a survey of clinical assays for proteins in plasma and serum. *Clinical Chemistry*, **56**(2), 177–185.

Anderson, N. L. and Anderson, N. G. (2002). The human plasma proteome: history, character, and diagnostic prospects. *Molecular & Cellular Proteomics: MCP*, **1**(11), 845–867.

Anderson, N. L., Anderson, N. G., Haines, L. R., Hardie, D. B., Olafson, R. W., and Pearson, T. W. (2004). Mass spectrometric quantitation of peptides and proteins using stable isotope standards and capture by Anti-Peptide antibodies (SISCAPA). *Journal of Proteome Research*, **3**(2), 235–244.

Anderson, N. L., Anderson, N. G., Pearson, T. W., Borchers, C. H., Paulovich, A. G., Patterson, S. D., Gillette, M., Aebersold, R., and Carr, S. A. (2009a). A human proteome detection and quantitation project. *Molecular & Cellular Proteomics: MCP*, **8**(5), 883–886.

Anderson, N. L., Jackson, A., Smith, D., Hardie, D., Borchers, C., and Pearson, T. W. (2009b). SISCAPA peptide enrichment on magnetic beads using an in-line bead trap device. *Molecular & Cellular Proteomics: MCP*, **8**(5), 995–1005.

Carr, S. A. and Anderson, L. (2008). Protein quantitation through targeted mass spectrometry: The way out of biomarker purgatory? *Clinical Chemistry*, **54**(11), 1749 –1752.

Cologna, S. M., Russell, W. K., Lim, P. J., Vigh, G., and Russell, D. H. (2010). Combining isoelectric point-based fractionation, liquid chromatography and mass spectrometry to improve peptide detection and protein identification. *Journal of the American Society for Mass Spectrometry*, **21**(9), 1612–1619.

Deutsch, E. W., Lam, H., and Aebersold, R. (2008). PeptideAtlas: a resource for target selection for emerging targeted proteomics workflows. *EMBO Reports*, **9**(5), 429–434.

Domon, B. and Aebersold, R. (2010). Options and considerations when selecting a quantitative proteomics strategy. *Nature Biotechnology*, **28**(7), 710–721.

Esparza-Gordillo, J., Soria, J. M., Buil, A., Almasy, L., Blangero, J., Fontcuberta, J., and Rodriguez de Cordoba, S. (2004). Genetic and environmental factors influencing the human factor h plasma levels. *Immunogenetics*, **56**(2), 77–82.

Everley, P. A., Krijgsveld, J., Zetter, B. R., and Gygi, S. P. (2004). Quantitative cancer proteomics: stable isotope labeling with amino acids in cell culture (SILAC) as a tool for prostate cancer research. *Molecular & Cellular Proteomics: MCP*, **3**(7), 729–735.

Fortin, T., Salvador, A., Charrier, J. P., Lenz, C., Lacoux, X., Morla, A., Choquet-Kastylevsky, G., and Lemoine, J. (2009a). Clinical quantitation of prostate-specific antigen biomarker in the low nanogram/milliliter range by conventional bore liquid chromatography-tandem mass spectrometry (multiple reaction monitoring) coupling and correlation with ELISA tests. *Molecular & Cellular Proteomics: MCP*, **8**(5), 1006–1015.

Fortin, T., Salvador, A., Charrier, J. P., Lenz, C., Bettsworth, F., Lacoux, X., Choquet-Kastylevsky, G., and Lemoine, J. (2009b). Multiple reaction monitoring cubed for protein quantification at the low nanogram/milliliter level in nondepleted human serum. *Analytical Chemistry*, **81**(22), 9343–9352.

Gerber, S. A., Rush, J., Stemman, O., Kirschner, M. W., and Gygi, S. P. (2003). Absolute quantification of proteins and phosphoproteins from cell lysates by tandem MS. *Proceedings of the National Academy of Sciences of the United States of America*, **100**(12), 6940–6945.

Glowinska, B., Urban, M., Koput, A., and Galar, M. (2003). [Selected new atherosclerosis risk factors and markers of fibrinolysis in children and adolescents with obesity, hypertension and diabetes]. *Przeglad Lekarski*, **60**(1), 12–17.

Gobom, J., Schuerenberg, M., Mueller, M., Theiss, D., Lehrach, H., and Nordhoff, E. (2001). Alpha-cyano-4-hydroxycinnamic acid affinity sample preparation. a protocol for MALDI-MS peptide analysis in proteomics. *Analytical Chemistry*, **73**(3), 434–438.

Granger, J., Siddiqui, J., Copeland, S., and Remick, D. (2005). Albumin depletion of human plasma also removes low abundance proteins including the cytokines. *Proteomics*, **5**(18), 4713–4718.

Gygi, S. P., Rist, B., Gerber, S. A., Turecek, F., Gelb, M. H., and Aebersold, R. (1999). Quantitative analysis of complex protein mixtures using isotope-coded affinity tags. *Nature Biotechnology*, **17**(10), 994–999.

Gygi, S. P., Rist, B., Griffin, T. J., Eng, J., and Aebersold, R. (2002). Proteome analysis of low-abundance proteins using multidimensional chromatography and isotope-coded affinity tags. *Journal of Proteome Research*, **1**(1), 47–54.

Hasholzner, U., Baumgartner, L., Stieber, P., Meier, W., Hofmann, K., and Fateh-Moghadam, A. (1994). Significance of the tumour markers CA 125 II, CA 72-4, CASA and CYFRA 21-1 in ovarian carcinoma. *Anticancer Research*, **14**(6B), 2743–2746.

Hillenkamp, F. and Peter-Katalinic, J. (2007). *MALDI MS: A Practical Guide to Instrumentation, Methods and Applications*. Wiley-VCH Verlag GmbH & Co. KGaA, Weinheim, Germany.

Hoeppe, S., Schreiber, T. D., Planatscher, H., Zell, A., Templin, M. F., Stoll, D., Joos, T. O., and Poetz, O. (2010). Targeting peptide termini - a novel immunoaffinity approach to reduce complexity in mass spectrometric protein identification. *Molecular & Cellular Proteomics: MCP*.

Hogasen, K., Mollnes, T. E., Tschopp, J., and Harboe, M. (1993). Quantitation of vitronectin and clusterin. pitfalls and solutions in enzyme immunoassays for adhesive proteins. *Journal of Immunological Methods*, **160**(1), 107–115.

Hoofnagle, A. N., Becker, J. O., Wener, M. H., and Heinecke, J. W. (2008). Quantification of thyroglobulin, a low-abundance serum protein, by immunoaffinity peptide enrichment and tandem mass spectrometry. *Clinical Chemistry*, **54**(11), 1796–1804.

Hortin, G. L., Sviridov, D., and Anderson, N. L. (2008). High-abundance polypeptides of the human plasma proteome comprising the top 4 logs of polypeptide abundance. *Clinical Chemistry*, **54**(10), 1608–1616.

Ichibangase, T., Moriya, K., Koike, K., and Imai, K. (2009). Limitation of immunoaffinity column for the removal of abundant proteins from plasma in quantitative plasma proteomics. *Biomedical Chromatography: BMC*, **23**(5), 480–487.

Jacobs, J. M., Adkins, J. N., Qian, W., Liu, T., Shen, Y., Camp, D. G., and Smith, R. D. (2005). Utilizing human blood plasma for proteomic biomarker discovery. *Journal of Proteome Research*, **4**(4), 1073–1085.

Jessome, L. L. and Volmer, D. A. (2006). Ion suppression: A major concern in mass spectrometry. *LCGC North America 2006*, **24**, 498–510.

Kalafatis, M. and Mann, K. G. (1997). Factor V Leiden and thrombophilia. *Arterioscler Thromb Vasc Biol*, **17**(4), 620–627.

Keller, B. O. and Li, L. (2000). Discerning matrix-cluster peaks in matrix-assisted laser desorption/ionization time-of-flight mass spectra of dilute peptide mixtures. *Journal of the American Society for Mass Spectrometry*, **11**(1), 88–93.

Keshishian, H., Addona, T., Burgess, M., Kuhn, E., and Carr, S. A. (2007). Quantitative, multiplexed assays for low abundance proteins in plasma by targeted mass spectrometry and stable isotope dilution. *Molecular & Cellular Proteomics: MCP*, **6**(12), 2212–2229.

Keshishian, H., Addona, T., Burgess, M., Mani, D. R., Shi, X., Kuhn, E., Sabatine, M. S., Gerszten, R. E., and Carr, S. A. (2009). Quantification of cardiovascular biomarkers in patient plasma by targeted mass spectrometry and stable isotope dilution. *Molecular & Cellular Proteomics: MCP*, **8**(10), 2339–2349.

Kim, C., Park, J. Y., Kim, J. Y., Choi, C. S., Kim, Y. I., Chung, Y. E., Lee, M. S., Hong, S. K., and Lee, K. (2002). Elevated serum ceruloplasmin levels in subjects with metabolic syndrome: a population-based study. *Metabolism: Clinical and Experimental*, **51**(7), 838–842.

Knochenmuss, R. and Zenobi, R. (2003). MALDI ionization: The role of in-plume processes. *Chemical Reviews*, **103**(2), 441–452.

Kratzer, R., Eckerskorn, C., Karas, M., and Lottspeich, F. (1998). Suppression effects in enzymatic peptide ladder sequencing using ultraviolet - matrix assisted laser desorption/ionization - mass spectrometry. *Electrophoresis*, **19**(11), 1910–1919.

Krause, E., Wenschuh, H., and Jungblut, P. R. (1999). The dominance of arginine-containing peptides in MALDI-Derived tryptic mass fingerprints of proteins. *Analytical Chemistry*, **71**(19), 4160–4165.

Kuhn, E., Addona, T., Keshishian, H., Burgess, M., Mani, D. R., Lee, R. T., Sabatine, M. S., Gerszten, R. E., and Carr, S. A. (2009). Developing multiplexed assays for troponin I and interleukin-33 in plasma by peptide immunoaffinity enrichment and targeted mass spectrometry. *Clinical Chemistry*, **55**(6), 1108–1117.

Kujiraoka, T., Oka, T., Ishihara, M., Egashira, T., Fujioka, T., Saito, E., Saito, S., Miller, N. E., and Hattori, H. (2000). A sandwich enzyme-linked immunosorbent assay for human serum paraoxonase concentration. *Journal of Lipid Research*, **41**(8), 1358–1363.

Kyrtsonis, M., Vassilakopoulos, T. P., Siakantaris, M. P., Kokoris, S. I., Gribabis, D. A., Dimopoulou, M. N., Angelopoulou, M. K., and Pangalis, G. A. (2004). Serum syndecan-1, basic fibroblast growth factor and osteoprotegerin in myeloma patients at diagnosis and during the course of the disease. *European Journal of Haematology*, **72**(4), 252–258.

Lee, S., Rhim, T., Choi, Y., Min, J., Kim, S., Cho, S., Paik, Y., and Park, C. (2006). Complement c3a and c4a increased in plasma of patients with aspirin-induced asthma. *American Journal of Respiratory and Critical Care Medicine*, **173**(4), 370–378.

Lei, K. I. and Johnson, P. J. (2000). The prognostic significance of serum levels of soluble intercellular adhesion molecules-1 in patients with primary extranodal non-Hodgkin lymphomas. *Cancer*, **89**(6), 1387–1395.

Lequin, R. M. (2005). Enzyme immunoassay (EIA)/Enzyme-Linked immunosorbent assay (ELISA). *Clinical Chemistry*, **51**(12), 2415 –2418.

Liu, T., Qian, W., Mottaz, H. M., Gritsenko, M. A., Norbeck, A. D., Moore, R. J., Purvine, S. O., Camp, D. G., and Smith, R. D. (2006). Evaluation of multiprotein immunoaffinity subtraction for plasma proteomics and candidate biomarker discovery using mass spectrometry. *Molecular & Cellular Proteomics: MCP*, **5**(11), 2167–2174.

Lottspeich, F., Engels, J. W., and Simeon, A. (2006). *Bioanalytik*. Spektrum Akademischer Verlag, Heidelberg, Germany.

Lueftner, D., Mesterharm, J., Akrivakis, C., Geppert, R., Petrides, P. E., Wernecke, K. D., and Possinger, K. (2000). Tumor type m2 pyruvate kinase expression in advanced breast cancer. *Anticancer Research*, **20**(6D), 5077–5082.

Luo, J. and Liu, B. (1994). [ELISA for measurement of human serum apolipoprotein a II]. *Hua Xi Yi Ke Da Xue Xue Bao = Journal of West China University of Medical Sciences = Huaxi Yike Daxue Xuebao / [bian Ji Zhe, Hua Xi Yi Ke Da Xue Xue Bao Bian Wei Hui*, **25**(2), 229–232.

Masaki, T., Matsuura, T., Ohkawa, K., Miyamura, T., Okazaki, I., Watanabe, T., and Suzuki, T. (2006). All-trans retinoic acid down-regulates human albumin gene expression through the induction of C/EBPbeta-LIP. *Biochemical Journal*, **397**(Pt 2), 345–353.

Melanson, J. E., Avery, S. L., and Pinto, D. M. (2006). High-coverage quantitative proteomics using amine-specific isotopic labeling. *Proteomics*, **6**(16), 4466–4474.

Minutti, C. Z., Lacey, J. M., Magera, M. J., Hahn, S. H., McCann, M., Schulze, A., Cheillan, D., Dorche, C., Chace, D. H., Lymp, J. F., Zimmerman, D., Rinaldo, P., and Matern, D. (2004). Steroid profiling by tandem mass spectrometry improves the positive predictive value of newborn screening for congenital adrenal hyperplasia. *The Journal of Clinical Endocrinology and Metabolism*, **89**(8), 3687–3693.

Miyagi, M. and Rao, K. C. S. (2007). Proteolytic ^{18}o-labeling strategies for quantitative proteomics. *Mass Spectrometry Reviews*, **26**(1), 121–136.

Montreuil, J., Vliegenthart, J. F. G., and Schachter, H. (1997). *Glycoproteins II*. Elsevier, Amsterdam, Netherlands.

Nielsen, U. B. and Geierstanger, B. H. (2004). Multiplexed sandwich assays in microarray format. *Journal of Immunological Methods*, **290**(1-2), 107–120.

Omenn, G. S., States, D. J., Adamski, M., Blackwell, T. W., Menon, R., Hermjakob, H., Apweiler, R., Haab, B. B., Simpson, R. J., Eddes, J. S., Kapp, E. A., Moritz, R. L., Chan, D. W., Rai, A. J., Admon, A., Aebersold, R., Eng, J., Hancock, W. S., Hefta, S. A., Meyer, H., Paik, Y., Yoo, J., Ping, P., Pounds, J., Adkins, J., Qian, X., Wang, R., Wasinger, V., Wu, C. Y., Zhao, X., Zeng, R., Archakov, A., Tsugita, A., Beer, I., Pandey, A., Pisano, M., Andrews, P., Tammen, H., Speicher, D. W., and Hanash, S. M. (2005). Overview of the HUPO plasma proteome project: results from the pilot phase with 35 collaborating laboratories and multiple analytical groups, generating a core dataset of 3020 proteins and a publicly-available database. *Proteomics*, **5**(13), 3226–3245.

Ong, S., Blagoev, B., Kratchmarova, I., Kristensen, D. B., Steen, H., Pandey, A., and Mann, M. (2002). Stable isotope labeling by amino acids in cell culture, SILAC, as a simple and accurate approach to expression proteomics. *Molecular & Cellular Proteomics: MCP*, **1**(5), 376–386.

Paulovich, A. G., Whiteaker, J. R., Hoofnagle, A. N., and Wang, P. (2008). The interface between biomarker discovery and clinical validation: The tar pit of the protein biomarker pipeline. *Proteomics. Clinical Applications*, **2**(10-11), 1386–1402.

Planatscher, H., Supper, J., Poetz, O., Stoll, D., Joos, T., Templin, M. F., and Zell, A. (2010). Optimal selection of epitopes for TXP-immunoaffinity mass spectrometry. *Algorithms for Molecular Biology: AMB*, **5**, 28.

Poetz, O., Hoeppe, S., Templin, M. F., Stoll, D., and Joos, T. O. (2009). Proteome wide screening using peptide affinity capture. *Proteomics*, **9**(6), 1518–1523.

Polanski, M. and Anderson, N. L. (2007). A list of candidate cancer biomarkers for targeted proteomics. *Biomarker Insights*, **1**, 1–48.

Pynn, C. J., Henderson, N. G., Clark, H., Koster, G., Bernhard, W., and Postle, A. D. (2010). The specificity and rate of human and mouse liver and plasma phosphatidylcholine synthesis analysed in vivo. *Journal of Lipid Research*, **52**(15), 399–407.

Quinn, K. A., Grimsley, P. G., Dai, Y. P., Tapner, M., Chesterman, C. N., and Owensby, D. A. (1997). Soluble low density lipoprotein receptor-related protein (LRP) circulates in human plasma. *The Journal of Biological Chemistry*, **272**(38), 23946–23951.

Ridker, P. M., Rifai, N., Stampfer, M. J., and Hennekens, C. H. (2000). Plasma concentration of interleukin-6 and the risk of future myocardial infarction among apparently healthy men. *Circulation*, **101**(15), 1767–1772.

Rifai, N., Gillette, M. A., and Carr, S. A. (2006). Protein biomarker discovery and validation: the long and uncertain path to clinical utility. *Nature Biotechnology*, **24**(8), 971–983.

Rush, J., Moritz, A., Lee, K. A., Guo, A., Goss, V. L., Spek, E. J., Zhang, H., Zha, X., Polakiewicz, R. D., and Comb, M. J. (2005). Immunoaffinity profiling of tyrosine phosphorylation in cancer cells. *Nature Biotechnology*, **23**(1), 94–101.

Schienk, S., Lienard, D., Gerain, J., Baumgartner, M., Lejeune, F. J., Chiquet-Ehrismann, R., and Rueegg, C. (1995). Rapid increase in plasma tenascin-C concentration after isolated limb perfusion with high-dose tumor necrosis factor (TNF), interferon gamma (IFN gamma) and melphalan for regionally advanced tumors. *International Journal of Cancer. Journal International Du Cancer*, **63**(5), 665–672.

Schulze, P. C., Kratzsch, J., Linke, A., Schoene, N., Adams, V., Gielen, S., Erbs, S., Moebius-Winkler, S., and Schuler, G. (2003). Elevated serum levels of leptin and soluble leptin receptor in patients with advanced chronic heart failure. *European Journal of Heart Failure: Journal of the Working Group on Heart Failure of the European Society of Cardiology*, **5**(1), 33–40.

Schwenk, J. M., Gry, M., Rimini, R., Uhlen, M., and Nilsson, P. (2008). Antibody suspension bead arrays within serum proteomics. *Journal of Proteome Research*, **7**(8), 3168–3179.

Secretion, F., Conjur, G. S., and Attitude, S. P. (1998). Interviews with the dead. using meta-life qualitative analysis to validate hippocrates' theory of humours. *CMAJ: Canadian Medical Association Journal = Journal De l'Association Medicale Canadienne*, **159**(12), 1472–1473.

Spencer, C. A. (2004). Challenges of serum thyroglobulin (Tg) measurement in the presence of tg autoantibodies. *The Journal of Clinical Endocrinology and Metabolism*, **89**(8), 3702–3704.

Stahl-Zeng, J., Lange, V., Ossola, R., Eckhardt, K., Krek, W., Aebersold, R., and Domon, B. (2007). High sensitivity detection of plasma proteins by multiple reaction monitoring of n-glycosites. *Molecular & Cellular Proteomics: MCP*, **6**(10), 1809–1817.

Stevens, R. G., Beasley, R. P., and Blumberg, B. S. (1986). Iron-binding proteins and risk of cancer in taiwan. *Journal of the National Cancer Institute*, **76**(4), 605–610.

Sun, W., Wu, S., Wang, X., Zheng, D., and Gao, Y. (2005). An analysis of protein abundance suppression in data dependent liquid chromatography and tandem mass spectrometry with tryptic peptide mixtures of five known proteins. *European Journal of Mass Spectrometry (Chichester, England)*, **11**(6), 575–580.

Svedberg, T. (1933). SEDIMENTATION CONSTANTS, MOLECULAR WEIGHTS, AND ISOELECTRIC POINTS OF THE RESPIRATORY PROTEINS. *Cold Spring Harbor Symposia on Quantitative Biology*, **1**, 51 –59.

Tengerdy, R. P. and Faust, C. H. (1971). Separation of soluble antigen-antibody complexes by acrylamide gel electrophoresis and ultracentrifugation. *Analytical Biochemistry*, **42**(1), 248–254.

Thompson, A. R. (1977). Factor IX antigen by radioimmunoassay. abnormal factor IX protein in patients on warfarin therapy and with hemophilia b. *The Journal of Clinical Investigation*, **59**(5), 900–910.

Veenstra, T. D., Conrads, T. P., Hood, B. L., Avellino, A. M., Ellenbogen, R. G., and Morrison, R. S. (2005). Biomarkers: mining the biofluid proteome. *Molecular & Cellular Proteomics: MCP*, **4**(4), 409–418.

Washburn, M. P., Wolters, D., and Yates, J. R. (2001). Large-scale analysis of the yeast proteome by multidimensional protein identification technology. *Nature Biotechnology*, **19**(3), 242–247.

Whiteaker, J. R., Zhao, L., Zhang, H. Y., Feng, L., Piening, B. D., Anderson, L., and Paulovich, A. G. (2007a). Antibody-based enrichment of peptides on magnetic beads for mass-spectrometry-based quantification of serum biomarkers. *Analytical Biochemistry*, **362**(1), 44–54.

Whiteaker, J. R., Zhang, H., Eng, J. K., Fang, R., Piening, B. D., Feng, L., Lorentzen, T. D., Schoenherr, R. M., Keane, J. F., Holzman, T., Fitzgibbon, M., Lin, C., Zhang, H., Cooke, K., Liu, T., Camp, D. G., Anderson, L., Watts, J., Smith, R. D., McIntosh, M. W., and Paulovich, A. G. (2007b). Head-to-head comparison of serum fractionation techniques. *Journal of Proteome Research*, **6**(2), 828–836.

Whiteaker, J. R., Zhao, L., Anderson, L., and Paulovich, A. G. (2010). An automated and multiplexed method for high throughput peptide immunoaffinity enrichment and multiple reaction monitoring mass spectrometry-based quantification of protein biomarkers. *Molecular & Cellular Proteomics: MCP*, **9**(1), 184–196.

Whiteaker, J. R., Lin, C., Kennedy, J., Hou, L., Trute, M., Sokal, I., Yan, P., Schoenherr, R. M., Zhao, L., Voytovich, U. J., Kelly-Spratt, K. S., Krasnoselsky, A., Gafken, P. R., Hogan, J. M., Jones, L. A., Wang, P., Amon, L., Chodosh, L. A., Nelson, P. S., McIntosh, M. W., Kemp, C. J., and Paulovich, A. G. (2011). A targeted proteomics-based pipeline for verification of biomarkers in plasma. *Nat Biotech*, **29**(7), 625–634.

Wingren, C., James, P., and Borrebaeck, C. A. K. (2009). Strategy for surveying the proteome using affinity proteomics and mass spectrometry. *Proteomics*, **9**(6), 1511–1517.

Wolters, D. A., Washburn, M. P., and Yates, J. R. (2001). An automated multidimensional protein identification technology for shotgun proteomics. *Analytical Chemistry*, **73**(23), 5683–5690.

Wu, J. T. (2002). C-erbB2 oncoprotein and its soluble ectodomain: a new potential tumor marker for prognosis early detection and monitoring patients undergoing herceptin treatment. *Clinica Chimica Acta; International Journal of Clinical Chemistry*, **322**(1-2), 11–19.

Yalow, R. S. and Berson, S. A. (1960). IMMUNOASSAY OF ENDOGENOUS PLASMA INSULIN IN MAN. *Journal of Clinical Investigation*, **39**, 1157–1175.

Yao, X., Freas, A., Ramirez, J., Demirev, P. A., and Fenselau, C. (2001). Proteolytic ^{18}o labeling for comparative proteomics: model studies with two serotypes of adenovirus. *Analytical Chemistry*, **73**(13), 2836–2842.

Zhang, H., Li, X., Martin, D. B., and Aebersold, R. (2003). Identification and quantification of N-linked glycoproteins using hydrazide chemistry, stable isotope labeling and mass spectrometry. *Nature Biotechnology*, **21**(6), 660–666.

Zhang, N. and Li, L. (2004). Effects of common surfactants on protein digestion and matrix-assisted laser desorption/ionization mass spectrometric analysis of the digested peptides using two-layer sample preparation. *Rapid Communications in Mass Spectrometry: RCM*, **18**(8), 889–896.

Appendix A.

Supplementals

A.1. Antibody binding assays - graphs

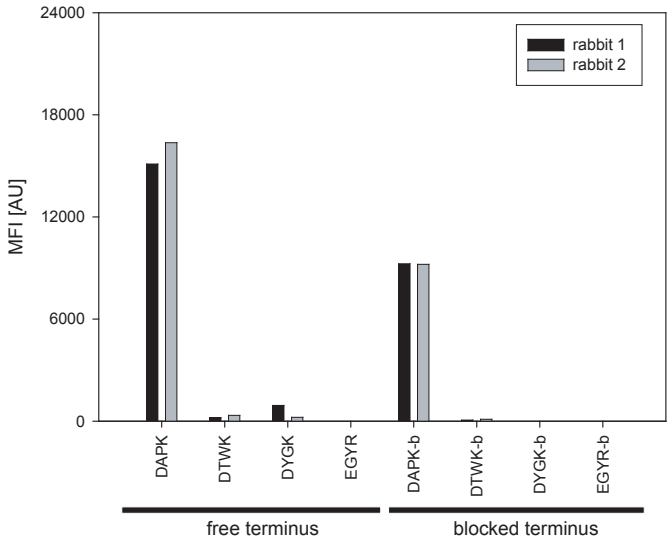

Figure A.1.: Antibody binding assay - anti-DAPK to test the rabbit sera (2 replicates) for the success of immunization respectively for the functionality of the containing antibodies. Serum Dilution: 1:10,000.

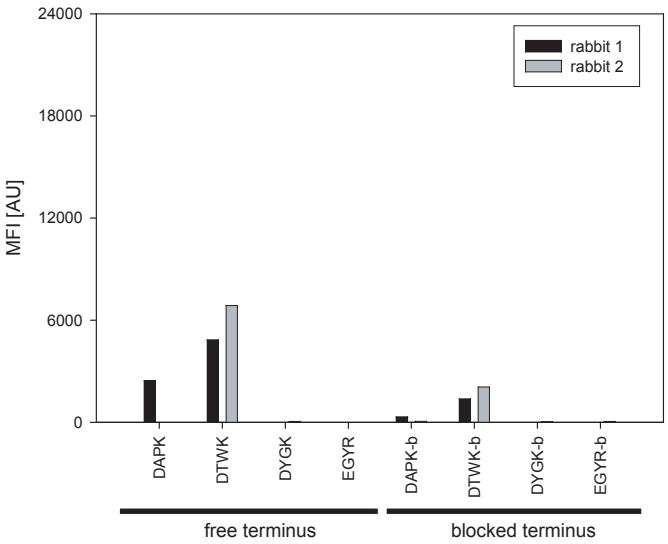

Figure A.2.: Antibody binding assay - anti-DTWK to test the rabbit sera (2 replicates) for the success of immunization respectively for the functionality of the containing antibodies. Serum Dilution: 1:10,000.

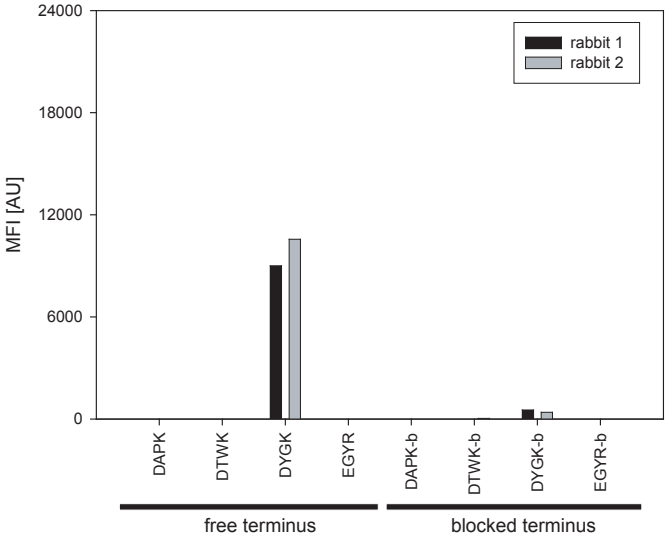

Figure A.3.: Antibody binding assay - anti-DYGK to test the rabbit sera (2 replicates) for the success of immunization respectively for the functionality of the containing antibodies. Serum Dilution: 1:10,000.

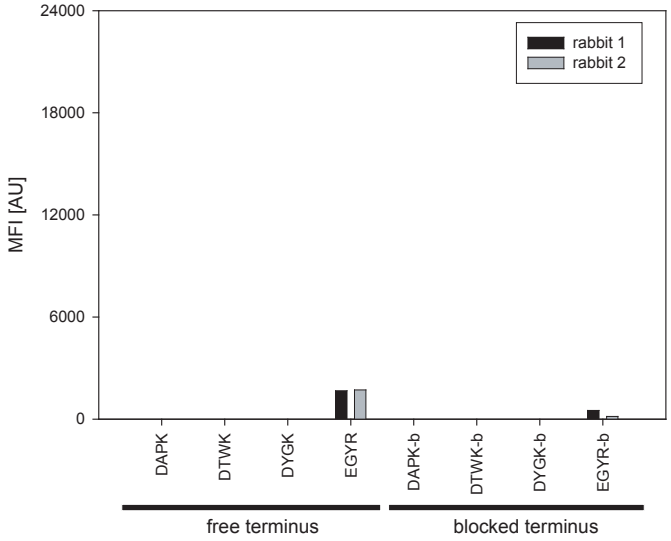

Figure A.4.: Antibody binding assay - anti-EGYR to test the rabbit sera (2 replicates) for the success of immunization respectively for the functionality of the containing antibodies. Serum Dilution: 1:10,000.

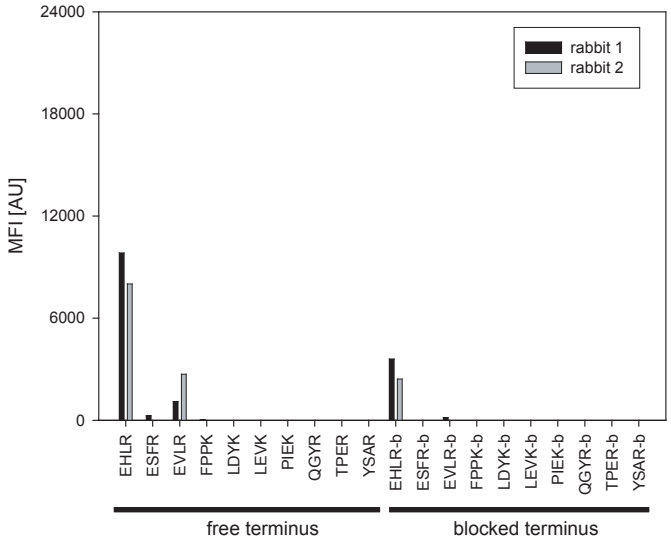

Figure A.5.: Antibody binding assay - anti-EHLR to test the rabbit sera (2 replicates) for the success of immunization respectively for the functionality of the containing antibodies. Serum Dilution: 1:10,000.

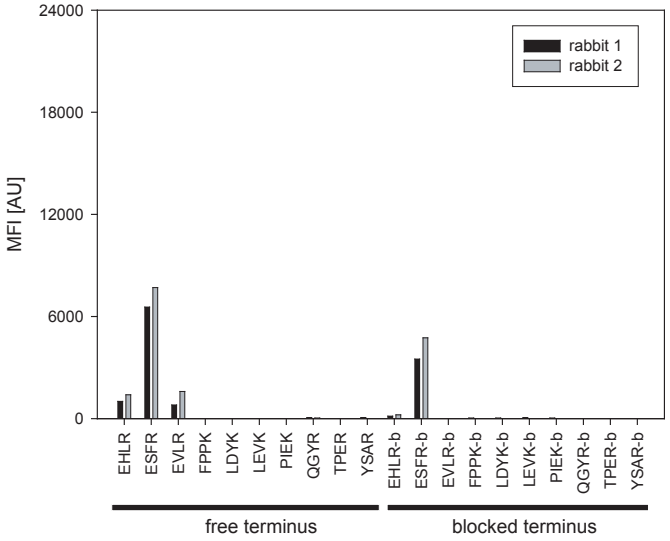

Figure A.6.: Antibody binding assay - anti-ESFR to test the rabbit sera (2 replicates) for the success of immunization respectively for the functionality of the containing antibodies. Serum Dilution: 1:10,000.

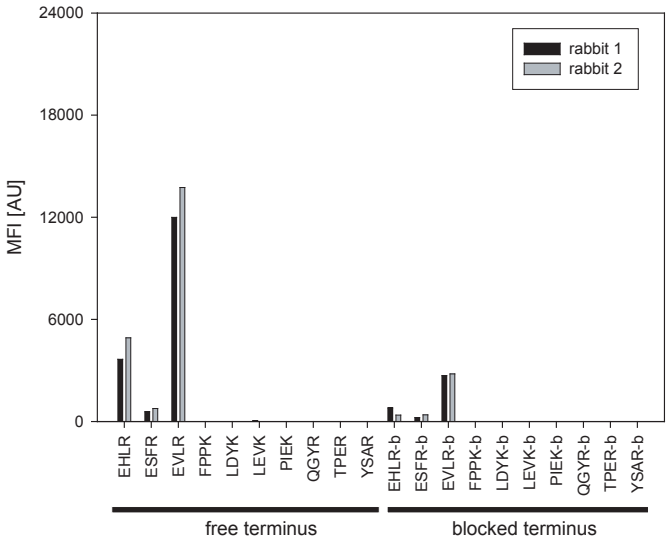

Figure A.7.: Antibody binding assay - anti-EVLR to test the rabbit sera (2 replicates) for the success of immunization respectively for the functionality of the containing antibodies. Serum Dilution: 1:10,000.

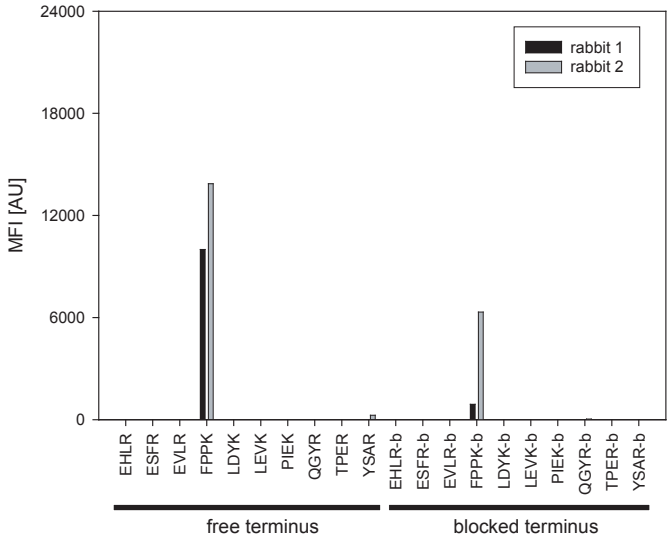

Figure A.8.: Antibody binding assay - anti-FPPK to test the rabbit sera (2 replicates) for the success of immunization respectively for the functionality of the containing antibodies. Serum Dilution: 1:10,000.

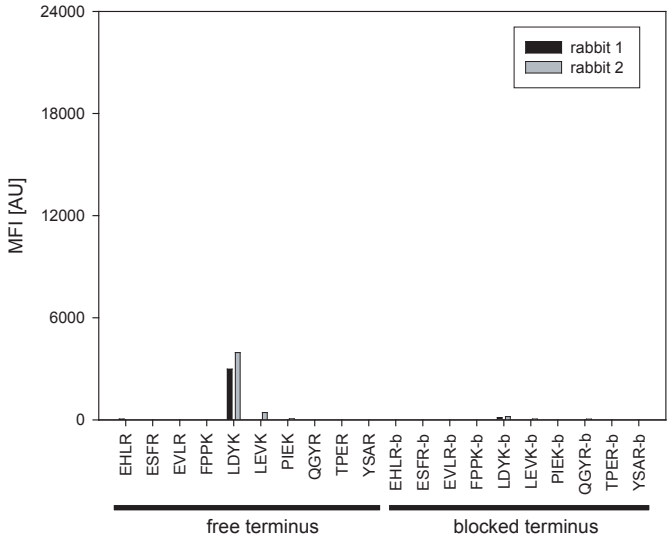

Figure A.9.: Antibody binding assay - anti-LDYK to test the rabbit sera (2 replicates) for the success of immunization respectively for the functionality of the containing antibodies. Serum Dilution: 1:10,000.

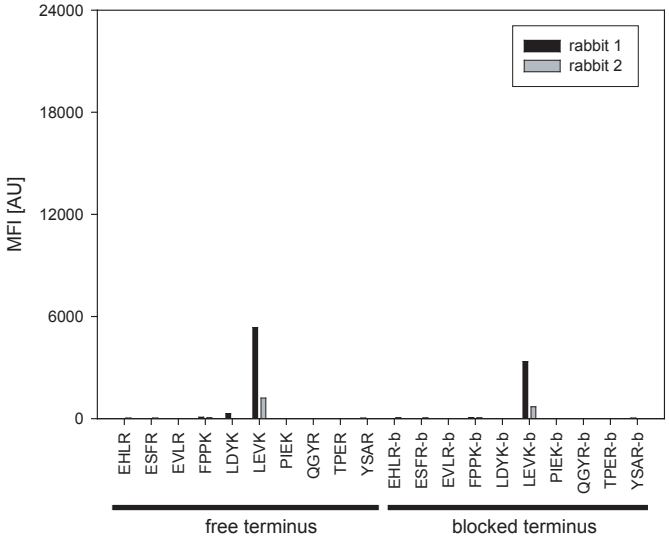

Figure A.10.: Antibody binding assay - anti-LEVK to test the rabbit sera (2 replicates) for the success of immunization respectively for the functionality of the containing antibodies. Serum Dilution: 1:10,000.

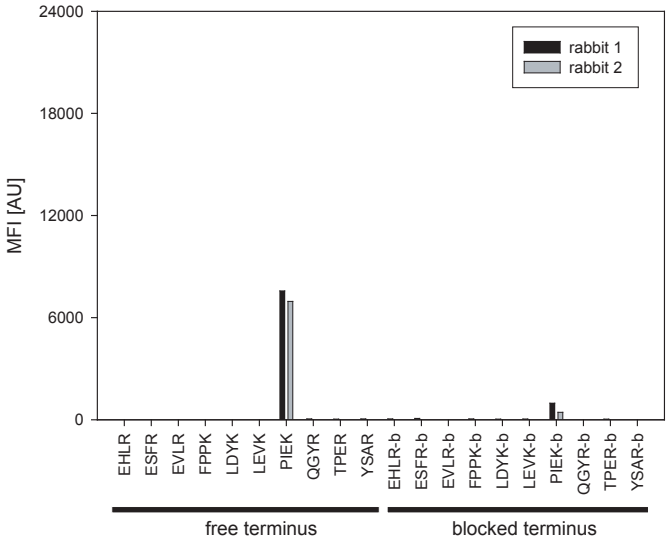

Figure A.11.: Antibody binding assay - anti-PIEK to test the rabbit sera (2 replicates) for the success of immunization respectively for the functionality of the containing antibodies. Serum Dilution: 1:10,000.

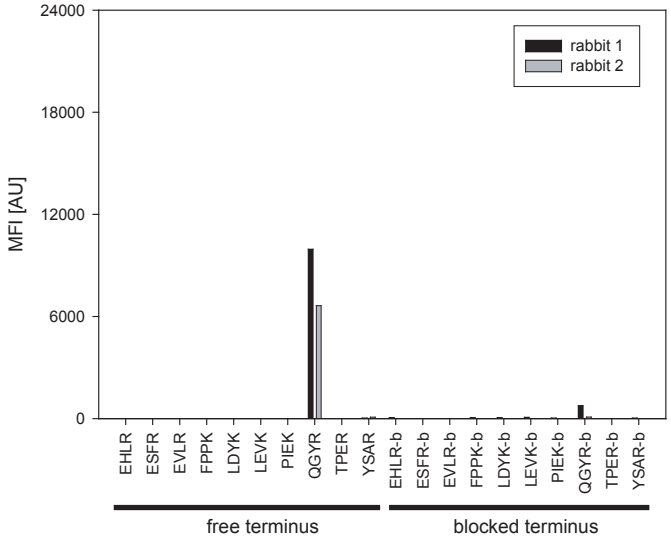

Figure A.12.: Antibody binding assay - anti-QGYR to test the rabbit sera (2 replicates) for the success of immunization respectively for the functionality of the containing antibodies. Serum Dilution: 1:10,000.

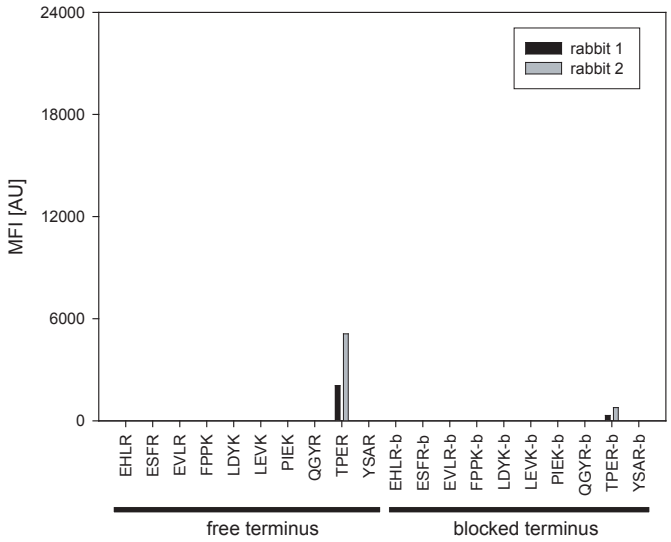

Figure A.13.: Antibody binding assay - anti-TPER to test the rabbit sera (2 replicates) for the success of immunization respectively for the functionality of the containing antibodies. Serum Dilution: 1:10,000.

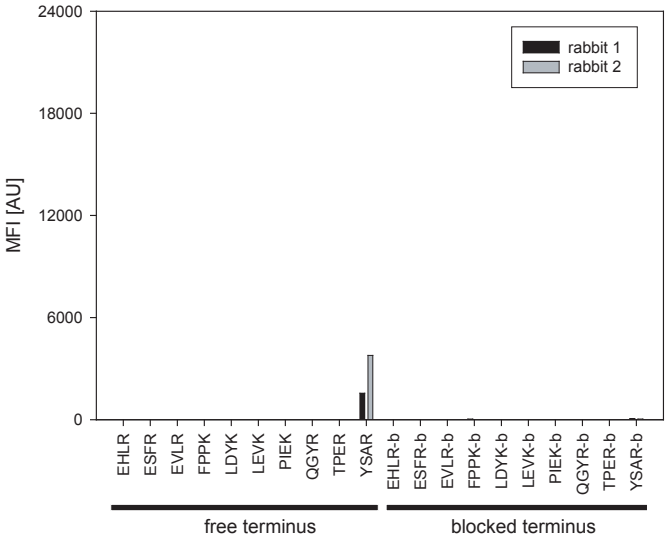

Figure A.14.: Antibody binding assay - anti-YSAR to test the rabbit sera (2 replicates) for the success of immunization respectively for the functionality of the containing antibodies. Serum Dilution: 1:10,000.

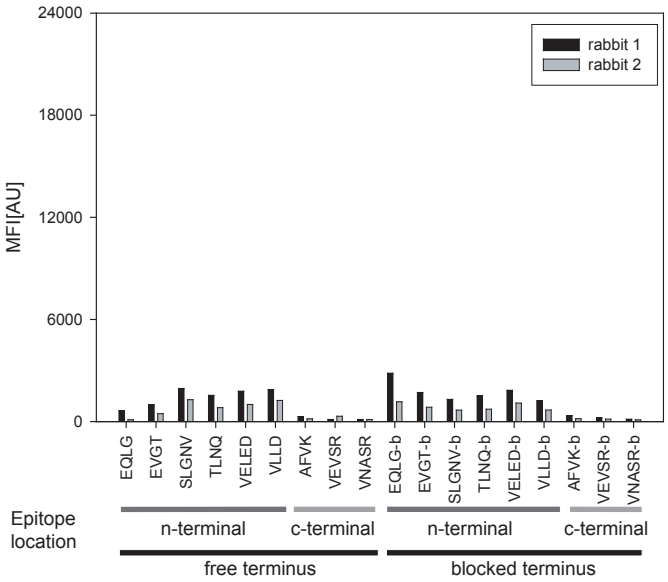

Figure A.15.: Antibody binding assay - anti-EQLG to test the rabbit sera (2 replicates) for the success of immunization respectively for the functionality of the containing antibodies. Serum Dilution: 1:20,000.

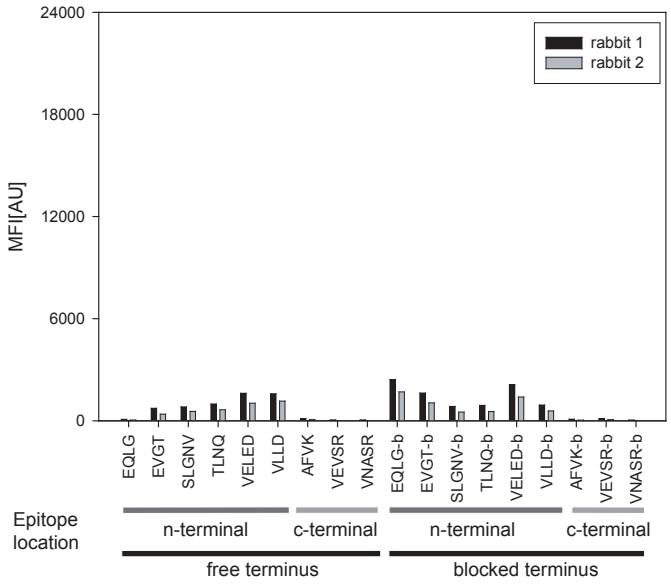

Figure A.16.: Antibody binding assay - anti-EVGT to test the rabbit sera (2 replicates) for the success of immunization respectively for the functionality of the containing antibodies. Serum Dilution: 1:20,000.

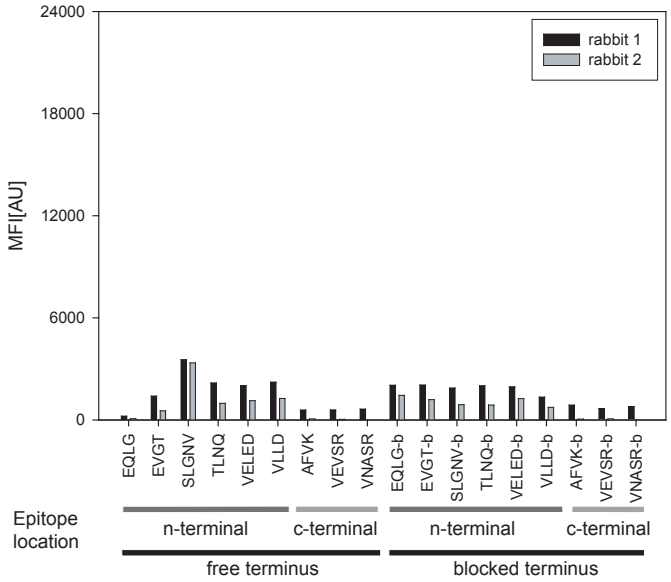

Figure A.17.: Antibody binding assay - anti-SLGNV to test the rabbit sera (2 replicates) for the success of immunization respectively for the functionality of the containing antibodies. Serum Dilution: 1:20,000.

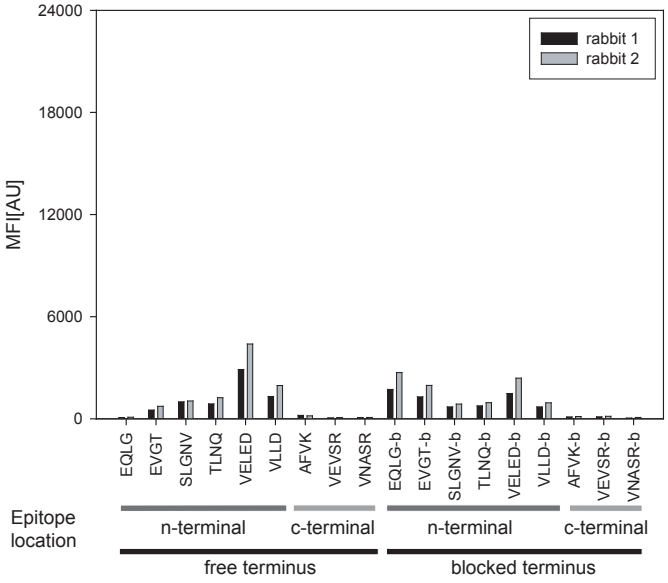

Figure A.18.: Antibody binding assay - anti-VELED to test the rabbit sera (2 replicates) for the success of immunization respectively for the functionality of the containing antibodies. Serum Dilution: 1:20,000.

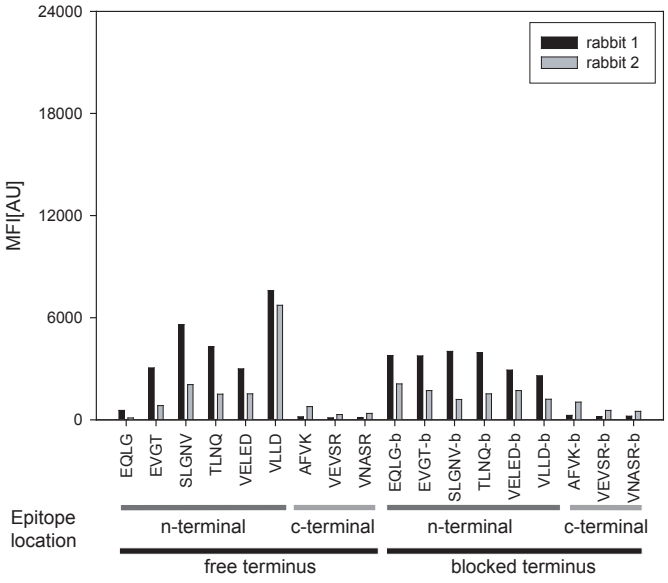

Figure A.19.: Antibody binding assay - anti-VLLD to test the rabbit sera (2 replicates) for the success of immunization respectively for the functionality of the containing antibodies. Serum Dilution: 1:20,000.

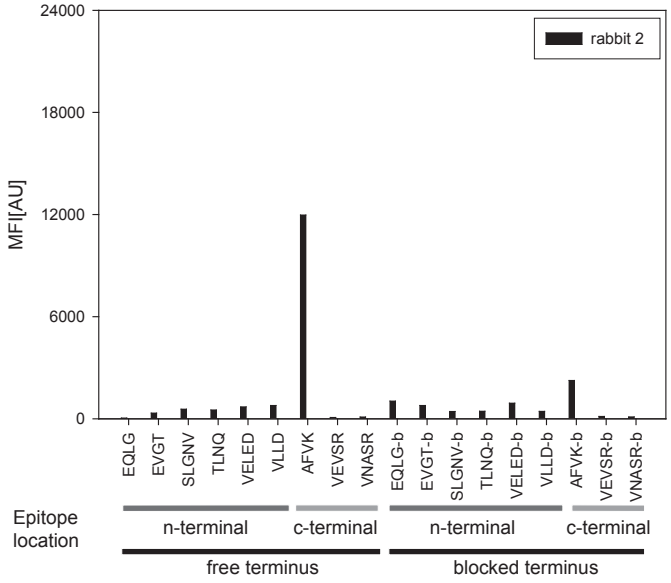

Figure A.20.: Antibody binding assay - anti-AFVK to test the rabbit sera (2 replicates) for the success of immunization respectively for the functionality of the containing antibodies. Serum Dilution: 1:20,000.

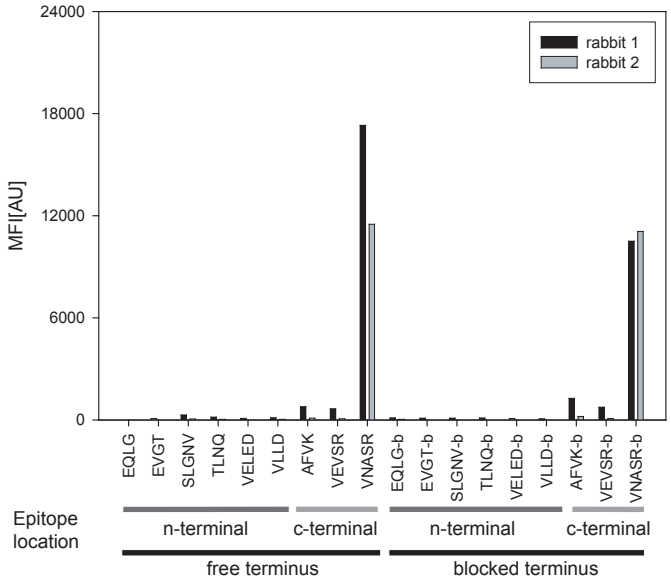

Figure A.21.: Antibody binding assay - anti-VNASR to test the rabbit sera (2 replicates) for the success of immunization respectively for the functionality of the containing antibodies. Serum Dilution: 1:20,000.

A.2. Peptide capture assays - graphs

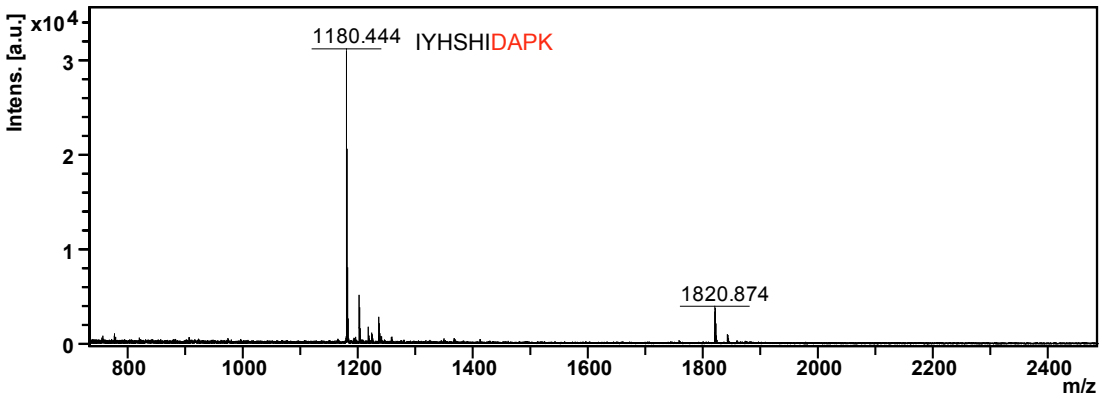

Figure A.22.: Peptide capture assay - anti-DAPK. MALDI read-out of a TXP assay using the C-terminal anti-DAPK antibody. The TXP antibody is capable of capturing the targeted standard peptide: IYHSHIDAPK. The mass 1820 Da is the peptide DAVEKPQEFTIVAFVK, which was bound non-specifically.

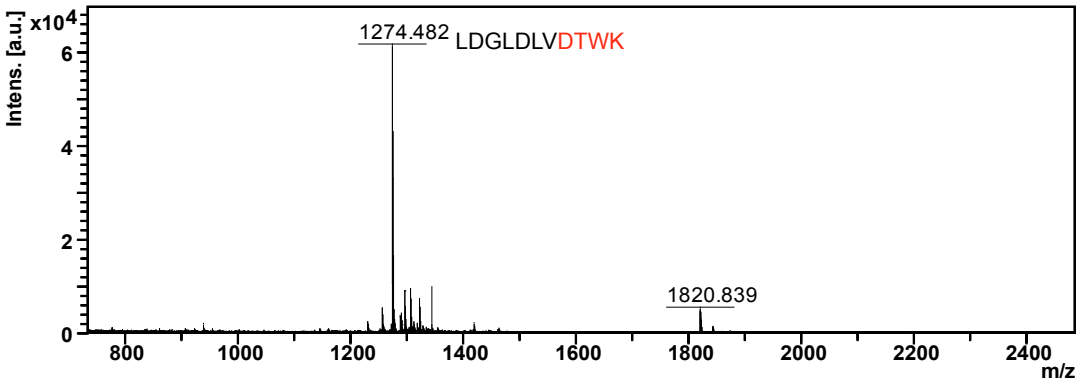

Figure A.23.: Peptide capture assay - anti-DTWK. MALDI read-out of a TXP assay using the C-terminal anti-DTWK antibody. The TXP antibody is capable of capturing the targeted standard peptide: LDGLDLVDTWK. The mass 1820 Da is the peptide DAVEKPQEFTIVAFVK, which was bound non-specifically.

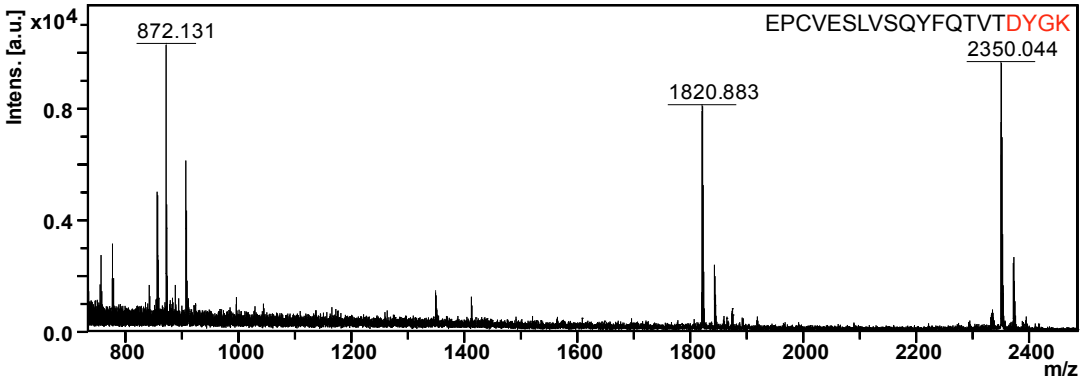

Figure A.24.: Peptide capture assay - anti-DYGK. MALDI read-out of a TXP assay using the C-terminal anti-DYGK antibody. The TXP antibody is capable of capturing the targeted standard peptide: EPCVESLVSQYFQTVTDYGK. The mass 1820 Da is the peptide DAVEKPQEFTIVAFVK, which was bound non-specifically.

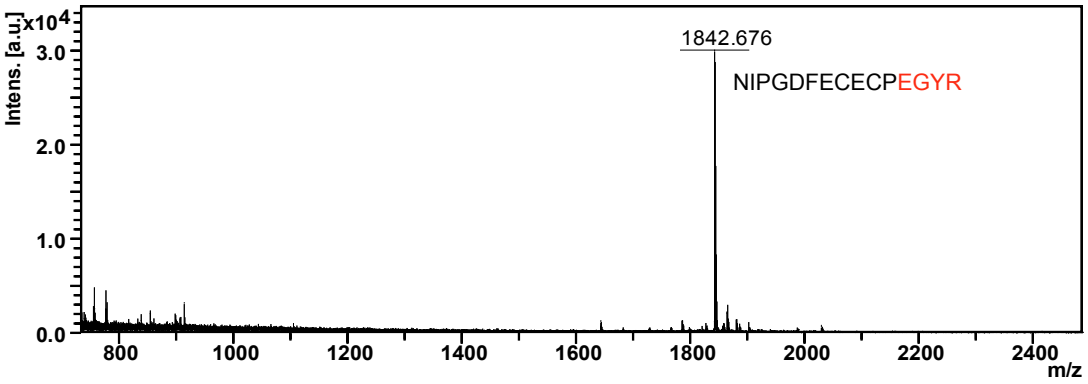

Figure A.25.: Peptide capture assay - anti-EGYR. MALDI read-out of a TXP assay using the C-terminal anti-EGYR antibody. The TXP antibody is capable of capturing the targeted standard peptide: NIPGDFECECPEGYR. The mass 1820 Da is the peptide DAVEKPQEFTIVAFVK, which was bound non-specifically.

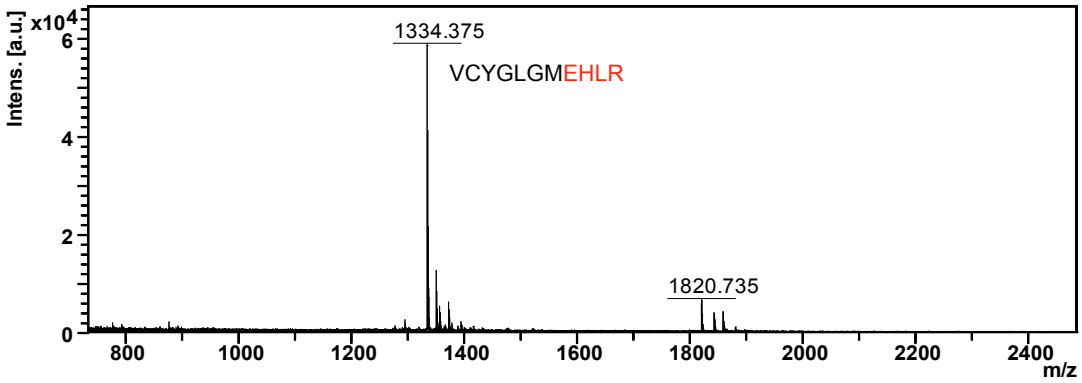

Figure A.26.: Peptide capture assay - anti-EHLR. MALDI read-out of a TXP assay using the C-terminal anti-EHLR antibody. The TXP antibody is capable of capturing the targeted standard peptide: VCYGLGMEHLR. The mass 1820 Da is the peptide DAVEKPQEFTIVAFVK, which was bound non-specifically.

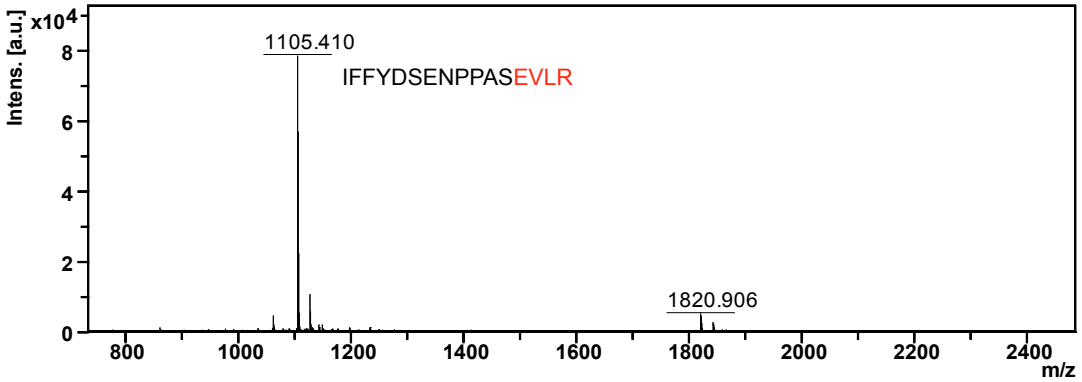

Figure A.27.: Peptide capture assay - anti-ESFR. MALDI read-out of a TXP assay using the C-terminal anti-ESFR antibody. The TXP antibody is capable of capturing the targeted standard peptide: APTAQVESFR. The mass 1820 Da is the peptide DAVEKPQEFTIVAFVK, which was bound non-specifically.

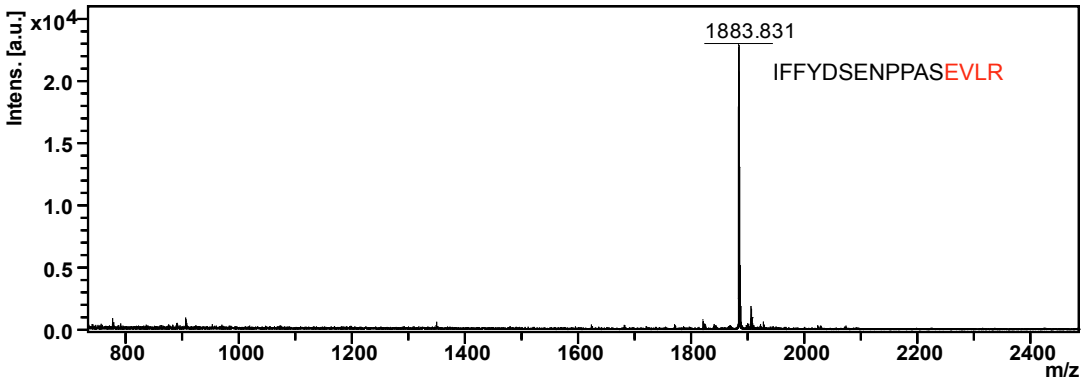

Figure A.28.: Peptide capture assay - anti-EVLR. MALDI read-out of a TXP assay using the C-terminal anti-EVLR antibody. The TXP antibody is capable of capturing the targeted standard peptide: IFFYDSENPPASEVLR. The mass 1820 Da is the peptide DAVEKPQEFTIVAFVK, which was bound non-specifically.

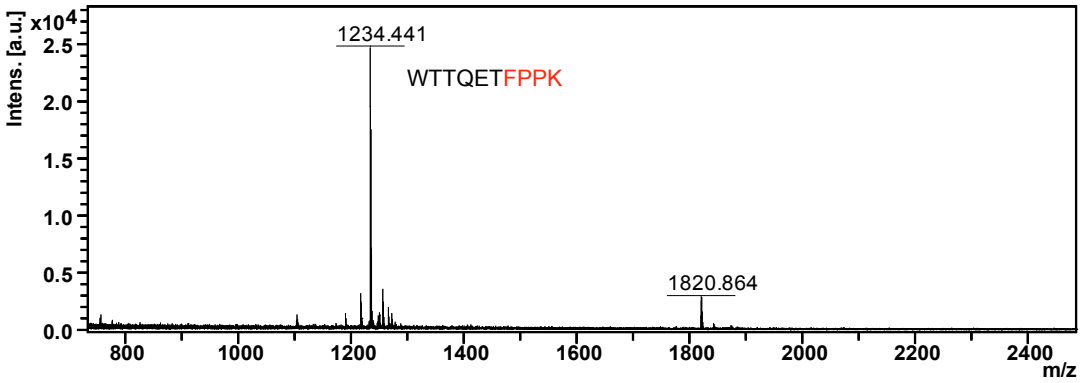

Figure A.29.: Peptide capture assay - anti-FPPK. MALDI read-out of a TXP assay using the C-terminal anti-FPPK antibody. The TXP antibody is capable of capturing the targeted standard peptide: WTTQETFPPK. The mass 1820 Da is the peptide DAVEKPQEFTIVAFVK, which was bound non-specifically.

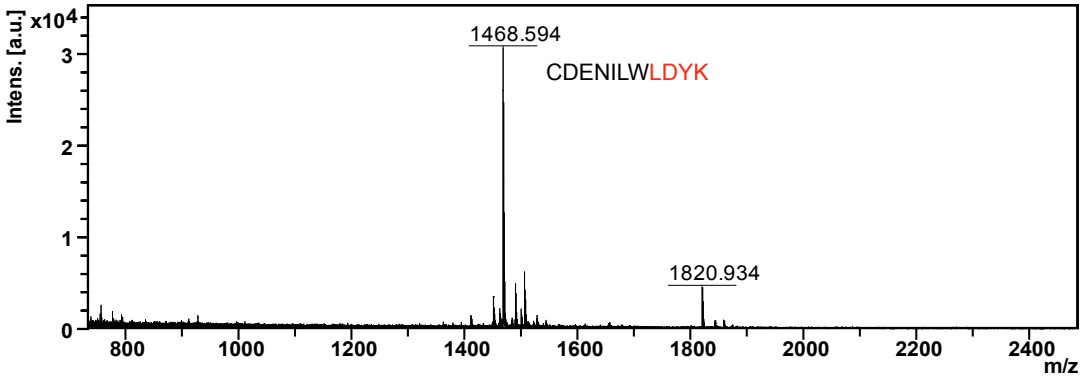

Figure A.30.: Peptide capture assay - anti-LDYK. MALDI read-out of a TXP assay using the C-terminal anti-LDYK antibody. The TXP antibody is capable of capturing the targeted standard peptide: CDENILWLDYK. The mass 1820 Da is the peptide DAVEKPQEFTIVAFVK, which was bound non-specifically.

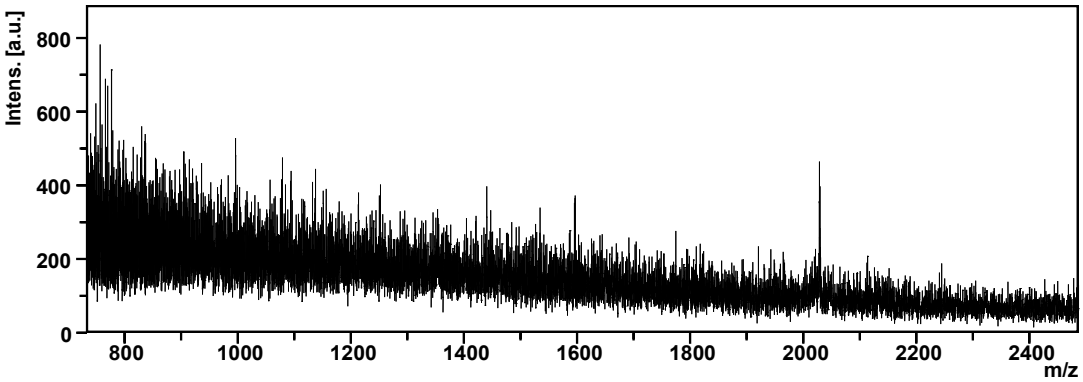

Figure A.31.: Peptide capture assay - anti-LEVK. MALDI read-out of a TXP assay using the C-terminal anti-LEVK antibody. The TXP antibody is not capable of capturing the targeted standard peptide: ALEAANGELEVK.

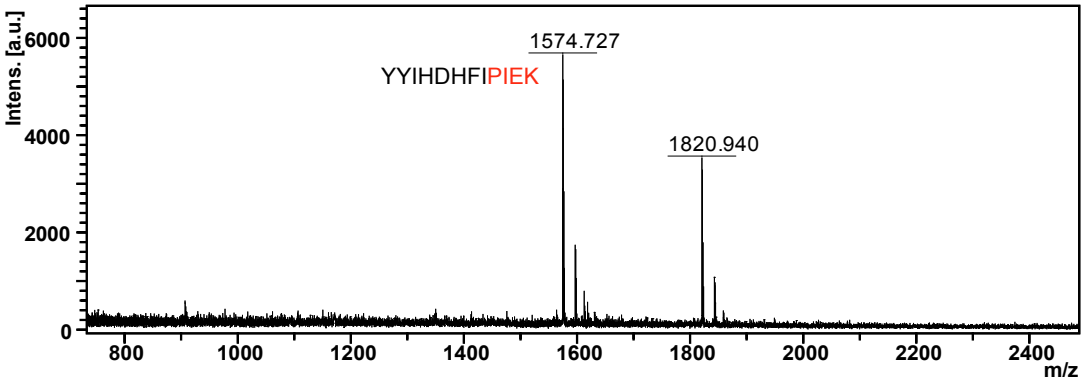

Figure A.32.: Peptide capture assay - anti-PIEK. MALDI read-out of a TXP assay using the C-terminal anti-PIEK antibody. The TXP antibody is capable of capturing the targeted standard peptide: YYIHDHFIPIEK. The mass 1820 Da is the peptide DAVEKPQEFTIVAFVK, which was bound non-specifically.

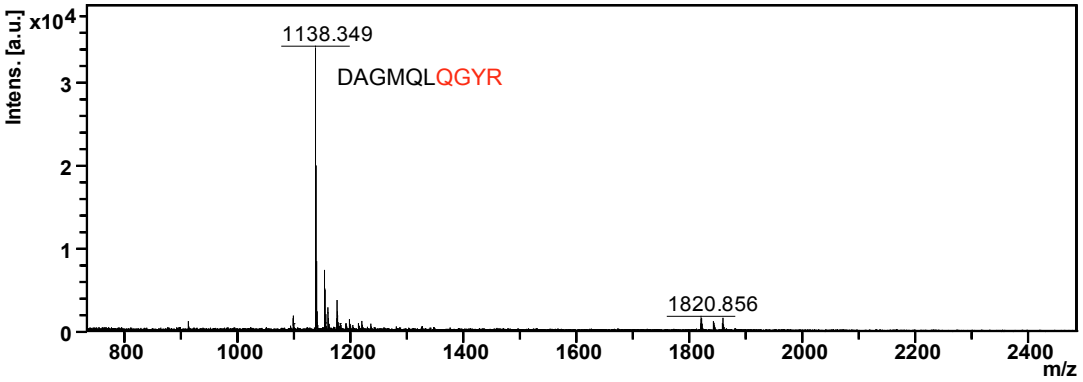

Figure A.33.: Peptide capture assay - anti-QGYR. MALDI read-out of a TXP assay using the C-terminal anti-QGYR antibody. The TXP antibody is capable of capturing the targeted standard peptide: DAGMQLQGYR. The mass 1820 Da is the peptide DAVEKPQEFTIVAFVK, which was bound non-specifically.

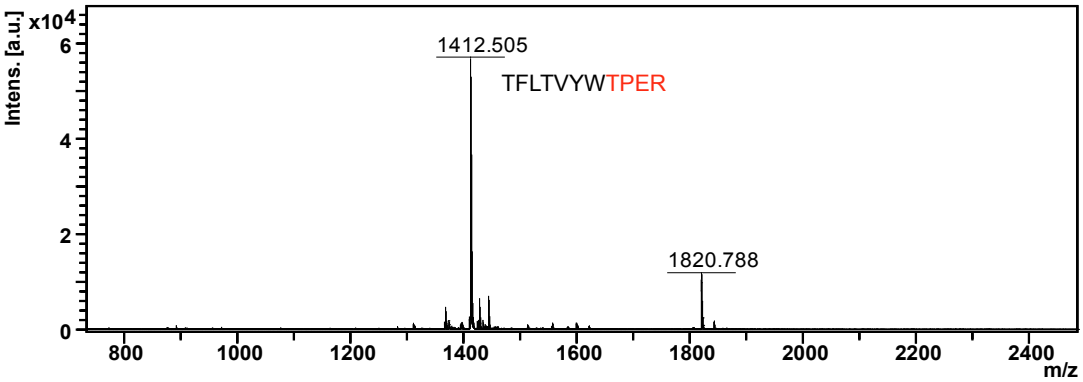

Figure A.34.: Peptide capture assay - anti-TPER. MALDI read-out of a TXP assay using the C-terminal anti-TPER antibody. The TXP antibody is capable of capturing the targeted standard peptide: TFLTVYWTPER. The mass 1820 Da is the peptide DAVEKPQEFTIVAFVK, which was bound non-specifically.

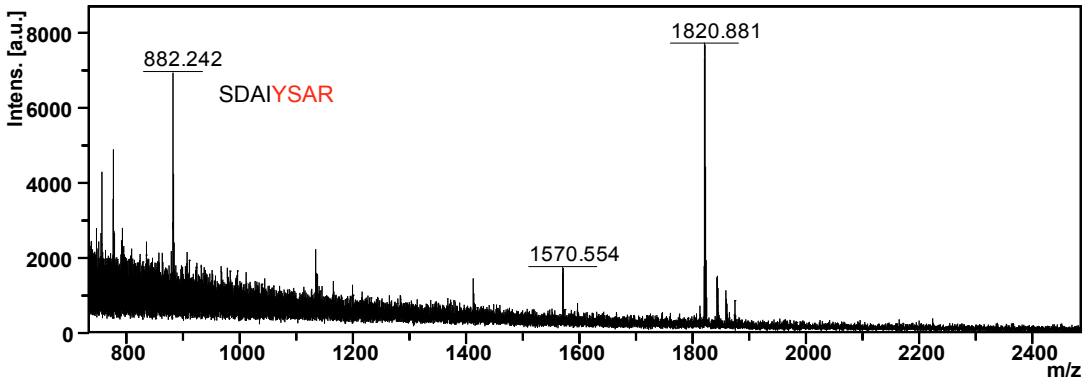

Figure A.35.: Peptide capture assay - anti-YSAR. MALDI read-out of a TXP assay using the C-terminal anti-YSAR antibody. The TXP antibody is capable of capturing the targeted standard peptide: SDAIYSAR. The mass 1820 Da is the peptide DAVEKPQEFTIVAFVK, which was bound non-specifically.

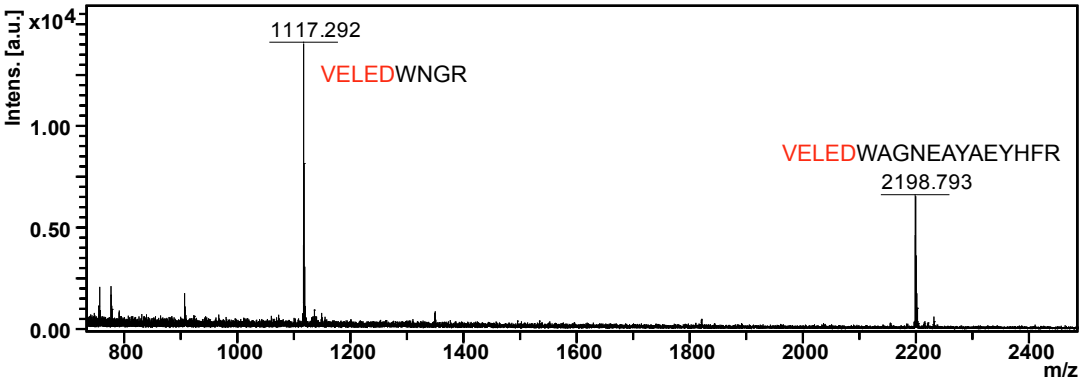

Figure A.36.: Peptide capture assay - anti-VELED. MALDI read-out of a TXP assay using the C-terminal anti-VELED antibody. The TXP antibody is capable of capturing the targeted standard peptides: VELEDWNGR and VELEDWAGNEAYAEYHFR.

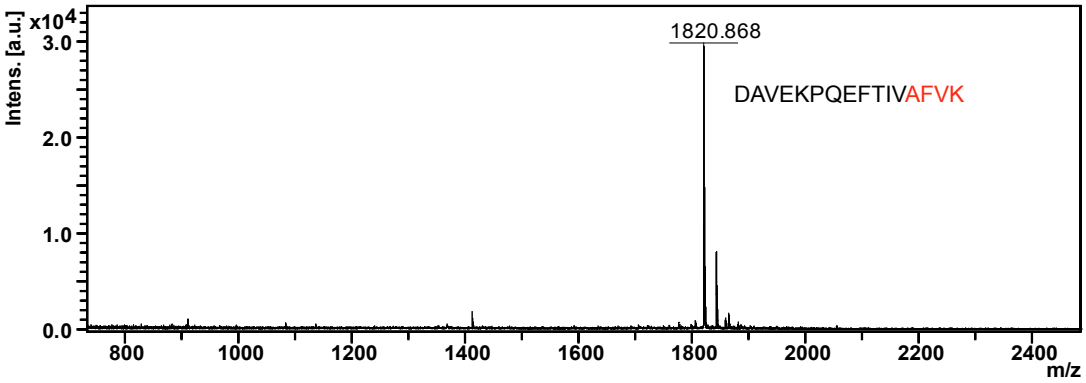

Figure A.37.: Peptide capture assay - anti-AFVK antibody. MALDI read-out of a TXP assay using the C-terminal anti-AFVK antibody. The TXP antibody is capable of capturing the targeted standard peptide: DAVEKPQEFTIVAFVK. The second target peptide DGAGDVAFVKwas not detected.

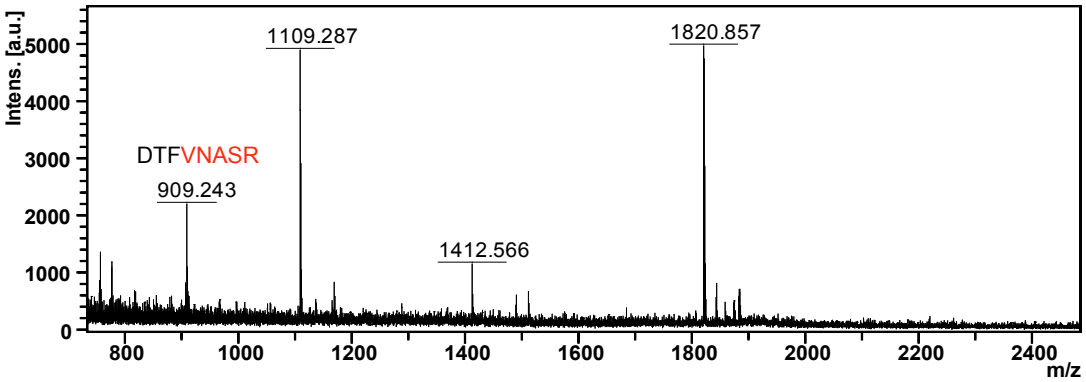

Figure A.38.: Peptide capture assay - anti-VNASR antibody. MALDI read-out of a TXP assay using the C-terminal anti-VNASR antibody. The TXP antibody is capable of capturing the targeted standard peptide: DTFVNASR. The mass 1820 Da is the peptide DAVEKPQEFTIVAFVK, which was bound non-specifically.

A.3. Immunaffinity enrichment using TXP antibodies - MSMS spectra

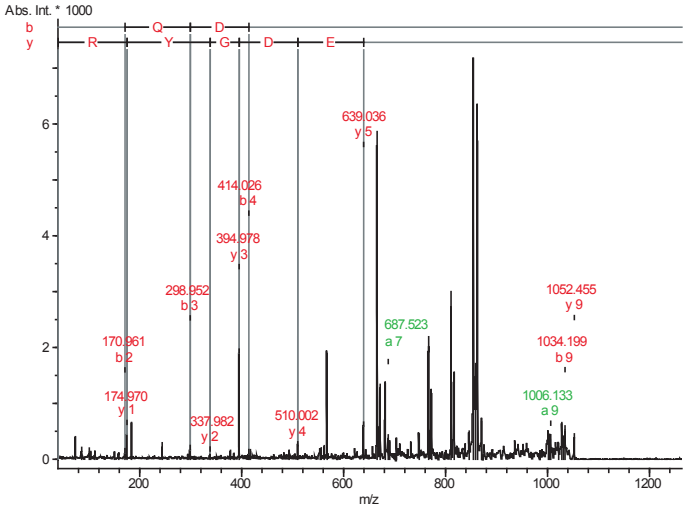

Figure A.39.: Fragment spectrum of a tryptic fragment of complement C4a containing the TXP tag DGYR with one exchanged amino acid D instead of E. b- and y-ion series were used for amino acid identification (red).

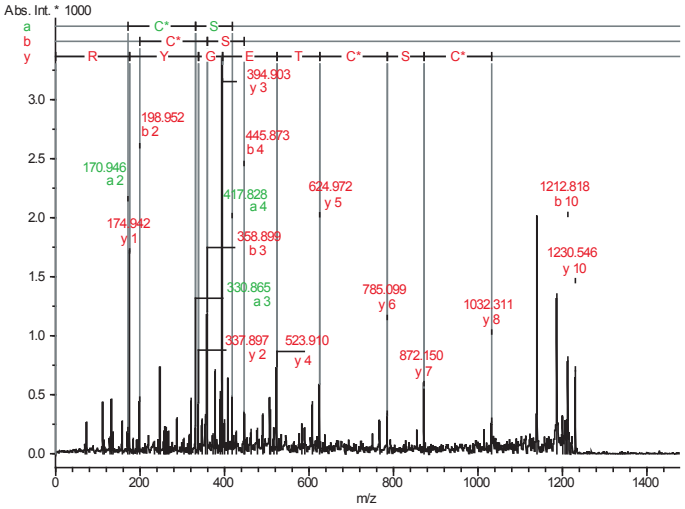

Figure A.40.: Fragment spectrum of a tryptic fragment of coagulation Factor IX containing the TXP tag EGYR. a- (green), b- and y-ion (red) series were used for amino acid identification.

A.4. Non-specific binding

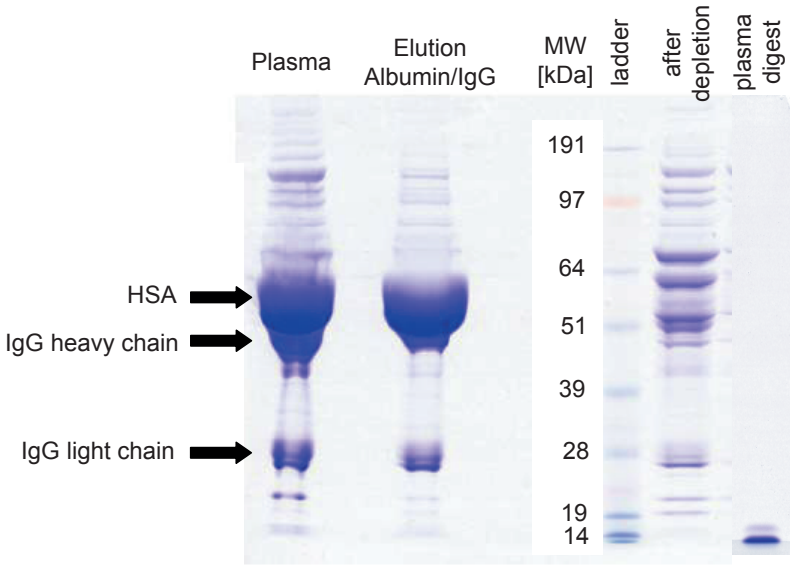

Figure A.41.: SDS PAGE depletion columns/digest. A huge content of albumin and IgG is found in plasma (left lane). The elution from the depletion columns show that mostly albumin and IgG was bound by the column, but also other proteins bands were detected in the elution, second lane. After passing the depletion column, the bands from albumin and IgG are significantly reduced, see lane "after depletion". The right lane shows the plasma digest.

Table A.1.: Non-specific binding peptides of high abundant proteins in human plasma.

m/z	protein	peptide sequence
940.46	Albumin	DDNPNLPR
960.59	Albumin	FQNALLVR
1,074.55	Albumin	LDELRDEGK
1,077.59	Albumin	DYSVVLLLR
1,083.65	Complement C3	GYTQQLAFR
1,138.51	Albumin	CCTESLVNR
1,160.70	Alpha-1-acid glycoprotein 1	WFYIASAFR
1,311.77	Albumin	HPDYSVVLLLR
1,468.00	Albumin	RHPDYSVVLLLR
1,545.79	Alpha-2-macroglobulin	LVHVEEPHTETVR
1,742.91	Albumin	HPYFYAPELLFFAK
1,797.91	Albumin	SGTASVVCLLNNFYPR
1,840.93	Alpha-2-macroglobulin	AHTSFQISLSVSYTGSR
1,899.02	Albumin	HPYFYAPELLFFAKR
2,045.26	Albumin	VFDEFKPLVEEPQNLIK
2,086.81	Albumin	VHTECCHGDLLECADDR
2,259.99	Albumin	EFNAETFTFHADICTLSEK
2,387.18	Albumin	PCAEDYLSVVLNQLCVLHEK
2,490.46	Albumin	ALVLIAFAQYLQQCPFEDHVK
2,518.24	Albumin	MPCAEDYLSVVLNQLCVLHEK
2,545.38	Albumin	EFNAETFTFHADICTLSEKER
2,650.20	Albumin	LVRPEVDVMCTAFHDNEETFLK
3,042.52	Albumin	PCAEDYLSVVLNQLCVLHEKTPVSDR
3,173.48	Albumin	MPCAEDYLSVVLNQLCVLHEKTPVSDR

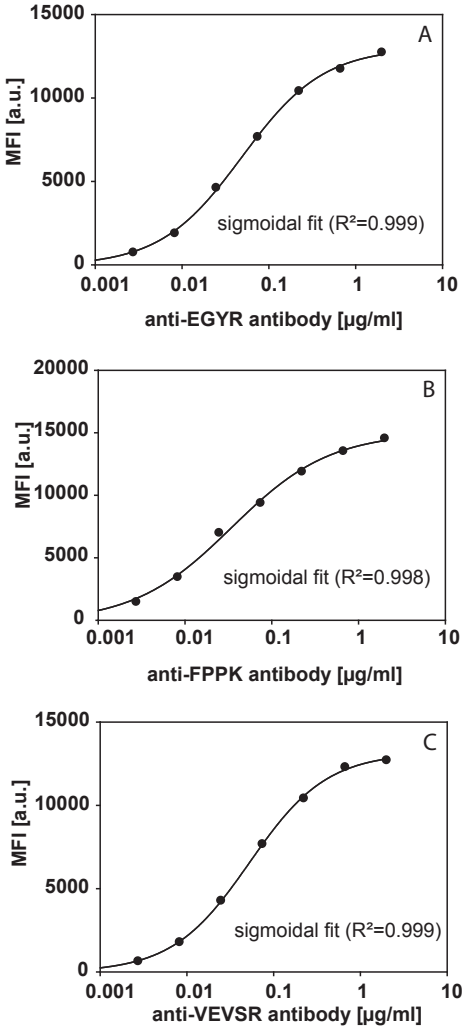

Figure A.42.: Bead-based immunoassays - linearity. Dilution series of 3 TXP antibodies: anti-EGYR, anti-FPPK and anti-VEVSR.

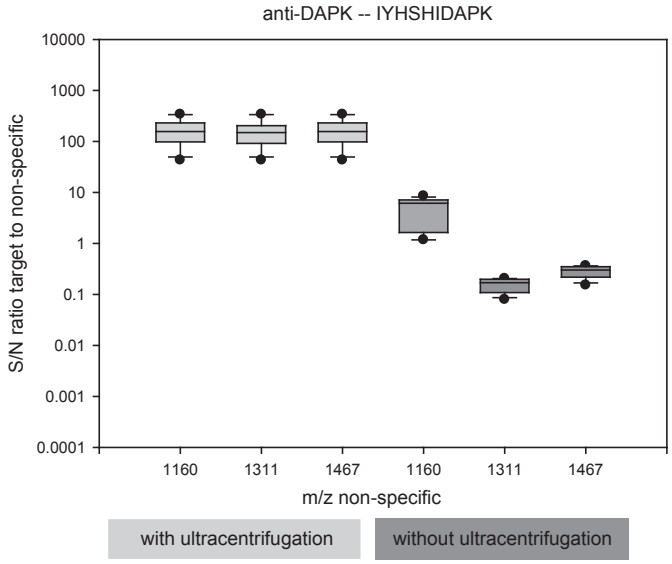

Figure A.43.: Distribution of signal-to-noise ratios of target peptide IYHSHIDAPK (m/z 1180, Ceruloplasmin) to selected non-specific peptides for assay conditions with and without ultracentrifugation. One target peptide was set in relation to each of three non-specific peptides from two different proteins: one peptide from Alpha-1-acid glycoprotein 1 (m/z 1,160.70, WFYIASAFR) and two peptides from Human serum albumin (m/z 1,311.77, HPDYSVVLLLR and m/z 1,467.85, RHPDYSVVLLLR). Data from 3 assay replicates were included in one box plot. The S/N ratios of the values generated with the ultracentrifugation procedure are significantly ($P<0.001$) higher compared to the respective values of the assays without ultracentrifugation. Statistical significances were calculated with Mann-Whitney test using StatistiXL 1.8.

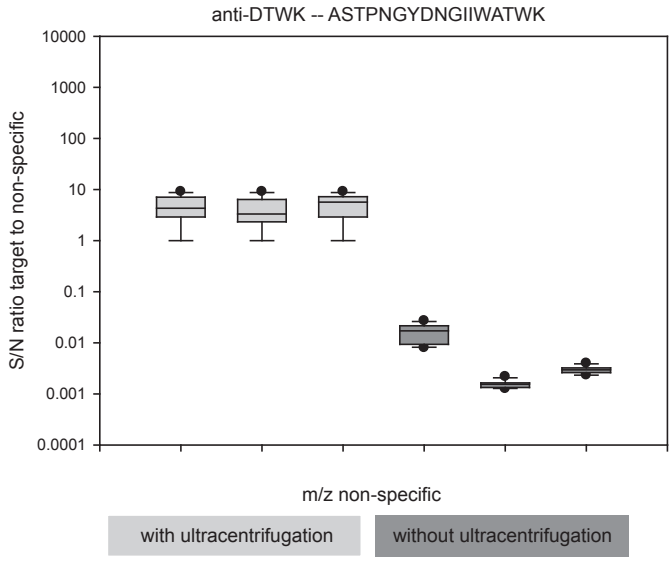

Figure A.44.: Distribution of signal-to-noise ratios of target peptide ASTPNGYDNGIIWATWK (m/z 1894, Fibrinogen) to selected non-specific peptides for assay conditions with and without ultracentrifugation. One target peptide was set in relation to each of three non-specific peptides from two different proteins: one peptide from Alpha-1-acid glycoprotein 1 (m/z 1,160.70, WFYIASAFR) and two peptides from Human serum albumin (m/z 1,311.77, HPDYSVVLLLR and m/z 1,467.85, RHPDYSVVLLLR). Data from 3 assay replicates were included in one box plot. The S/N ratios of the values generated with the ultracentrifugation procedure are significantly ($P<0.001$) higher compared to the respective values of the assays without ultracentrifugation. Statistical significances were calculated with Mann-Whitney test using StatistiXL 1.8.

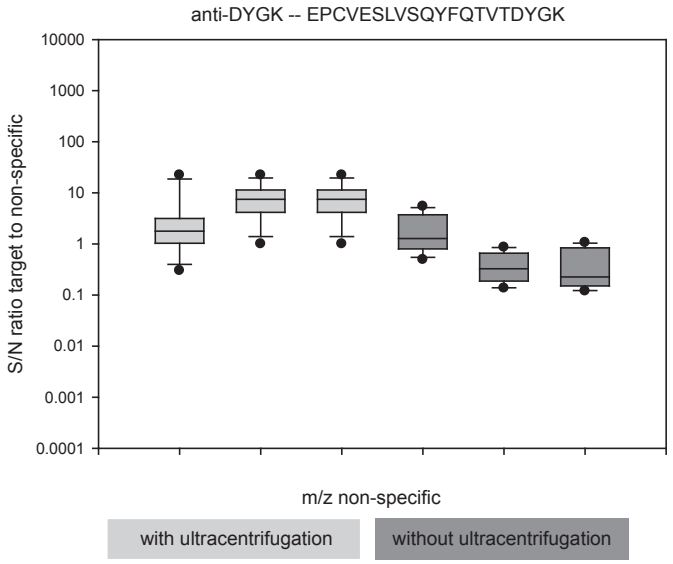

Figure A.45.: Distribution of signal-to-noise ratios of target peptide EPCVESLVSQYFQTVTDYGK (m/z 2350, Apolipoprotein A-II) to selected non-specific peptides for assay conditions with and without ultracentrifugation. One target peptide was set in relation to each of three non-specific peptides from two different proteins: one peptide from Alpha-1-acid glycoprotein 1 (m/z 1,160.70, WFYIASAFR) and two peptides from Human serum albumin (m/z 1,311.77, HPDYSVVLLLR and m/z 1,467.85, RHPDYSVVLLLR). Data from 3 assay replicates were included in one box plot. The S/N ratios of the values generated with the ultracentrifugation procedure are not significantly higher compared to the respective values of the assays without ultracentrifugation. Statistical significances were calculated with Mann-Whitney test using StatistiXL 1.8.

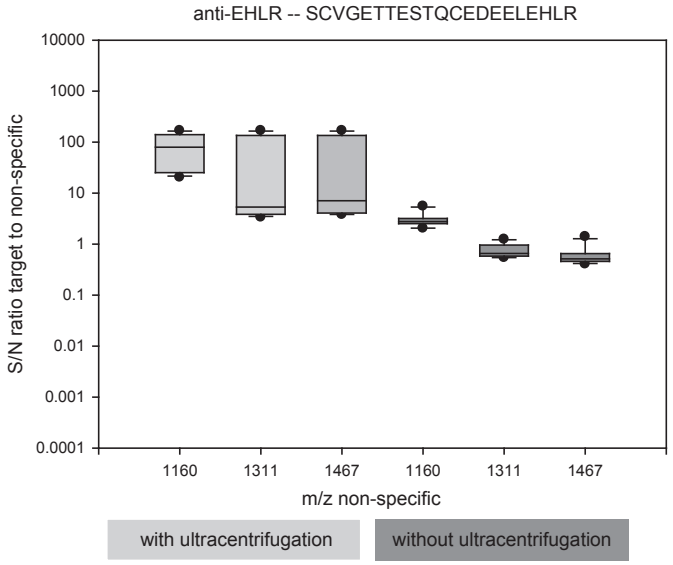

Figure A.46.: Distribution of signal-to-noise ratios of target peptide SCVGETTESTQCEDEELEHLR (m/z 2509, Complement component C7) to selected non-specific peptides for assay conditions with and without ultracentrifugation. One target peptide was set in relation to each of three non-specific peptides from two different proteins: one peptide from Alpha-1-acid glycoprotein 1 (m/z 1,160.70, WFYIASAFR) and two peptides from Human serum albumin (m/z 1,311.77, HPDYSVVLLLR and m/z 1,467.85, RHPDYSVVLLLR). Data from 3 assay replicates were included in one box plot. The S/N ratios of the values generated with the ultracentrifugation procedure are significantly ($P<0.001$) higher compared to the respective values of the assays without ultracentrifugation. Statistical significances were calculated with Mann-Whitney test using StatistiXL 1.8.

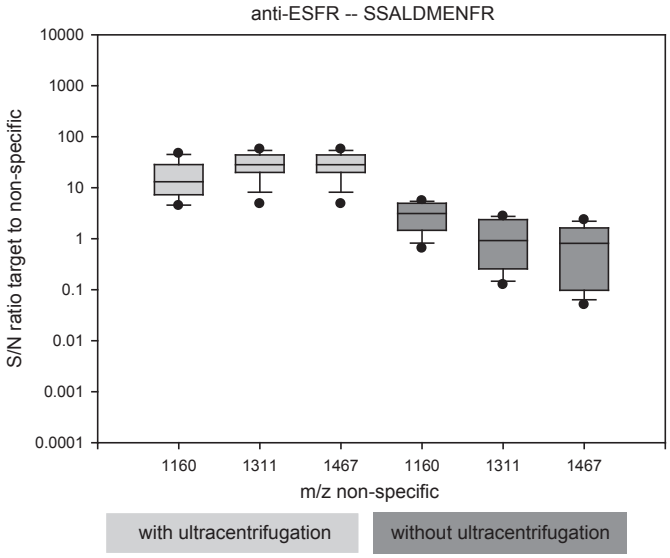

Figure A.47.: Distribution of signal-to-noise ratios of target peptide SSALDMENFR (m/z 1169, Inter-alpha-trypsin inhibitor heavy chain H2) to selected non-specific peptides for assay conditions with and without ultracentrifugation. One target peptide was set in relation to each of three non-specific peptides from two different proteins: one peptide from Alpha-1-acid glycoprotein 1 (m/z 1,160.70, WFYIASAFR) and two peptides from Human serum albumin (m/z 1,311.77, HPDYSVVLLLR and m/z 1,467.85, RHPDYSVVLLLR). Data from 3 assay replicates were included in one box plot. The S/N ratios of the values generated with the ultracentrifugation procedure are significantly ($P<0.001$) higher compared to the respective values of the assays without ultracentrifugation. Statistical significances were calculated with Mann-Whitney test using StatistiXL 1.8.

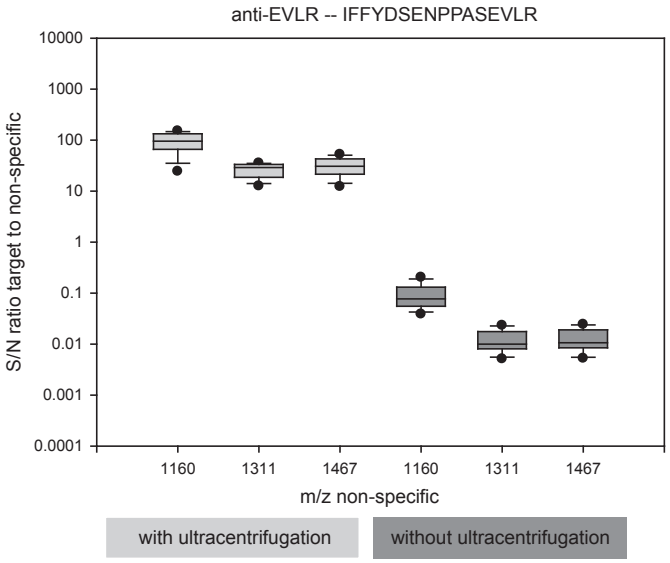

Figure A.48.: Distribution of signal-to-noise ratios of target peptide IFFYDSENPPASEVLR (m/z 1884, Serum paraoxonase/arylesterase 1) to selected non-specific peptides for assay conditions with and without ultracentrifugation. One target peptide was set in relation to each of three non-specific peptides from two different proteins: one peptide from Alpha-1-acid glycoprotein 1 (m/z 1,160.70, WFYIASAFR) and two peptides from Human serum albumin (m/z 1,311.77, HPDYSVVLLLR and m/z 1,467.85, RHPDYSVVLLLR). Data from 3 assay replicates were included in one box plot. The S/N ratios of the values generated with the ultracentrifugation procedure are significantly ($P<0.001$) higher compared to the respective values of the assays without ultracentrifugation. Statistical significances were calculated with Mann-Whitney test using StatistiXL 1.8.

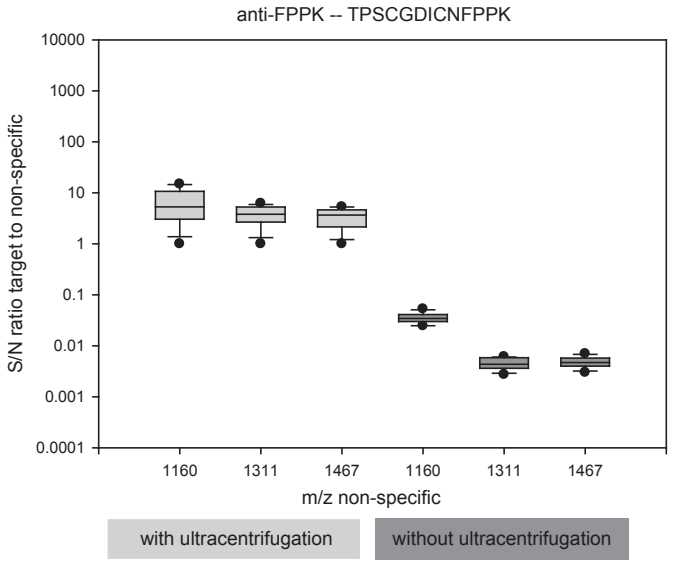

Figure A.49.: Distribution of signal-to-noise ratios of target peptide TPSCGDICNFPPK (m/z 1492, C4b-binding protein alpha chain) to selected non-specific peptides for assay conditions with and without ultracentrifugation. One target peptide was set in relation to each of three non-specific peptides from two different proteins: one peptide from Alpha-1-acid glycoprotein 1 (m/z 1,160.70, WFYIASAFR) and two peptides from Human serum albumin (m/z 1,311.77, HPDYSVVLLLR and m/z 1,467.85, RHPDYSVVLLLR). Data from 3 assay replicates were included in one box plot. The S/N ratios of the values generated with the ultracentrifugation procedure are significantly ($P<0.001$) higher compared to the respective values of the assays without ultracentrifugation. Statistical significances were calculated with Mann-Whitney test using StatistiXL 1.8.

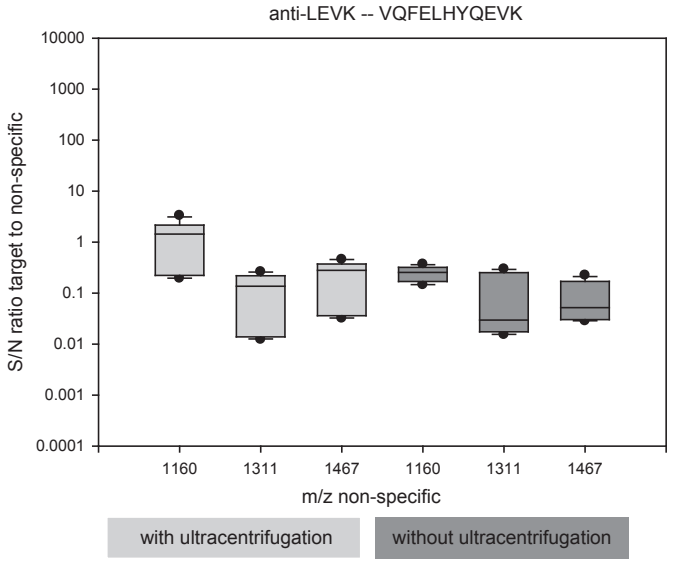

Figure A.50.: Distribution of signal-to-noise ratios of target peptide VQFELHYQEVK (m/z 1420, Inter-alpha-trypsin inhibitor heavy chain H2) to selected non-specific peptides for assay conditions with and without ultracentrifugation. One target peptide was set in relation to each of three non-specific peptides from two different proteins: one peptide from Alpha-1-acid glycoprotein 1 (m/z 1,160.70, WFYIASAFR) and two peptides from Human serum albumin (m/z 1,311.77, HPDYSVVLLLR and m/z 1,467.85, RHPDYSVVLLLR). Data from 3 assay replicates were included in one box plot. The S/N ratios of the values generated with the ultracentrifugation procedure are not significantly higher compared to the respective values of the assays without ultracentrifugation. Statistical significances were calculated with Mann-Whitney test using StatistiXL 1.8.

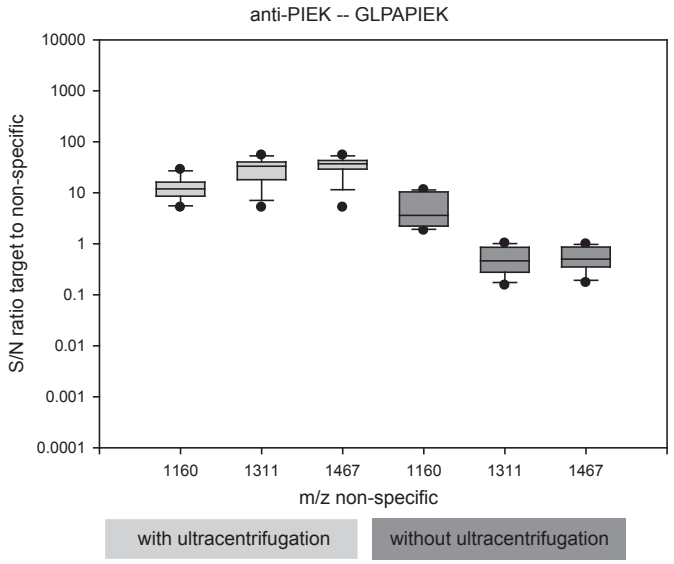

Figure A.51.: Distribution of signal-to-noise ratios of target peptide GLPAPIEK (m/z 824, Ig gamma-2 chain C region) to selected non-specific peptides for assay conditions with and without ultracentrifugation. One target peptide was set in relation to each of three non-specific peptides from two different proteins: one peptide from Alpha-1-acid glycoprotein 1 (m/z 1,160.70, WFYIASAFR) and two peptides from Human serum albumin (m/z 1,311.77, HPDYSVVLLLR and m/z 1,467.85, RHPDYSVVLLLR). Data from 3 assay replicates were included in one box plot. The S/N ratios of the values generated with the ultracentrifugation procedure are significantly ($P<0.001$) higher compared to the respective values of the assays without ultracentrifugation. Statistical significances were calculated with Mann-Whitney test using StatistiXL 1.8.

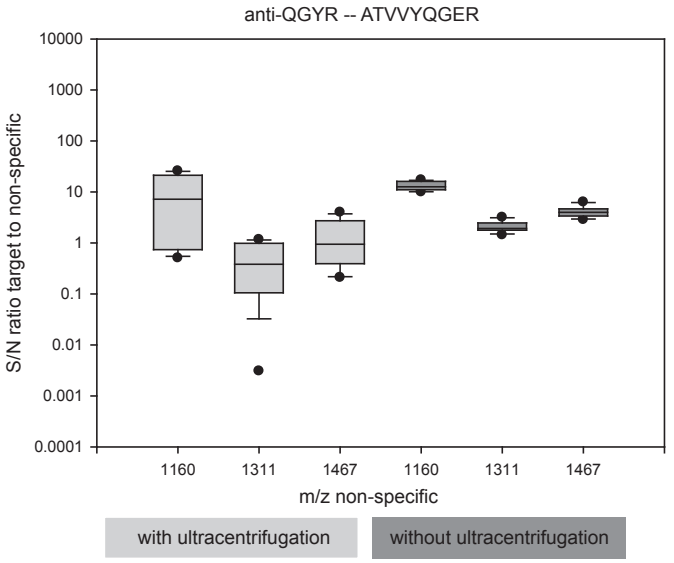

Figure A.52.: Distribution of signal-to-noise ratios of target peptide ATVVYQGER (m/z 1022, Beta-2-glycoprotein 1) to selected non-specific peptides for assay conditions with and without ultracentrifugation. One target peptide was set in relation to each of three non-specific peptides from two different proteins: one peptide from Alpha-1-acid glycoprotein 1 (m/z 1,160.70, WFYIASAFR) and two peptides from Human serum albumin (m/z 1,311.77, HPDYSVVLLLR and m/z 1,467.85, RHPDYSVVLLLR). Data from 3 assay replicates were included in one box plot. The S/N ratios of the values generated with the ultracentrifugation procedure are not significantly higher compared to the respective values of the assays without ultracentrifugation. Statistical significances were calculated with Mann-Whitney test using StatistiXL 1.8.

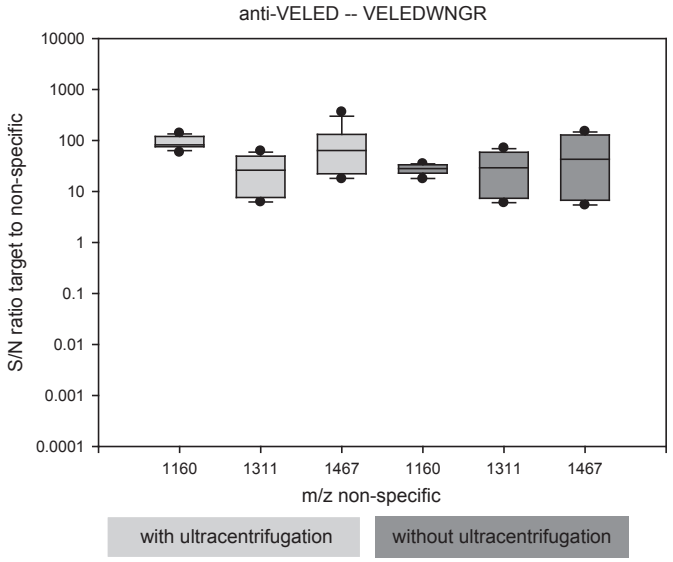

Figure A.53.: Distribution of signal-to-noise ratios of target peptide VELEDWNGR (m/z 1118, Fibrinogen) to selected non-specific peptides for assay conditions with and without ultracentrifugation. One target peptide was set in relation to each of three non-specific peptides from two different proteins: one peptide from Alpha-1-acid glycoprotein 1 (m/z 1,160.70, WFYIASAFR) and two peptides from Human serum albumin (m/z 1,311.77, HPDYSVVLLLR and m/z 1,467.85, RHPDYSVVLLLR). Data from 3 assay replicates were included in one box plot. The S/N ratios of the values generated with the ultracentrifugation procedure are not significantly higher compared to the respective values of the assays without ultracentrifugation. Statistical significances were calculated with Mann-Whitney test using StatistiXL 1.8.

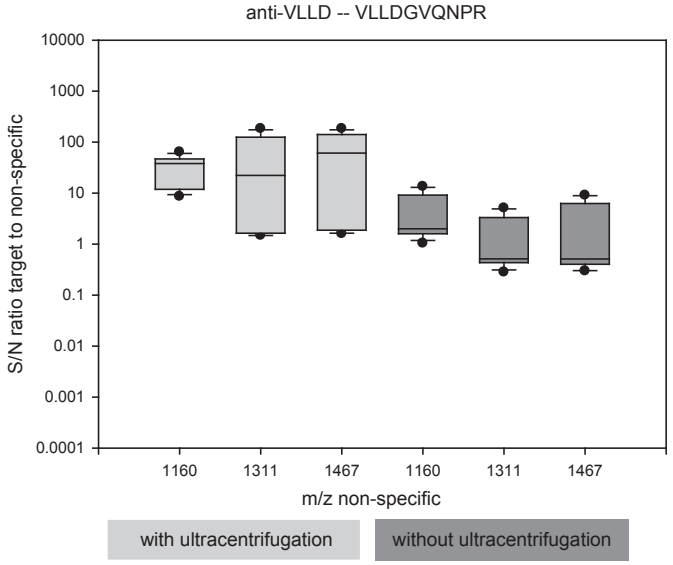

Figure A.54.: Distribution of signal-to-noise ratios of target peptide VLLDGVQNPR (m/z 1111, Complement C3) to selected non-specific peptides for assay conditions with and without ultracentrifugation. One target peptide was set in relation to each of three non-specific peptides from two different proteins: one peptide from Alpha-1-acid glycoprotein 1 (m/z 1,160.70, WFYIASAFR) and two peptides from Human serum albumin (m/z 1,311.77, HPDYSVVLLLR and m/z 1,467.85, RHPDYSVVLLLR). Data from 3 assay replicates were included in one box plot. The S/N ratios of the values generated with the ultracentrifugation procedure are significantly ($P<0.001$) higher compared to the respective values of the assays without ultracentrifugation. Statistical significances were calculated with Mann-Whitney test using StatistiXL 1.8.

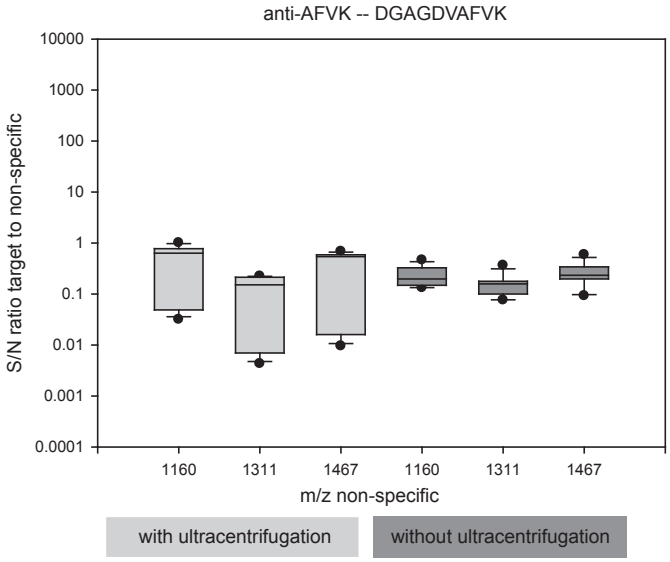

Figure A.55.: Distribution of signal-to-noise ratios of target peptide DGAGDVAFVK (m/z 978, Serotransferrin) to selected non-specific peptides for assay conditions with and without ultracentrifugation. One target peptide was set in relation to each of three non-specific peptides from two different proteins: one peptide from Alpha-1-acid glycoprotein 1 (m/z 1,160.70, WFYIASAFR) and two peptides from Human serum albumin (m/z 1,311.77, HPDYSVVLLLR and m/z 1,467.85, RHPDYSVVLLLR). Data from 3 assay replicates were included in one box plot. The S/N ratios of the values generated with the ultracentrifugation procedure are not significantly higher compared to the respective values of the assays without ultracentrifugation. Statistical significances were calculated with Mann-Whitney test using StatistiXL 1.8.

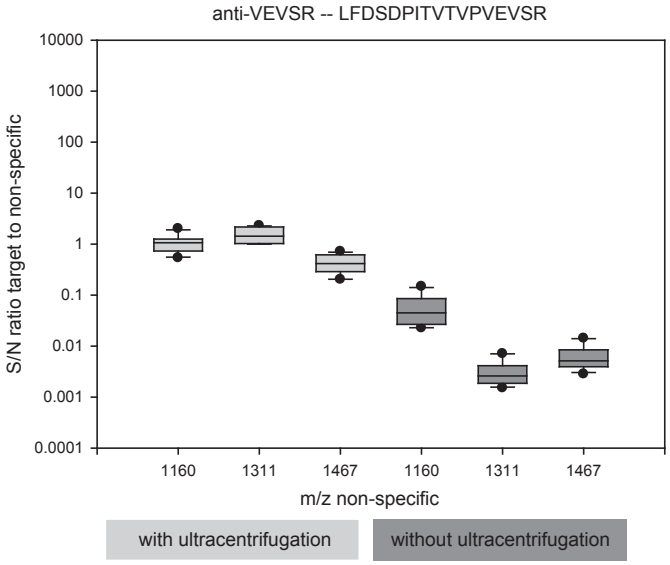

Figure A.56.: Distribution of signal-to-noise ratios of target peptide LFDSDPITVTVPVEVSR (m/z 1874, Clusterin) to selected non-specific peptides for assay conditions with and without ultracentrifugation. One target peptide was set in relation to each of three non-specific peptides from two different proteins: one peptide from Alpha-1-acid glycoprotein 1 (m/z 1,160.70, WFYIASAFR) and two peptides from Human serum albumin (m/z 1,311.77, HPDYSVVLLLR and m/z 1,467.85, RHPDYSVVLLLR). Data from 3 assay replicates were included in one box plot. The S/N ratios of the values generated with the ultracentrifugation procedure are significantly ($P<0.001$) higher compared to the respective values of the assays without ultracentrifugation. Statistical significances were calculated with Mann-Whitney test using StatistiXL 1.8.

Appendix B.

List of publications

Publications

Paper **Sonja Schneider**, Thomas D. Schreiber, David Eisen, Calvin Wiese, Hannes Planatscher, Andreas Zell, Dieter Stoll, Markus Templin, Thomas O. Joos, Oliver Pötz. Combining ultracentrifugation and peptide termini group-specific immunoprecipitation for multiplex plasma protein analysis.

Paper Oliver Poetz, Anke Schnabel, **Sonja Schneider**, Hannes Planatscher, Bettina Serschnitzki, Helmut Meyer, Andreas Zell, Dieter Stoll, Markus F. Templin, Katrin Marcus, Thomas O. Joos. Absolute quantification of CYP3A4, 3A5 and 3A7 and MDR1 using a single peptide-terminus specific antibody. (in preparation)

Talk **Sonja Volk**, Thomas D. Schreiber, Calvin Wiese, Hannes Planatscher, Andreas Zell, Dieter Stoll, Markus Templin, Thomas O. Joos, Oliver Pötz. Immunoaffinitätsanreicherung für die MS basierte Proteomanalyse. *5. Tübinger Massenspektrometrie Seminar, 25th June 2009*

Talk **Sonja Volk**, Thomas D. Schreiber, David Eisen, Calvin Wiese, Hannes Planatscher, Andreas Zell, Dieter Stoll, Markus Templin, Thomas O. Joos, Oliver Pötz. Plasma Proteome Analysis By Immunoaffinity Triple X Proteomics. *Proteomic Summer School, Brixen 2009*

Poster **Sonja Volk**, Tobias Niels, Bernd Mühlbauer, Dieter Stoll, Markus Templin, Thomas O. Joos, Oliver Pötz. Analysis Of Cancer Specific Proteolytic Peptides. *Proteomic Summer School, Brixen 2008*

Poster **Sonja Volk**, Thomas D. Schreiber, David Eisen, Calvin Wiese, Hannes Planatscher, Andreas Zell, Dieter Stoll, Markus Templin, Thomas O. Joos, Oliver Pötz. Plasma Proteome Analysis By Immunoaffinity Triple X Proteomics. *Proteomic Summer School, Brixen 2009.* Posterprize